

DISSERTATION FOR THE DEGREE OF DOCTOR OF PHILOSOPHY (PHD)

Investigation of biocompatibility of polyethylene glycol derivatives  
and preparation of solid dispersion containing ketoprofen

by Dr. Pham Le Khanh Ha

Supervisor: Prof. Dr. Ildikó Bácskay



UNIVERSITY OF DEBRECEN  
DOCTORAL SCHOOL OF PHARMACEUTICAL SCIENCES

DEBRECEN, 2024

## Table of Contents

<b>1. AUTHOR'S DECLARATION.....</b>	<b>1</b>
<b>2. LIST OF FIGURES.....</b>	<b>2</b>
<b>3. LIST OF TABLES.....</b>	<b>3</b>
<b>4. ABBREVIATION.....</b>	<b>4</b>
<b>5. Introduction.....</b>	<b>6</b>
<b>5.1. General characterization of PEGS.....</b>	<b>6</b>
<b>5.2. Application in different dosage forms based on PEGS.....</b>	<b>10</b>
<b>5.3. Biocompatibility of PEGs, structure, properties biocompatibility correlation.....</b>	<b>14</b>
5.3.1. The biocompatibility of polyethylene glycols (PEGs).....	20
<b>5.4. Ketoprofen formulations and preparations.....</b>	<b>24</b>
5.4.1. Characterization of ketoprofen.....	24
5.4.2. Effect of ketoprofen.....	26
5.4.3. Increase of solubility and permeability in pharmaceutical formulations.....	28
5.4.4. New formulations of Ketoprofen.....	32
5.4.5. Solid dispersion introduction.....	34
<b>6. THESIS OBJECTIVES.....</b>	<b>44</b>
<b>7. EXPERIMENTAL PART.....</b>	<b>46</b>
<b>7.1. Materials and sample preparation.....</b>	<b>46</b>
<b>7.2. Methods.....</b>	<b>47</b>
7.2.1. Cell culture.....	47
7.2.2. Cytotoxicity tests.....	47
7.2.3. Osmolality measurement.....	48
7.2.4. Flow cytometry analysis.....	48
7.2.5. Autophagy Assay.....	49
7.2.6. G. mellonella larvae survivability tests.....	49
7.2.7. Statistical analysis.....	50
7.2.8. Phase solubility.....	50
7.2.9. Preparation of solid dispersions and physical mixtures.....	51
7.2.10. Fourier-transform infrared spectroscopy (FTIR).....	51
7.2.11. Powder X-ray Diffraction (PXRD).....	51
7.2.12. Scanning Electron Microscopy (SEM).....	52

7.2.13. In Vitro Dissolution Test .....	52
<b>8. RESULTS I. ....</b>	<b>54</b>
8.1. Osmolality results .....	54
8.2. Cytotoxicity assay results .....	55
8.3. Autophagy assay results .....	57
8.4. Flow cytometry results .....	58
8.5. In vivo toxicity test.....	60
8.6. Correlation of results with molecular weight .....	61
<b>9. RESULTS II. ....</b>	<b>63</b>
9.1. Phase solubility.....	63
9.2. Fourier-transform infrared spectroscopy (FT-IR).....	64
9.3. Powder X-ray Diffraction (PXRD) .....	66
9.4. Scanning Electron Microscopy (SEM) .....	67
9.5. In Vitro Dissolution Test .....	68
<b>10. DISCUSSION I.....</b>	<b>72</b>
<b>11. DISCUSSION II.....</b>	<b>77</b>
<b>12. SUMMARY .....</b>	<b>81</b>
<b>13. REFERENCES .....</b>	<b>83</b>
<b>14. KEYWORDS .....</b>	<b>118</b>
<b>15. PUBLICATIONLIST RELATED TO THE DISSERTATION .....</b>	<b>119</b>
<b>16. FUNDING .....</b>	<b>120</b>
<b>17. ACKNOWLEDGEMENT .....</b>	<b>121</b>

## **1. AUTHOR'S DECLARATION**

I hereby declare that I am the sole author of this thesis. This is a true copy of the thesis, including any required final revisions, as accepted by my examiners. I understand that my thesis may be made electronically available to the public.

Ha Pham Le Khanh

## 2. LIST OF FIGURES

Figure 1: Chemical structure of PEGs and its derivatives -----	7
Figure 2: Chemical structure of PEGs -----	8
Figure 3: Various application of Polyethylene glycols (PEGs) -----	11
Figure 4: Main advantages of PEGSylated protein -----	13
Figure 5: Reduction of MTT (yellow) to formazan crystals (purple) -----	17
Figure 6: Caco-2 cell morphology after seeding the 2nd; 7th day; and 21 <sup>st</sup> day -----	19
Figure 7: The brush conformation of PEGs -----	20
Figure 8: Molecular structures of (S)-and (R)-Ketoprofen -----	24
Figure 9: Biopharmaceutics drug classification system (BCS) -----	29
Figure 10: Pharmaceutical particle technologies for improved solubility, dissolution, and bioavailability of drugs -----	32
Figure 11: Components of solid dispersion system -----	35
Figure 12: Classification of solid dispersions -----	39
Figure 13: Techniques for solid dispersion preparation -----	41
Figure 14: Experimental design of the thesis -----	45
Figure 15: Osmolality of PEGs and sorbitol solutions measured by vapor pressure osmometer OSMOMAT 070-----	55
Figure 16: Cytotoxicity of PEGs and sorbitol solutions measured by MTT assay -----	56
Figure 17: Cytotoxicity of PEGs and sorbitol solutions measured by NR assay -----	57
Figure 18: Effect of PEGs and sorbitol solutions on the number of autophagosomes-----	58
Figure 19: Flow cytometric measurement of Caco-2 cells -----	59
Figure 20: Survival curve of G. mellonella larvae -----	60
Figure 21: Phase-solubility diagram of ketoprofen in simulated gastric juice-----	64
Figure 22: FTIR spectra of KT, pure PEGs, PM, SD for PEG 1000,1500, 2000-----	65
Figure 23: PXRD spectra of KT, pure PEGs, PM, SD for PEG 1000,1500, 2000 -----	66
Figure 24: SEM images of PEG 2000,1500,1000, and crystalline ketoprofen -----	67
Figure 25: SEM images of PM and SD of PEG 2000, PEG 1500, PEG 1000-----	68
Figure 26: Dissolution profiles of SDs and PMs in simulated gastric juice-----	69

### 3. LIST OF TABLES

Table 1: Summary of physicochemical characteristics of PEGs-----	9
Table 2: Preliminary evaluation tests of the materials.-----	15
Table 3: Quantitative analysis of biocompatibility.-----	16
Table 4: Characteristics of Caco-2 cells -----	19
Table 5: Summary of physicochemical properties of ketoprofen-----	26
Table 6: Solubility criteria according to USP -----	30
Table 7: Mathematical models for comparison of dissolution profiles -----	37
Table 8: Different class of carriers used in solid dispersion method -----	40
Table 9: Market products with solid dispersion technique -----	42
Table 10: Mathematical calculations of drug release profiles. -----	53
Table 11: Correlation of measured data (only PEGs) with average MW. -----	61
Table 12: Correlation of matrix of all measured data sets (only PEGs). -----	62
Table 13: Gibbs free energy values of ketoprofen and the tested PEGs. -----	64
Table 14: Difference and similarity factors of the dissolution profiles -----	69
Table 15: Coefficient determination for different models of the dissolution profiles--	70
Table 16: Some publications about the correlation between MW of PEGs -----	71
Table 17: Some review of SDs dissolution studies, prepared with multiple PEGs ----	79

## 4. ABBREVIATION

<b>Abbreviations</b>	<b>Definitions</b>
<b>ANOVA</b>	Analysis of Variance
<b>API</b>	Active Pharmaceutical Ingredient
<b>AUC</b>	Area under the curve
<b>AV</b>	Annexin V
<b>BCS</b>	Biopharmaceutics drug Classification System
<b>BP</b>	British Pharmacopoeia
<b>Caco-2</b>	Human colorectal adenocarcinoma cells
<b>CHS-CS</b>	Chitosan-chondroitin sulfate
<b>COLO205</b>	Human adenocarcinoma cells
<b>COX</b>	Cyclooxygenase
<b>DMEM</b>	Dulbecco's Modified Eagle's Medium
<b>DMSO</b>	Dimethyl sulfoxide
<b>DSC</b>	Differential scanning calorimetry
<b>ECACC</b>	European Collection of Cell Cultures
<b>EDTA</b>	Ethylenediaminetetraacetic acid
<b>EO</b>	Ethylene oxide
<b>ER</b>	Enhancement ratio
<b>FA</b>	Fumaric acid
<b>FBS</b>	Foetal bovine serum
<b>FDA</b>	Food and Drug Administration
<b>FHC</b>	Human foetal mucosa cells
<b>FLC</b>	Fluconazole
<b>FLC-NP</b>	Fluconazole nanoparticles
<b>FT-IR</b>	Fourier-transform infrared spectroscopy
<b>GI</b>	Gastrointestinal
<b>GRAS</b>	Generally Recognized as Safe
<b>HEC</b>	Hydroxyethyl cellulose
<b>HPMC</b>	Hydroxypropyl Methylcellulose
<b>HT29</b>	Human adenocarcinoma cells
<b>i.v</b>	intravenous
<b>ICH</b>	International Council for Harmonisation of Technical Requirements of Pharmaceuticals for Human Use
<b>IND</b>	Indomethacin
<b>ISO</b>	International Organization for Standardization
<b>IU</b>	International units
<b>Jss</b>	Steady-state flux
<b>Kp</b>	Permeability coefficient
<b>KT</b>	Keptoprofen
<b>LDH</b>	Lactate dehydrogenase
<b>LMW</b>	Lower molecular weight

<b>MAG</b>	Magnolol
<b>MANOVA</b>	Multivariate analysis of variance
<b>mPEGSA</b>	PEGS methyl ether acrylate
<b>mPEGsMA</b>	PEGS methyl ether methacrylate
<b>MTT</b>	3-(4,5-dimethylthiazol-2-yl)-2,5-diphenyltetrazolium bromide
<b>MW</b>	Molecular weight
<b>NR</b>	Neutral Red
<b>NSAID</b>	Non-steroidal anti-inflammatory drug
<b>OLM</b>	Olmesartan medoxomil
<b>P</b>	permeability
<b>PBS</b>	Phosphate-buffered saline
<b>PEG</b>	Polyethylene glycol
<b>PEGs</b>	Polyethylene glycols
<b>PEO</b>	Poly(ethylene) oxide
<b>PI</b>	propidium iodide
<b>PM</b>	Physical mixture
<b>POE</b>	Poly(oxyethylene)
<b>POED</b>	polyoxyethylene 32 distearate
<b>PVC</b>	Polyvinyl Chloride
<b>PVP</b>	Polyvinylpyrrolidone
<b>PWS</b>	Poorly water-soluble
<b>PXRD</b>	Powder X-ray Diffraction
<b>S</b>	solubility
<b>SCF</b>	Supercritical fluid
<b>SD</b>	Solid dispersions
<b>SEDDD</b>	Self-emulsifying drug delivery systems
<b>SEM</b>	Scanning Electron Microscopy
<b>SLN</b>	Solid lipid nanoparticles
<b>TEG</b>	Triethylene glycol
<b>TPP</b>	Tripolyphosphate
<b>USP</b>	United States Pharmacopoeia

## 5. Introduction

### 5.1. General characterization of PEGs

Polyethylene glycols (PEGs) are widely used polymers that have a variety of applications in many fields, including biomedical, chemical, and industrial processes. These compounds are important group of excipients due to their widespread use in different pharmaceutical formulations, especially is a favorable choice to reach the optimal drug delivery system. PEGs are also recognized as Macrogols in the European Pharmacopoeia. PEGs refer to oligomers of polyethylene oxide with different molecular weight (MW) and they are commercially available in a wide range of MW from 200 to 10.000.000 g/mol.<sup>1,2</sup> Poly(ethylene) oxide (PEO) or poly(oxyethylene) (POE) are also known as PEGs.<sup>3</sup> However, PEO and POE are common names for higher molecular weight polymers, whereas polymer with MW < 30.000g/mol are referred to as PEGS.<sup>2</sup> However, for medical applications, in general, the abbreviation “PEGs” is common and exclusively used.

Polyethylene glycols are synthetic, water-soluble, odorless and tasteless polymer made up of repeating units of ethylene oxide (EO) units. They are polyether compounds which are synthesized by polymerization of EO with water, mono ethylene glycol or diethylene glycol (hydroxyl initiators) as starting material under alkaline and acidic catalysis. The final PEGs product structure is  $\text{HO} - [\text{CH}_2 - \text{CH}_2 - \text{O}]_n - \text{H}$ , where (n) is the number of ethylene oxide (EO) units and defines the molecular weight of the polymer.<sup>4</sup> The molecular structure of PEGs imparts several key characteristics that makes it highly attractive for pharmaceutical applications. The amphiphilic nature of PEGs, characterized by hydrophilic ether linkages (C-O bonds) and hydrophobic methylene groups (-CH<sub>2</sub> groups), contributes to their versatility and compatibility with both aqueous and organic environments.<sup>5</sup> The chemical structure of PEGs and their derivatives are illustrated in Figure 1.

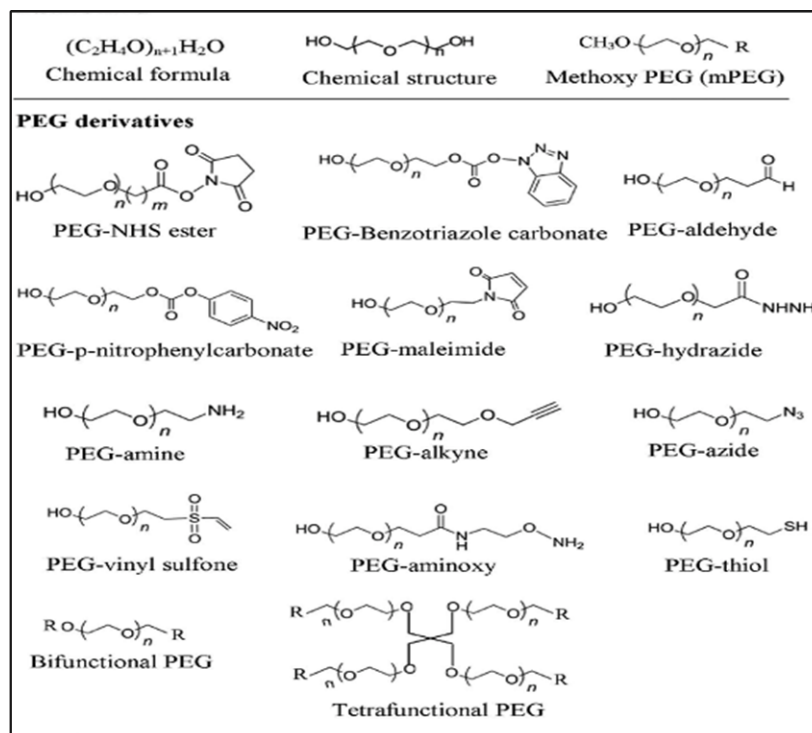


Figure 1: Chemical structure of PEGs and its derivatives. <sup>6</sup>

PEGs may manifest in diverse physical states, spanning from a transparent, non-volatile liquid at room temperature (for low molecular weight PEGs ranging from 200 to 700) to a semi-solid state (having a pasty consistency, characteristic of medium molecular weight PEGs within the range of 800 to 2000) and ultimately transitioning to a solid form (either as a white waxy solid, flakes, or powder for high molecular weight PEGs of 3000 and above).<sup>2,6</sup> PEGs become harder as their molecular weight increases, however, the melting range only extends to the maximum value of about 60°C.<sup>4</sup>

The molecular weight of PEGs plays a critical role in determining its physical properties and biomedical applications. PEGs with different molecular weights possess distinct characteristics.<sup>7</sup> Lower molecular weight PEGs (e.g., PEGS 200) are typically used as solvents, while higher molecular weight PEGs (e.g., PEGS 20,000) are more commonly employed in drug delivery systems. The choice of PEGs molecular weight depends on the desired drug release kinetics, circulation time, and biodistribution profile.

One of the most significant properties of PEGs is their hydrophilicity, which makes it an ideal compound for use in aqueous solutions.<sup>8</sup> The molecular weight of PEGs affects their water solubility. The polymer chains are hydroxyl-terminated at both ends. The high polarity characteristic of PEGs, which is depicted in Figure 2, is largely attributed to the terminal hydroxyl and ether groups.<sup>2,6</sup> The low molecular weight PEGs have more

hydroxyl groups compared to their structure, thus as the molecular weight of the PEGs increase, their solubility in water and other solvents decreases.<sup>9</sup>

Moreover, PEGs can also be dissolved in many other solvents such as tetrahydrofuran, chloroform, dimethyl sulfoxide and alcohol chlorinated solvents.<sup>10</sup> Under normal conditions, PEGs can be considered relatively stable, the chemical and physical changes are limited and few. However, the interaction of PEGs with given compounds might induce precipitation such as phenol, cresol, resorcinol, tannin, hence, PEGs can be used as the antidote for removing certain toxic substances.<sup>11</sup> Additionally, PEGs have an excellent property of retaining moisture. LMW PEGs are hygroscopic and thus are preferred for various applications to their moisture retention feature as a humectant in skincare products.<sup>3,12</sup> PEGs is also quite stable and will not be hydrolysed or deteriorated or get rancid under normal circumstances.

PEGs exhibit remarkable viscosity-enhancing properties, making them useful in various applications, including drug formulation and as a lubricant. The viscosity of PEGs is influenced by their molecular weight, concentration, and temperature.<sup>13</sup> Higher molecular weight PEGs generally have higher viscosities, while increasing the concentration of PEGs in a solution also leads to an increase in viscosity.<sup>14</sup> Temperature affects the viscosity of PEGs, as higher temperatures reduce the intermolecular interactions among polymer chains and consequently decrease viscosity.

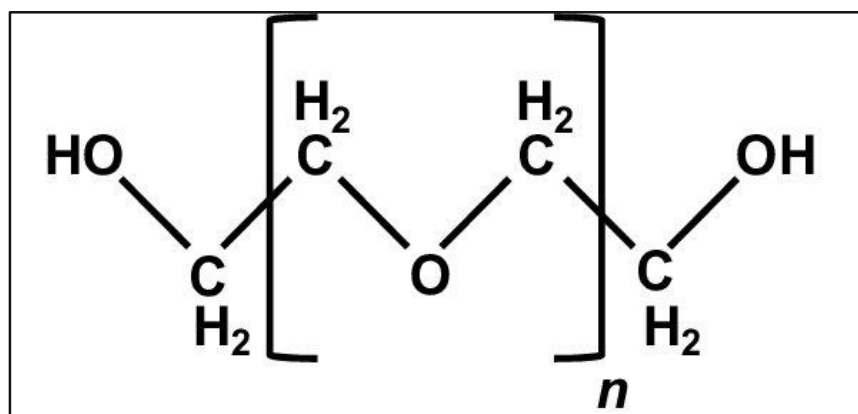


Figure 2: Chemical structure of PEGs <sup>15</sup>

The general physicochemical properties of PEGs are summarized in the Table 1.

<b>Molar mass (g/mol)</b>	Commercially available from 300 g/mol to 10.000.000 g/mol
<b>Chemical formula (g/mol)</b>	$\text{HO} - [\text{CH}_2 - \text{CH}_2 - \text{O}]_n - \text{H}$
<b>Physical state/Appearance (at room temperature)</b>	<ul style="list-style-type: none"> <li>• PEG 200-700: liquid</li> <li>• PEG 1000-2000 (MW &gt;700): semi-solid to soft solids, waxy solid</li> <li>• PEGs MW &gt;2000: solid, powder/flakes</li> </ul>
<b>Solubility</b>	<ul style="list-style-type: none"> <li>• Soluble in water, ethanol, benzene, acetonitrile, dichloromethane</li> <li>• Insoluble in ether and hexane</li> </ul>
<b>Melting point <math>T_m</math> (°C)</b>	<70 °C regardless of molecular weight
<b>Boiling point (°C)</b>	>150 °C
<b>Viscosity</b>	increase with higher MW PEGs

**Table 1: Summary of physicochemical characteristics of PEGs<sup>16,17</sup>**

In summary, polyethylene glycols (PEGs) possess a range of physicochemical properties that make it an invaluable polymer in pharmaceutical sciences. Its solubility, viscosity, molecular weight, thermal behavior, and interactions with biological systems play pivotal roles in drug delivery system, formulation design, and therapeutic applications. In addition, PEGs have a favourable safety profile. It is non-toxic and has been extensively studied for its use in various pharmaceutical applications. PEGs are also biodegradable, which means they can be broken down and eliminated from the body. PEGs have a low toxicity level which are classified as the Generally Recognized as Safe (GRAS) category by the FDA, making it safe for use in many applications.<sup>18</sup> PEGs are non-toxic and non-immunogenic and non-antigenic.<sup>19</sup> This makes them a safe ingredient for use in medical applications. PEGs have low toxicity with systemic absorption less than 0.5%.

PEGs are ideal excipients due to their excellent features such as inert, non-immunogenicity, hydrophilicity, high biocompatibility and solubility improving capacity, making them ideal for pharmaceutical formulations. For PEGs to be used to their full potential in the creation of novel drug delivery systems, a thorough understanding of these properties is essential.

## 5.2. Application in different dosage forms based on PEGs

The applications of PEGs are summarized in Figure 3. Considering the *medical application*, PEGs are well-known to be applied as laxatives or in preparation for surgery or colonoscopy, because PEGs can apply osmotic pressure and cause water to be retained with the stool. This increases the number of bowel movements and softens the stool, providing a laxative effect.<sup>20,21</sup> They are frequently employed in the medical industry as a drug carrier, wound dressing, and tissue engineering scaffold.<sup>22,23</sup> In the case of cells and tissues, PEGs are demonstrated by their minimal cytotoxicity and ability to support cellular functions. PEGs-based hydrogels, for example, provide an excellent three-dimensional matrix for cell encapsulation and tissue engineering applications.<sup>24,25</sup> These hydrogels mimic the extracellular matrix, promoting cell adhesion, proliferation, and differentiation. PEGs' high-water content and mechanical properties resembling soft tissues contribute to its successful integration into biological systems.<sup>26</sup> In tissue engineering, PEGs hydrogels are utilized in tissue engineering as scaffolds to support cell growth and direct tissue regeneration.<sup>27,28</sup> PEGs hydrogels are extremely adaptable platforms because of their flexible physical and mechanical characteristics, as well as their capacity to incorporate bioactive molecules.

Besides, polyethylene glycol (PEGs) has been widely used in various industries, including the *pharmaceutical industry*. These properties have also made PEGs ideal for use in *cosmetics and personal care products*. In cosmetic products, PEGs is used as an emulsifier, a moisturizer, and a thickener, where it can improve product stability, texture, and appearance.

Specifically, PEGs are used as an excipient in drug formulations, where it can improve drug solubility, stability and bioavailability in *pharmaceutical industry*. PEGs are frequently employed in the production of tablets and capsules as a lubricant.<sup>29</sup> During the manufacturing process, tablets and capsules need to be able to move freely without getting stuck to machinery or one another. PEGs can be used as to reduce adhesion and improve the flowability of the powder mixtures. The coating of the tablets or capsules

with PEGs can also make them easier to swallow and lower their risk of causing gastrointestinal tract irritation.

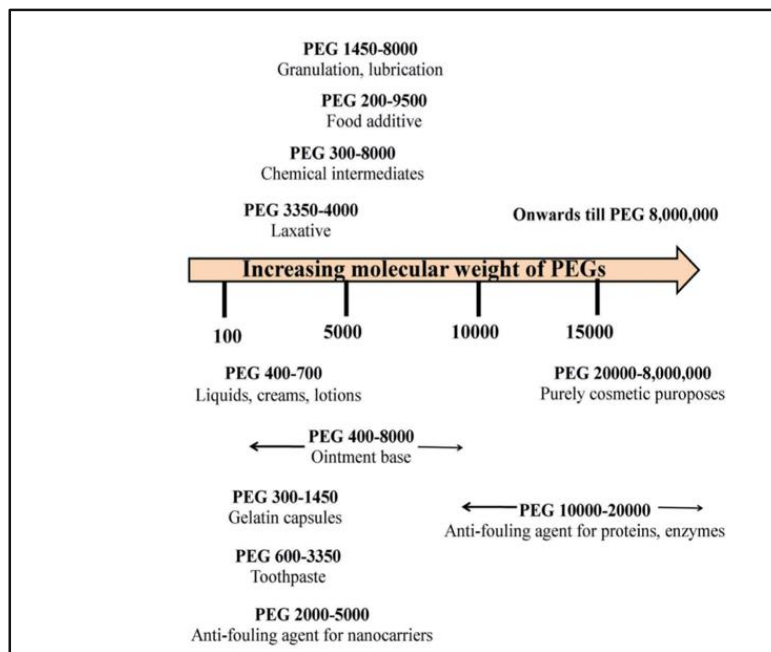


**Figure 3: Various application of Polyethylene glycols (PEGs) <sup>6</sup>**

PEGs are also useful in the manufacturing of coatings, adhesives, and plastics, among other industrial products. When making PVC, PEGs can be used as a plasticizer to increase the flexibility and toughness of the material. The performance and durability of adhesives and coatings can be enhanced by adding PEGs as a binder during production. Another important use of PEGs in drug formulation is as a viscosity modifier. Viscosity is an important property in the preparation of liquid formulations such as suspensions and emulsions. These formulations' viscosity can be increased by PEGs, which can enhance their stability and prevent sedimentation. Additionally, PEGs can be used to modify the rheological properties of gels and ointments, which can improve their spread ability and skin adherence. Another important application of PEGs is in biotechnology and biomedical research. PEGs can be used as a protein stabilizer, where it can increase protein solubility and stability.

PEGs are likely to play an important role in the formulation and delivery of new drugs. One of the primary uses of PEGs in drug formulation is as a solubilizer. Many drugs have poor solubility in water, which can limit their bioavailability and efficacy. PEGs can increase the solubility of drugs in water, making them more readily absorbed by the body. The use of PEGs as a solubilizer has been shown to improve the oral

bioavailability of poorly soluble drugs such as griseofulvin and fenofibrate. Oliveria. et al reported that the solubility of griseofulvin in water was increased by 6-8-fold using PEGS 6000 and PEGS 35000.<sup>30</sup> In comparison to other polymers tested (PVP K30 and PVP K90) in their research, the addition of a relatively small amount of PEGS 3500 even allows for a lesser amount of F127 solution to be required for solubilization while still achieving a similar or improved solubilization capacity. The solubility of weakly water-soluble substance Olmesartan medoxomil (OLM) was also found to be improved in the binary system using PEGs 400. The OLM solubility was enhanced significantly by increasing the temperature and the amount of PEGs 400 in the cosolvent mixture.<sup>31</sup>

PEGs are great as solubilizers and permeation enhancers for many poorly soluble and low permeability compounds, particularly those falling under BCS classes II and IV. They substantially enhance the bioavailability of the respective drugs, attributed to PEGs' miscibility with aqueous fluids. At 30°C, it was shown that the solubility of benzodiazepines such as diazepam and temazepam increased by 3.5 and 2.5 times, respectively.<sup>6</sup>

An example of enhanced permeability is the improved absorption of Digoxin (classified as BCS class IV) within the gastrointestinal tract when formulated as a PEGs 400 solution encapsulated in soft gels (Lanoxincaps®), as opposite to the tablet dosage form (Lanoxin®).<sup>2</sup> Moreover, some PEGs and their derivatives, such as surfactants, humectants, and emulsifiers, are used as penetration enhancers in topical dermatological preparations or cosmetics.<sup>32</sup> The study of Ahmed et al. used an ex vivo permeation experiment to demonstrate how coating fluconazole nanoparticles (FLC-NP) with PEGs 4000, PEGs 10000, and PEGs 20000 improved their permeability.<sup>33</sup> The amount of FLC coated permeated across the abdominal rat skin was much higher compared to permeability of the FLC without coating ( $3.45 \pm 0.108 \text{ mg/cm}^2$  vs  $1.650 \pm 0.97 \text{ mg/cm}^2$ ).

PEGs are also used as a drug delivery system, where they can be conjugated to drugs or nanoparticles to improve their pharmacokinetics and biodistribution. PEGs are frequently selected to cover the particles surfaces of the specialized carriers employed in targeted drug delivery system.<sup>34</sup> This choice is attributed to the neutral, hydrophilic, and flexible characteristics of these polymers, forming a surface layer on nanoparticles to create stealth nanocarriers in cancer therapy. Consequently, opsonin adhesion is minimized, and evasion of uptake by the reticuloendothelial system prolongs systemic circulation.<sup>6,35</sup> A highly successful approach in this regard involves using polyethylene glycol (PEGs) as a modifying polymer, a strategy termed PEGSylation, which has yielded

significant outcomes in therapy, diagnosis, and organic biocatalysis.<sup>7</sup> Notable examples of this PEGSylation technique include Doxorubicin, Taxol, and Camptothecin.<sup>6</sup> The Figure 4 illustrates a polymer-protein conjugate and its advantages, where PEGs shield the protein surface from degrading agents through steric hindrance. Furthermore, the increased size of the conjugate is foundational to the diminished kidney clearance of the PEGSylated protein.

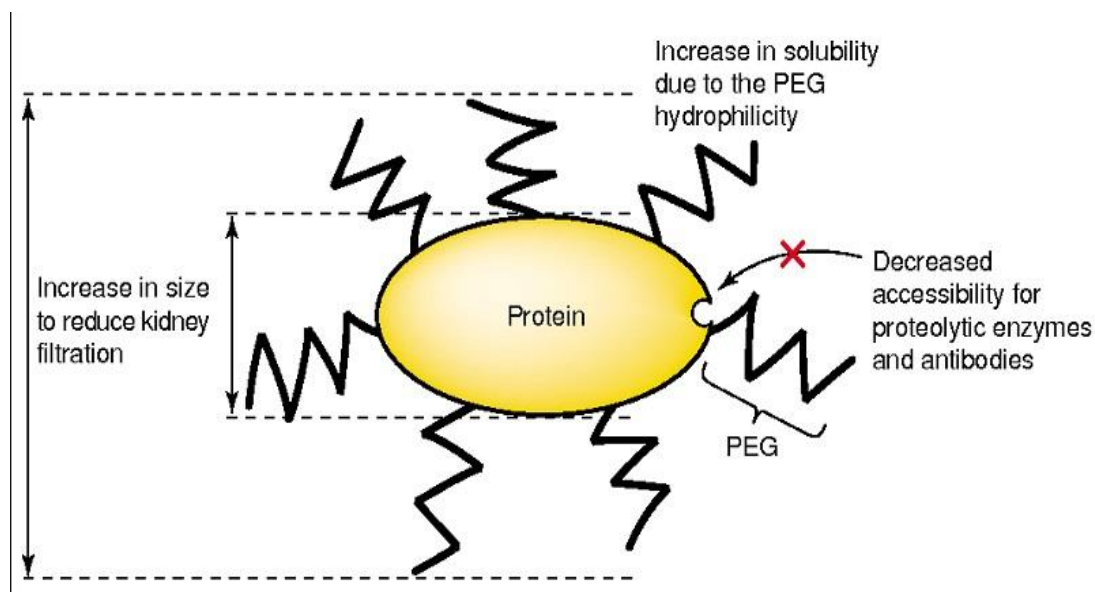


**Figure 4: Main advantages of PEGSylated protein<sup>6</sup>**

In drug delivery, PEGSylation—the covalent attachment of PEGs chains to therapeutic molecules—has been used to improve drug stability, extend circulation time, and reduce immunogenicity. PEGs-based nanoparticles and micelles offer efficient carriers for targeted drug delivery, demonstrating improved pharmacokinetics and reduced toxicity compared to traditional drug formulations.

In conclusion, PEGs are versatile polymers that has found numerous applications in a wide range of industries. They have many applications in various industries, including pharmaceuticals, cosmetics, and food. PEGs functions as a lubricant, binder, and solubilizing agent. It is also used in the manufacture of polyurethane foams, surfactants, and plasticizers. In medicine, PEGs are used in drug delivery systems, such as PEGSylated proteins and liposomes, and as a laxative. Its ability to increase solubility and stability of drugs makes it a valuable tool in pharmaceutical and biomedical research. Its hydrophilicity, low toxicity, and biocompatibility make it an attractive choice for use

in medical and pharmaceutical applications. PEGs' properties can be tuned to meet the specific requirements of different applications, making it an essential component in many products and processes.

### **5.3. Biocompatibility of PEGs, structure, properties biocompatibility correlation**

In recent years, the quest for biocompatible materials has become paramount in biomedical research and applications. Every stage of the drug formulation process must take the drug safety profile into consideration. In order to ensure the safe and efficient interaction of biomedical materials with living systems, *biocompatibility is a crucial component* in their development. According to Klinkmann et. al. (1984), biocompatibility is specifically described as the compatibility with living tissue or a living system by not being toxic, harmful, or physiologically reactive and not resulting in immunological rejection.<sup>37</sup> A device that will be implanted into a human body must be safe for the patients, which necessitates that it be biologically compatible with the tissues. The aim of biocompatibility testing is to make sure that a substance or device will offer the patient the greatest benefit with the least amount of risk.<sup>38</sup>

According to the major standards organizations, both national and international, who have published guidelines about the selection of tests for the biological evaluation of materials and medical and dental devices, any program of assessment on biomaterials must include biocompatibility tests on cell cultures. The guideline document 'Biological Testing of Medical Devices--Part 1: Guidance on Selection of Tests' (ISO 10933-1), which incorporates all national and international documents, was created by ISO in order to harmonize the existing guidelines. In this draft, the devices are grouped according to how they interact with the body (surface contacting, implant and external communicating).

Additionally, this document categorizes the devices into 3 groups based on how long they interact with the body: limited exposure, prolonged exposure, and permanent contact. The choice of tests to evaluate device compatibility is influenced by the amount of time and type of contact that the device has with tissues. Cytotoxicity tests must be performed on all categories, as can be seen in Table 2. Tests for the initial evaluation of the biological compatibility of medical devices are listed in this table.<sup>39</sup>

Device categories		Biological effect								
Body contact	Contact duration A-Limited exposure (< 24 h) B-Prolonged exposure (> 24 h < 30 days) C-Permanent contact (> 30 days)	Cytotoxicity	Sensitization	Irritation or intracutaneous reactivity	Systemic toxicity (acute)	Sub-chronic toxicity	Genotoxicity	Implantation	Haemocompatibility	
Surface devices	Skin	A	X	X	X					
		B	X	X	X					
		C	X	X	X					
	Mucous membrane	A	X	X	X					
		B	X	X	X					
		C	X	X	X		X	X		
	Broken surface	A	X	X	X					
		B	X	X	X					
		C	X	X	X		X	X		
External communicating devices	Blood path indirect	A	X	X	X				X	
		B	X	X	X				X	
		C	X	X		X	X	X		X
	Tissue/bone /dentine communicating	A	X	X	X					
		B	X	X				X	X	
		C	X	X				X	X	
	Circulating blood	A	X	X	X	X				X
		B	X	X	X	X		X		X
		C	X	X	X	X	X	X		X
Implant devices	Bone/tissue	A	X	X	X					
		B	X	X				X	X	
		C	X	X				X	X	
	Blood	A	X	X	X	X			X	X
		B	X	X	X	X		X	X	X
		C	X	X	X	X	X	X	X	X

Table 2: Preliminary evaluation tests of the materials.<sup>39</sup>

Quantitative tests are required to go beyond the simple morphological analysis of biomaterial/tissue interaction in order to assess a material or device's biocompatibility. According to the stage of the biomaterial evaluation, the quantitative analysis of biocompatibility is summarized in Table 3.<sup>39</sup> Depending on the characteristics of the material and its intended use, this list is adaptable and flexible.

<b>Screening tests</b>	<b>Supplementary tests</b>
Cytotoxicity	Cell response
Histotoxicity	Blood response
Hemotoxicity	Tissue response
Genotoxicity	Immune and allergic response
	Irritation response
	Systemic acute, subacute and chronic toxicity
	Reproductive toxicity
	Carcinogenesis
<b>Infection tests</b>	<b>Structural tests</b>
Bacterial adhesion	<i>Biomaterial and peri-prosthetic tissue</i>
Bacterial growth	Crystal habit
Antibiotic resistance	Microhardness
Macrophage inhibition	Ion release
	Resorption kinetics

**Table 3: Quantitative analysis of biocompatibility.<sup>39</sup>**

#### Cytotoxicity assay:

The evaluation of a biomaterial's biocompatibility at the cellular and tissue levels is one of the primary requirements for its suitability for clinical use.<sup>40</sup> Cytotoxicity testing, which illustrates how cultured cells are exposed directly to the test material or to its extract, is the fundamental and required component of biocompatibility evaluation at early stages of drug development. The cytotoxicity assays are a quick in vitro techniques that assess the impact of drugs on cultured cells.<sup>41</sup> This assay is applied to evaluate and characterize the potentially harmful/toxic effect of the tested compound to the cells. They are low-cost methods that provides crucial details about biological characteristics of the substance, with a particular emphasis on its basic tolerability. Based on the concept that living cells have quantifiable intrinsic metabolic activities, cytotoxicity assays are designed to measure the toxicity of a sample. The reduction in cell viability due to drug exposure can be measured through various endpoints, including cell proliferation, membrane integrity, enzymatic activity, and mitochondrial function.<sup>42</sup>

One of the commonly employed cytotoxicity assays is the *MTT (3-(4,5-dimethylthiazol-2-yl)-2,5-diphenyltetrazolium bromide) assay*, which is a quantitative colorimetric method (George F et al.). The mechanism of MTT assay is briefly summarized in Figure 5.<sup>43</sup> MTT is a water-soluble tetrazolium salt that succinate dehydrogenase within the mitochondria cleaves to produce an insoluble purple formazan. Given that the cell membranes are impermeable to the formazan product, therefore it

accumulates in healthy cells. A solubilization solution, such as DMSO, acidic ethanol, or sodium dodecyl sulfate in diluted hydrochloric acid, is added to the insoluble formazan to dissolve it into a colored solution.<sup>44</sup> A spectrometer can be used to measure the absorbance of this colored solution, which is typically between 500 and 600 nm in wavelength. Light absorption varies depending on the solvent.

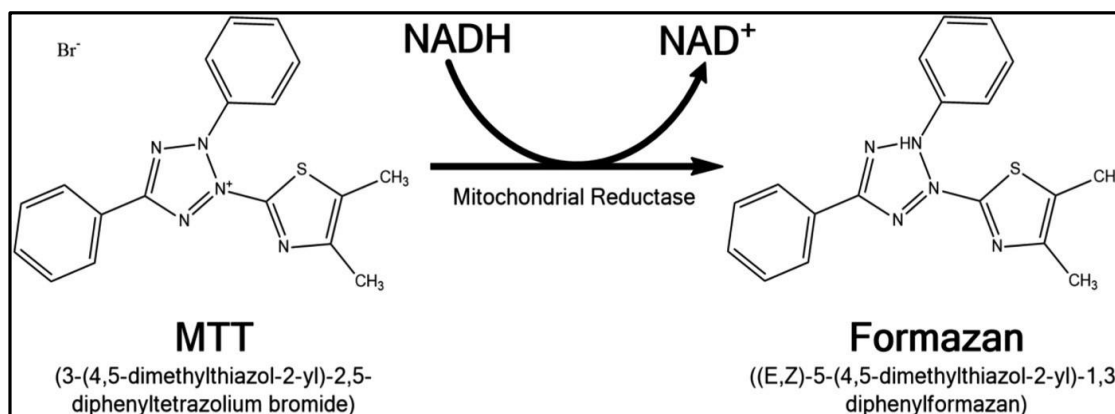


**Figure 5: Reduction of MTT (yellow) to formazan crystals (purple)<sup>43</sup>**

The *neutral red (NR) assay* is also one of the most used methods to determine the cytotoxic properties of compounds. Neutral red (3-amino-7-dimethylamini-2-methylphenazine hydrochloride) is a dye used to stain lysosomes. In this assay, the NR dye is incorporated and bound in the lysosomes of living cells.<sup>45</sup> The dye has a net charge close to zero at physiological pH, which allows it to pass through cell membranes. A proton gradient inside the lysosomes helps to keep the pH there lower than the cytoplasm. The dye becomes charged as a result and is kept in the lysosomes. The capacity of cells to incorporate neutral red decreases as they start to die. Loss of neutral red uptake therefore indicates a loss of cell viability.

#### Cell culture models:

The term "cell culture" refers to laboratory procedures that enable eukaryotic or prokaryotic cells to develop in physiological conditions, such as temperature, osmolality and pH.<sup>46</sup> It was first used in the early 20th century to research tissue growth, virus biology and vaccine, the function of genes in both health and disease, and the application of large-scale hybrid cell lines to manufacture biopharmaceuticals. By using isolated cells in vitro, cell culture assays are useful for determining the biocompatibility of substances or extracts.

In order to maintain the stability of particular phenotypes and behaviors over a period of time in culture, a population of cells is defined as a cell line.<sup>47</sup> The selection of a cell line for cell culture is largely influenced by the cell model's functional properties and specific readouts. Choosing a specific cell line is a crucial issue since the compound activity may be particular.<sup>48-50</sup> Cell lines can be finite or continuous. Cells cultured in the lab can be classified into three different types: primary cells, transformed cells, and self-renewing cells. Primary cells isolated directly from living animal or human tissues are typically referred to as "finite" and thus require a constant supply of stocks because their proliferation stops after a certain number of cell divisions and cell growth is frequently not possible.<sup>46</sup> On the other hand, an *immortalized or continuous cell line* has acquired the capacity to replicate itself indefinitely, either through genetic mutations or artificial modifications. The main advantage of using cell lines—a batch of clonal cells—for any applications, such as cytotoxicity testing, in vitro drug screening, and antineoplastic drug screening, is the consistency and reproducibility of the results.<sup>51</sup> Cell cultures have a tightly controlled physiological environment that can be continuously observed, as well as a highly controlled physicochemical environment (i.e., pH, temperature, osmotic pressure, oxygen, and carbon dioxide tension) that can be adjusted with extreme precision.

#### Caco-2 cells:

Various cell lines are used such as Caco-2, HeLa, HaCaT, L929, WI-38 cell lines as an in vitro biocompatibility model.<sup>52</sup> They are categorized mostly on the basis of the cell type they originated from. For example, L929 is a fibroblast cell line derived from a mouse, HeLa cells were isolated from a naturally occurring cervical cancer; HaCaT is a spontaneously immortalized keratinocyte cell line collected from adult human skin. In my research, *Caco-2 cell line* was used for the testing of the cytotoxicity of all PEGs derivatives.

The human epithelial cell line Caco-2 (**C**ancer **co**il-2) has been widely used as a model of the intestinal epithelial barrier.<sup>53</sup> These cells were established by Jorfen Fogh at the Sloan -Kettering Cancer Research Institute.<sup>54</sup> Caco-2 cells are immortalized lines of heterogenous epithelial adenocarcinoma cells isolated from the human colon.<sup>55</sup> The Caco-2 cells grow in culture media as an adherent monolayer of epithelial cells. As they approach confluence, they differentiate and polarize, acquiring a characteristic apical brush border with microvilli. Between adjacent cells, tight junctions develop and express enzymes that are typical of enterocytes. Differentiated Caco-2 cells expressed several morphological and functional properties of small bowel enterocytes. The differentiation of Caco-2 cells when cultured on the filter support is illustrated in Figure 6 and the properties of the Caco-2 cell monolayer are given in Table 4 .

Growth	Grows in culture as an adherent monolayer of epithelial cells
Differentiation	Takes 14–21 days after confluence under standard culture conditions
Cell morphology	Polarized cells with tight junctions and brush border at the apical side
Electrical parameters	High electrical resistance
Digestive enzymes	Expresses typical digestive enzymes, membrane peptidases and disaccharidases of the small intestine (lactase, aminopeptidase N, sucrase-isomaltase and dipeptidylpeptidase IV)
Active transport	Amino acids, sugars, vitamins, hormones
Membrane ionic transport	Na <sup>+</sup> /K <sup>+</sup> ATPase, H <sup>+</sup> /K <sup>+</sup> ATPase, Na <sup>+</sup> /H <sup>+</sup> exchange, Na <sup>+</sup> /K <sup>+</sup> /Cl <sup>-</sup> cotransport, apical Cl <sup>-</sup> channels
Membrane non-ionic transporters	Permeability glycoprotein (P-gp, multidrug resistance protein), multidrug resistance-associated protein, lung cancer-associated resistance protein
Receptors	Vitamin B12, vitamin D3, EGFR (epidermal growth factor receptor), sugar transporters (GLUT1, GLUT2, GLUT3, GLUT5, SGLT1)
Cytokine production	IL-6, IL-8, TNF $\alpha$ , TGF- $\beta$ 1, thymic stromal lymphopietin (TSLP), IL-15

**Table 4: Characteristics of Caco-2 cells**<sup>55</sup>

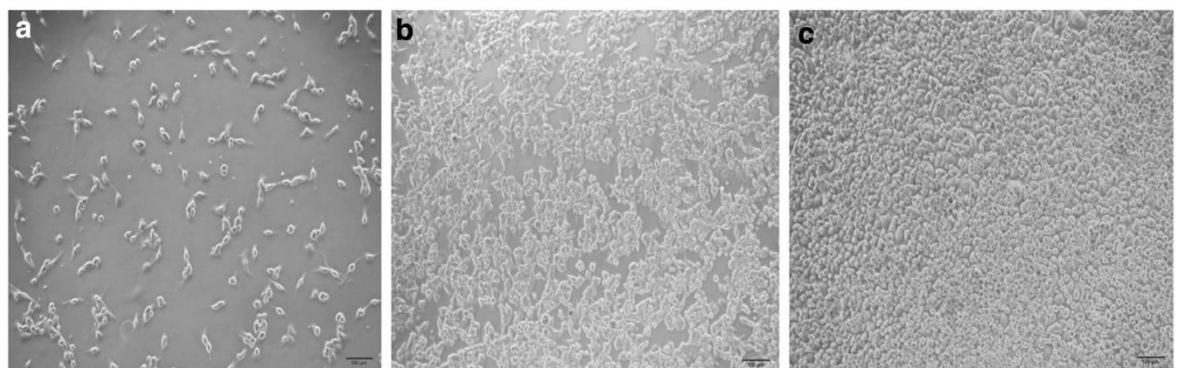


**Figure 6: Caco-2 cell morphology after seeding the 2nd; 7th day; and 21st day**<sup>56</sup>

### 5.3.1. *The biocompatibility of polyethylene glycols (PEGs)*

From those points mentioned above, drug safety profile is one of the essential factors in every stage of drug formulation. Biocompatibility is a critical factor in the development of biomedical materials, ensuring their safe and effective interaction with living systems. Polyethylene glycols (PEGs) is a versatile polymer that has gained significant attention in the field of biomedical research due to its remarkable biocompatibility properties.

PEGs' water solubility, low toxicity, and thermal stability make it a favorable choice for biomedical applications. Its flexible chain conformation allows for easy entanglement with other polymers and biomolecules, facilitating the formation of stable biocompatible coatings and hydrogels.<sup>7</sup> Furthermore, PEGs exhibit resistance to protein adsorption and fouling, reducing the risk of immune responses and enhancing its biocompatibility.<sup>57</sup>

One of the key factors determining PEGs' biocompatibility is its interaction with biological entities, such as proteins, cells, and tissues. PEGs' hydrophilic nature prevents nonspecific interactions with proteins, minimizing the risk of denaturation or aggregation. The formation of a hydrated PEGs layer on its surface, often referred to as the "brush" effect, acts as a steric barrier that repels proteins, preventing their adsorption and subsequent activation of immune responses.<sup>58</sup> The brush conformation of PEG polymers, which is illustrated in Figure 7, control the cellular interactions of nanocarrier.<sup>59</sup> A prerequisite for successful in vivo translation of nanomedicine to achieve long blood circulation and targeted delivery is that the nanocarriers exhibit a stealth behavior with inhibited uptake by phagocytic cells due to the brush conformation of PEGs.

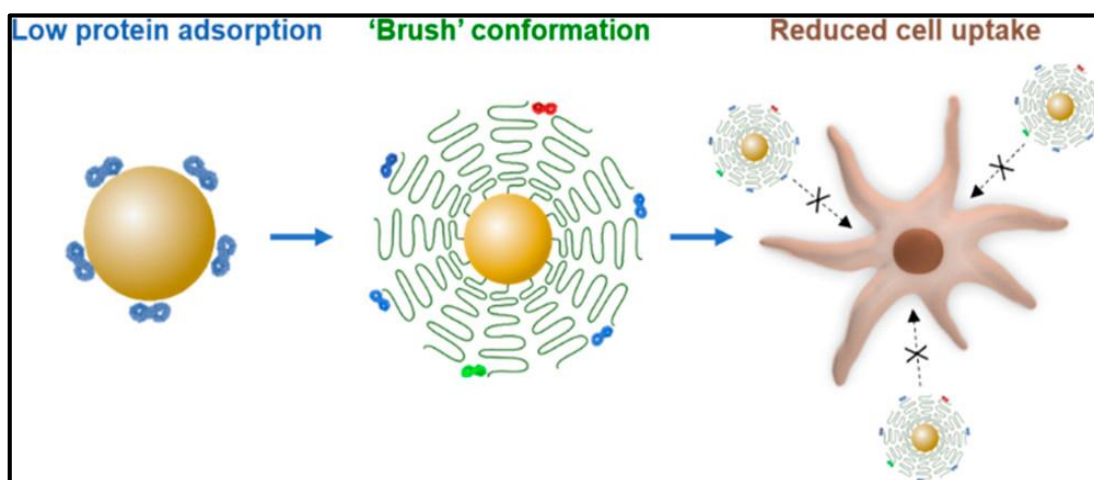


Figure 7: The brush conformation of PEGs<sup>59</sup>

### In vitro biocompatibility testing:

In vitro studies are essential for evaluating PEGs' compatibility with various cell types. These studies involve exposing cells to PEGs materials and assessing their viability, proliferation, and functionality. Common assays include the MTT assay, which measures cell metabolic activity, and the LDH release assay, which detects cellular membrane damage. Additionally, tests such as cell adhesion assays and morphological evaluations provide insights into cell-material interactions. Several studies have demonstrated PEGs's biocompatibility through in vitro testing. For example, Hinderer et al. (2015) evaluated the impact of PEGs-based hydrogels on neural stem cells, demonstrating their ability to support cell viability, proliferation, and differentiation.<sup>60</sup> Similarly, Wang et al. (2018) assessed the cytocompatibility of PEGs hydrogels with human mesenchymal stem cells, highlighting their favourable interactions and potential applications in tissue engineering.<sup>61</sup>

### Cytotoxicity evaluations:

Assessing PEGs' cytotoxicity is crucial for determining its impact on cellular viability and function. Various assays, such as the MTT assay, cell membrane integrity assays, and apoptosis assays, are employed to evaluate PEGs's cytotoxic effects. These tests help determine safe PEGS concentrations and exposure durations, ensuring minimal harm to cells and tissues. In a study by Lee et. al.(2000), the cytotoxicity of PEGs hydrogels was assessed using human dermal fibroblasts. The results indicated negligible cytotoxic effects, suggesting the suitability of PEGS hydrogels for tissue engineering applications.<sup>28</sup> Additionally, a study by Soppimath et. al. (2000) investigated the cytotoxicity of PEGs-modified nanoparticles.<sup>62</sup> The researchers examined the impact of PEGSylation on the biocompatibility of nanoparticles and assessed their cytotoxic effects on various cell lines. The study revealed that PEGSylation significantly reduced the cytotoxicity of nanoparticles, thereby enhancing their biocompatibility and potential for biomedical applications. The findings emphasized the importance of PEGS modification in improving the safety profile of nanoparticles and highlighted PEGS's role in minimizing adverse cellular responses.

In a separate study, PEGs 4000, PEGs 6000, PEGs 10000 demonstrated no cytotoxic effects on Caco-2 cells. However, PEGs 400 and PEGs 15000, both at 4 w/v%, exhibited considerable toxicity to the cells.<sup>63</sup> Another investigation by Parnaud et al. explored the cytotoxicity of PEGS 8000 on various cell lines, including human adenocarcinoma HT29 and COLO 205 cells, the human foetal mucosa FHC cells and Caco-2 cells.<sup>64</sup> Their

findings indicated that PEGs 8000 did not significantly induce toxicity on Caco-2 and FHC cells, however, it markedly inhibited the proliferation of HT29 and COLO205 cells. The researchers proposed that PEGS 8000 might possess a selectively cytostatic effect on proliferating cancer cells, potentially attributed to its high osmotic effect.

Overall, comprehensive biocompatibility testing is necessary to determine whether polyethylene glycols (PEGs) materials are appropriate for use in biomedical applications. The compatibility of PEGs with biological systems can be thoroughly investigated through in vitro and in vivo studies, cytotoxicity assessments, and immunological assessments. These testing procedures provide valuable insights into interactions of PEGs with cells and tissues, its potential impact on cellular viability and function, and its ability to elicit immunological responses. The studies reviewed above demonstrate the favourable biocompatibility of PEGs, highlighting its potential for applications such as tissue engineering scaffolds, implantable devices, and drug delivery systems. Due to its excellent biocompatibility properties, PEGs have become an attractive choice for use in medical and pharmaceutical applications. However, it is crucial to note that biocompatibility testing should be carried out thoroughly and with consideration for the specific application and intended use of PEGs-based materials.

#### In vivo biocompatibility testing:

In vivo studies are crucial for assessing PEGs' compatibility with living organisms and investigating its long-term effects. Animal models, ranging from small animals to non-human primates, are employed to evaluate PEGs' biocompatibility, tissue responses, and systemic effects. Implantation studies involve surgically inserting PEGS-based materials into animal models, followed by thorough analysis of tissue reactions, inflammation, and biodegradation. In a notable study by Hachim et al. (2020), the biocompatibility of PEGs-based nanoparticles was evaluated in a rat model.<sup>65</sup> The results indicated minimal inflammatory responses and favourable tissue integration, highlighting the potential of PEGs nanoparticles as drug delivery carriers. Similarly, in a study by Kim et al. (2007), PEGs-based hydrogels were implanted in a rabbit model, demonstrating favourable tissue responses and minimal adverse reactions.<sup>66</sup>

Despite their numerous advantages, there have been reports on the potential adverse effects of PEGs. In an animal experiment involving New Zealand white rabbits with open wounds, topically treating them with a PEGs-based antimicrobial cream resulted in elevated serum osmolality, hypercalcemia, and renal failure.<sup>67</sup> Additionally, a study on Cynomolgus monkeys (*Macaca fascicularis*) revealed kidney lesions, including

intratubular deposition of oxalate crystals, at an oral dose of 2.2 to 4.4 g/kg of PEGs 200 during a 13-week treatment.<sup>68</sup> Apart from animal studies, there is evidence indicating PEGs toxicity in humans. Three burned patients, treated with a PEGs-based burn cream (containing 63% PEGs 300, 5% PEGs 1000, 32% PEGs 4000, and approximately 0.01% ethylene glycol), experienced fatalities, with autopsy findings revealing tubular necrosis affecting the proximal tube.<sup>69</sup> This led to metabolic acidosis, an increase in serum calcium levels, renal failure, and cytotoxicity as the primary adverse effects associated with PEGs. The autopsy of the patients revealed tubular necrosis which affected the proximal tube. Metabolic acidosis increased the serum calcium level and renal osmotic pressure. In summary, the main adverse effects of PEGs included metabolic acidosis, the increase in serum calcium, renal failure and cytotoxicity.<sup>2,67-69</sup>

Long-term intravenous (i.v) injection studies in dogs reveal the polyethylene glycol have very low toxicity. Bao-qiu Li et.al. investigated the systemic toxicity and toxicokinetics of PEGs 400 i.v injection with high dose in dogs.<sup>70</sup> These 24 dogs were divided into 4 groups and received 4.23, 6.34, 8.45 g/kg of PEGs per day for 30 days with a control group treated with normal saline. In this study, dry mouth and dry nasal mucous membrane were commonly observed in PEGS-400 (8.45 and 6.34g/ kg) treated groups. The hematological and urine tests had no obvious abnormalities. There is no significant difference in the organs weights (liver, spleen, kidney and adrenal glands). The histopathological changes were detected only in kidney. PEGS-400 toxicokinetic parameters in dogs did not significantly differ between single and repeated doses. This study has shown that the toxicity of a high dose of PEGS-400 following repeated i.v injections is low, and alterations produced are reversible.<sup>70</sup>

## 5.4. Ketoprofen formulations and preparations

### 5.4.1. Characterization of ketoprofen

Ketoprofen (KT), which has chemical name that is 2-(3-benzoylphenyl)-propionic acid, belongs to a propionic acid group of a non-steroidal anti-inflammatory drug (NSAID).<sup>71,72</sup> There are 2 enantiomers of ketoprofen: (R)- and (S)-ketoprofen which is shown in Figure 8.<sup>73,74</sup> However, the S-isomer is the more potent one, compared to the R-isomer, multiple reviews, state, that the cheaper to manufacture racemic mixture is still more potent than several other NSAIDs.<sup>75,76</sup>

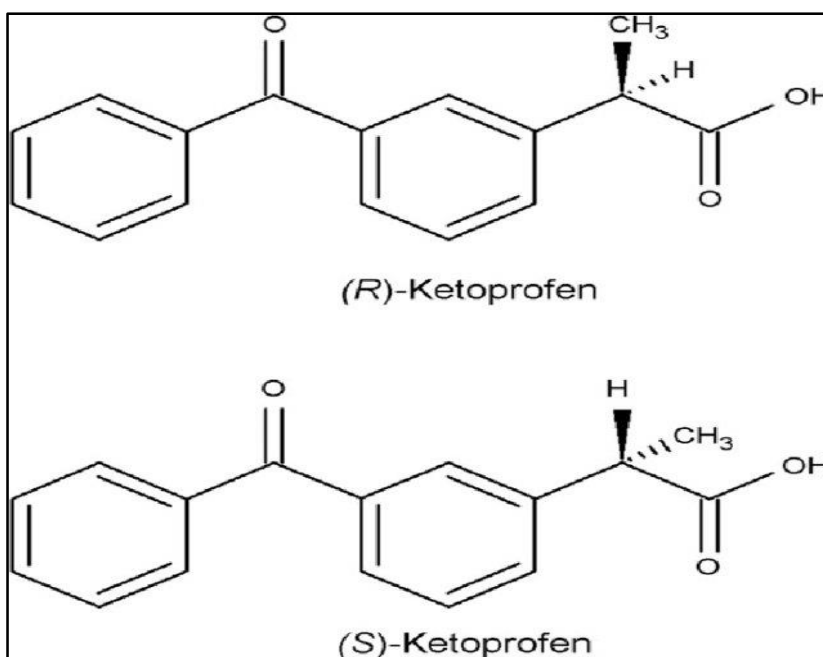


Figure 8: Molecular structures of (S)-and (R)-Ketoprofen <sup>73</sup>

It exists in white solid form, fine to granular powder with a molecular weight of 254.3 g/mol.<sup>77</sup> The molecular weight plays a significant role in determining the drug's pharmacokinetics, bioavailability, and interactions with target receptors. It influences parameters such as membrane permeability and distribution within the body. Ketoprofen can be melted around 94°C and has a boiling point at roughly 431.3°C.<sup>78</sup> Marketed since 1973, multiple clinical using KT can be listed, such as osteoarthritis, rheumatoid arthritis, gout, traumatic soft tissue injuries, low back pain, post-operative pain, headache, toothache and fever and is still widely consumed.<sup>71,79,80</sup>

The solubility of ketoprofen is an important characteristic that affects its dissolution rate, absorption, and bioavailability. The solubility of ketoprofen in water is 51 mg/L at 22°C which means that ketoprofen is practically insoluble in water.<sup>81,82</sup> However, it is

freely soluble in organic solvents such as ethanol, chloroform, acetone, and ether. In general, and because it contains a carboxylic acid group, KT dissolves more easily in polar protic solvents than polar aprotic or non-polar solvents.<sup>83</sup> This solubility profile is critical for formulation development, as it affects the choice of appropriate solvents, co-solvents, and surfactants to enhance drug solubility and bioavailability.

Lipophilicity refers to the affinity of a compound towards lipid-based environments. It is a crucial property that influences a drug's permeability across biological membrane, solubility distribution within the body and metabolic fate. Ketoprofen exhibits lipophilic properties, which play a crucial role in its absorption, distribution, and tissue penetration.<sup>84</sup> The lipophilicity of KT is attributed to its aromatic ring structure and the presence of a carboxylic acid moiety. The presence of these lipophilic moieties contributes to the compound's affinity for lipid-based environment. Lipophilicity is often characterized by the logarithm of the partition coefficient (log P). Ketoprofen has a log P value of 2.66 according to Andrzej's study, indicating its high affinity for lipid-rich environments.<sup>84</sup> This lipophilicity enables effective permeation across biological membranes, contributing to its therapeutic effectiveness. The pKa value of ketoprofen determines its acid-base properties and influences its solubility and stability in different pH environments. Ketoprofen exhibits a weak acidic character, with a pKa value of approximately 4.45 at 25 °C.<sup>85</sup> These properties are important in understanding its behavior in different physiological conditions, such as the gastrointestinal tract, where pH variations can affect drug dissolution and absorption. The physicochemical parameters of ketoprofen are summarized in the Table 5.

Physicochemical properties	Ketoprofen
<b>Molecular Formula</b>	C <sub>16</sub> H <sub>14</sub> O <sub>3</sub>
<b>Molecular Weight</b>	254.28 g/mol
<b>Melting point (T<sub>m</sub>)</b>	93-96 °C
<b>Boiling point (T<sub>b</sub>)</b>	460.5°C at 760 mmHg
<b>Solubility (S)</b>	51mg/L Practically insoluble in water Highly soluble in organic solvents (ethanol, methanol, dimethyl sulfoxide (DMSO))
<b>Log P (octanol/water partition coefficient)</b>	Appr. 3.8 moderate lipophilicity
<b>pKa</b>	4.42-4.69 Weakly acidic
<b>Elimination half-life (T<sub>1/2</sub>)</b>	2-5 hours

**Table 5: Summary of physicochemical properties of ketoprofen<sup>85</sup>**

The gastric absorption of pure ketoprofen powder is approximately 27%, but with an innovative proliposomal powder, this absorption can be enhanced to 37%.<sup>87</sup> However, it's crucial to note that absorption also takes place in significant amounts in the jejunum and colon. In these anatomical locations, pH dependence plays a crucial role, with pH 6.5 resulting in higher plasma levels of ketoprofen compared to pH 7.4.<sup>88</sup> The apparent permeation coefficient is also influenced by pH, reaching its maximum at the pKa value of the molecule, which is pH 4.45.<sup>89</sup>

#### **5.4.2. Effect of ketoprofen**

Ketoprofen is a NSAID drug that is commonly used for the treatment of pain, inflammation, and fever. Its pharmacokinetics refers to the way the drug is absorbed, distributed, metabolized and eliminated by the body. Ketoprofen can be administered orally, topically, or intravenously.<sup>90</sup> Ketoprofen is quickly and nearly completely absorbed when taken orally,<sup>91</sup> it is rapidly absorbed from the gastrointestinal (GI) tract.<sup>74</sup> The presence of food in the stomach may slightly delay its absorption. When applied topically, KT can penetrate the skin and reach underlying tissues. Once absorbed, ketoprofen is extensively distributed throughout the body. It has a high affinity for plasma proteins, mostly albumin. Ketoprofen undergoes hepatic metabolism, primarily through

glucuronidation and to a lesser extent through oxidation and reduction process. It is primarily metabolized to a glucuronide conjugate, which creates an unstable acyl-glucuronide. The drug and its metabolites are eliminated in the urine. The half-life time of ketoprofen is approximately 2-5 hours in healthy individuals. However, this can be prolonged in individuals with impaired renal or hepatic function.

Prescribed ketoprofen is used to relieve pain, tenderness, swelling, and stiffness caused by osteoarthritis and rheumatoid-arthritis. Non-prescribed ketoprofen is used to relieve minor aches and pain from headaches, menstrual periods, toothaches, common cold, muscle aches, back pain, and also to reduce fever. The mechanism of action of Ketoprofen, like other NSAIDs, is to reduce inflammation by inhibiting enzyme cyclooxygenase (COX).<sup>92</sup> These enzymes facilitate the conversion from arachidonic acid into prostanoids (thromboxanes, prostaglandins and prostacyclins), which play the main role in inflammatory reactions.

a. Mechanism of action:

Ketoprofen exerts its pharmacological effects primarily through the inhibition of cyclooxygenase (COX) enzymes, an enzyme responsible for the synthesis of prostaglandins and thromboxanes,<sup>93</sup> specifically COX-1 and COX-2. Ketoprofen works by inhibiting the production of certain chemicals in the body called prostaglandins. Prostaglandins are responsible for mediating pain, inflammation, and fever. COX-1 inhibition disrupts the production of prostaglandins involved in maintaining physiological functions, such as gastric mucosal integrity and renal blood flow.<sup>94,95</sup> On the other hand, COX-2 inhibition reduces the synthesis of prostaglandins associated with pain, inflammation, and fever. Ketoprofen's anti-inflammatory actions arise from the inhibition of COX-2, while its analgesic effects are attributed to modulation of peripheral and central pain pathways. Based on the mechanism of action of the drug, ketoprofen is used for these therapeutic applications below.<sup>72</sup>

b. Application of ketoprofen:

- **Pain Management:**

Ketoprofen is widely utilized in the management of various pain conditions, including musculoskeletal pain, osteoarthritis, and postoperative pain. Its analgesic effects stem from both peripheral and central mechanisms.<sup>96</sup> Ketoprofen attenuates the production of inflammatory mediators at the site of injury and modulates pain transmission in the central nervous system, providing effective pain relief in acute and chronic pain scenarios.

- **Inflammatory Disorders:**

Due to its potent anti-inflammatory properties, ketoprofen is frequently employed in the treatment of inflammatory disorders, such as rheumatoid arthritis, ankylosing spondylitis, and gout.<sup>97</sup> By inhibiting COX-2, ketoprofen reduces the production of prostaglandins responsible for the inflammatory response, thus alleviating pain, swelling, and joint stiffness associated with these conditions.

- **Fever Reduction:**

Ketoprofen's antipyretic effects result from its ability to inhibit prostaglandin synthesis in the hypothalamus, which plays a pivotal role in regulating body temperature.<sup>98</sup> By blocking the production of pyrogen-induced prostaglandins, ketoprofen effectively reduces fever in various infectious and non-infectious febrile conditions.

In short, ketoprofen is a nonsteroidal anti-inflammatory drug (NSAID). By blocking the production of prostaglandins, ketoprofen helps to reduce pain, swelling, and inflammation.<sup>72,74,90,93</sup> This medication is commonly used to relieve symptoms associated with various conditions, including rheumatoid arthritis, osteoarthritis, ankylosing spondylitis, gout, menstrual cramps, and musculoskeletal injuries such as sprains and strains. It is available in various formulations, including oral tablets, capsules, extended-release capsules, and topical gels. As with any medication, ketoprofen may cause side effects. Common side effects include gastrointestinal disturbances such as stomach pain, heartburn, and nausea. It can also cause dizziness, headache, rash, and fluid retention. In rare cases, ketoprofen may lead to more serious side effects, such as gastrointestinal bleeding, liver or kidney problems, and allergic reactions. This medication should not be used by individuals who have a history of allergic reactions to NSAIDs, aspirin, or other similar medications.

#### ***5.4.3. Increase of solubility and permeability in pharmaceutical formulations***

As solubility and permeability play a critical role in determining the bioavailability, drugs are classified into 4 main categories as the Biopharmaceutics drug Classification System (BCS classification).<sup>99</sup> The BCS is a system that categorizes a drug (API) based on aqueous solubility and permeability across intestinal membrane properties which is classified into four classes which include (Figure 9)<sup>100,101</sup>

- Class I: high solubility (S), high permeability (P)
- Class II: low S, high P
- Class II: high S, low P

- Class IV: low S, low P

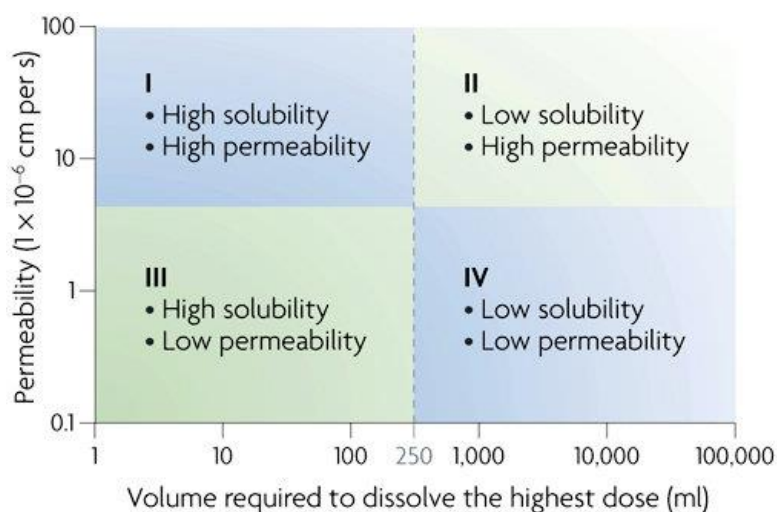


**Figure 9: Biopharmaceutics drug classification system (BCS) <sup>101</sup>**

For the selection and design of the formulation of any drug substance, this is a useful tool for formulation scientists. The most recent advancements have also made it possible for us to predict the solubility and permeability properties of the drug molecule in the early stages of development, allowing us to make the necessary changes to the drug molecules to optimize the pharmacokinetic parameters. The BCS guidance considers three main factors, dissolution, solubility, and intestinal permeability, which influence the rate and degree of drug absorption from immediate release solid dosage forms. The concept of BCS provides a better understanding of the relationship between drug release from the product and the absorption process. The creation of efficient drug formulations presents many difficulties in the field of pharmaceutical sciences, especially when dealing with poorly soluble drugs. Poor solubility and limited permeability significantly hinder the successful delivery of therapeutic compounds. Therefore, addressing solubility and permeability issues is crucial for improving drug bioavailability, therapeutic effectiveness, and patient outcomes.

The solubility of a drug refers to its ability to dissolve in a solvent, such as water, and form a homogeneous solution.<sup>102</sup> Poorly soluble drugs, characterized by low aqueous solubility, often exhibit slow dissolution rates and reduced bioavailability. Consequently, their therapeutic effectiveness is compromised, leading to inefficient treatment outcomes. By improving drug solubility, the delivery of the drugs can be improved. Various techniques have been employed to enhance drug solubility, including particle size

reduction, solid dispersion formation, and complexation.<sup>103</sup> Nanosizing techniques, such as high-pressure homogenization and media milling, reduce drug particle size to the sub-micron range, thereby increasing the surface area available for dissolution. Solid dispersions, obtained through methods like melt extrusion and spray drying, involve dispersing the drug in a hydrophilic carrier matrix, promoting its solubility and dissolution rate.<sup>105</sup> Complexation techniques, such as cyclodextrin inclusion complexes, utilize host-guest interactions to enhance solubility and stability.<sup>106</sup>

The United States Pharmacopoeia (USP) and British Pharmacopoeia (BP) have categorized the solubility classes provided in Table 6 based on the parts of solvent required for the solute to dissolve.<sup>107,108</sup> According to ICH M9 guideline, if the highest dose of a drug compound must be completely soluble in 250 mL or less of aqueous media with a pH range of 1.2 to 6.8 at 37.1 °C, that drug can be classified as highly soluble compound (ICH 2019).<sup>109,110</sup>

Descriptive term (Solubility definition)	Parts of solvent required for one part if solute	Solubility (mg/mL) range
Very soluble (vs)	$\leq 1$	$\geq 1000$
Freely soluble (fs)	1 – 10	100 – 1000
Soluble (s)	10 - 30	33 - 100
Sparingly soluble (sps)	30 - 100	10 - 33
Slightly soluble (s)	100 - 1000	1 - 10
Very slightly soluble (vss)	1000 - 10000	0.1 - 1
Practically insoluble (pi), or insoluble	$\geq 1000$	$\leq 0.1$

**Table 6: Solubility criteria according to USP**

Drug **permeability** is a term used to describe the ability of a drug to cross through biological barriers and reach its target. Permeability is an important factor in drug delivery as poor membrane permeability leads to poor or non-existent efficacy or therapeutic response.<sup>111</sup> The therapeutic efficacy of drugs with poor permeation is often constrained by difficulties in achieving sufficient systemic absorption. Therefore, improving drug permeability is crucial for ensuring efficient drug delivery and optimizing therapeutic results. Advancements in drug permeability enhancement strategies have revolutionized

pharmaceutical research. Promising results have been obtained using methods like prodrug design, formulation strategies using permeation enhancers, and the use of nanotechnology. Prodrug design involves chemically modifying the drug to enhance its lipophilicity or exploit specific transporter systems, facilitating better absorption through biological barriers.<sup>112</sup> Formulation approaches incorporating permeation enhancers, such as surfactants or penetration enhancers, improve drug permeability by altering the physicochemical properties of the drug or the epithelial membrane.<sup>113</sup> Nanotechnology-based formulations, such as lipid-based nanocarriers or nanoemulsions, provide unique opportunities to enhance drug permeability through improved solubilization, cellular uptake, and targeting capabilities.<sup>114</sup>

More than 70% of medications are reported to be poorly soluble and belong to BCS classes II and IV.<sup>115</sup> Therefore, improving the solubility and permeability of poorly soluble/permeable drugs is necessary to increase the drugs' bioavailability. Several methods have been used to increase the bioavailability of substances which include.<sup>99,115-118</sup>

1. Physical methods: Particle size reduction (micronization, milling and nanonization, high pressure homogenization) and engineered particle size control (cryogenic spray process, crystal engineering)

2. Chemical methods: Changes in pH of the solvent, use of buffers and permeation enhancers, salt formation, derivatization and complexation.

3. Formulation development: Nanoparticles (nanosuspensions, nanoemulsions, nanocrystals, polymeric nanoparticles and others), micelles, solid dispersions, lipid based drug delivery systems (self-emulsifying drug delivery systems (SEDD), solid lipid nanoparticles (SLNs), liposomes, microemulsions), liquid solid techniques, and targeted therapy (surface modified drug delivery systems).

4. Miscellaneous methods: Super critical fluid process, use of adjuvants such as surfactants, solubilizers, cyclodextrins, co-solvents, and novel excipients.

The technologies to improve the bioavailability of drugs are summarized in Figure 10.

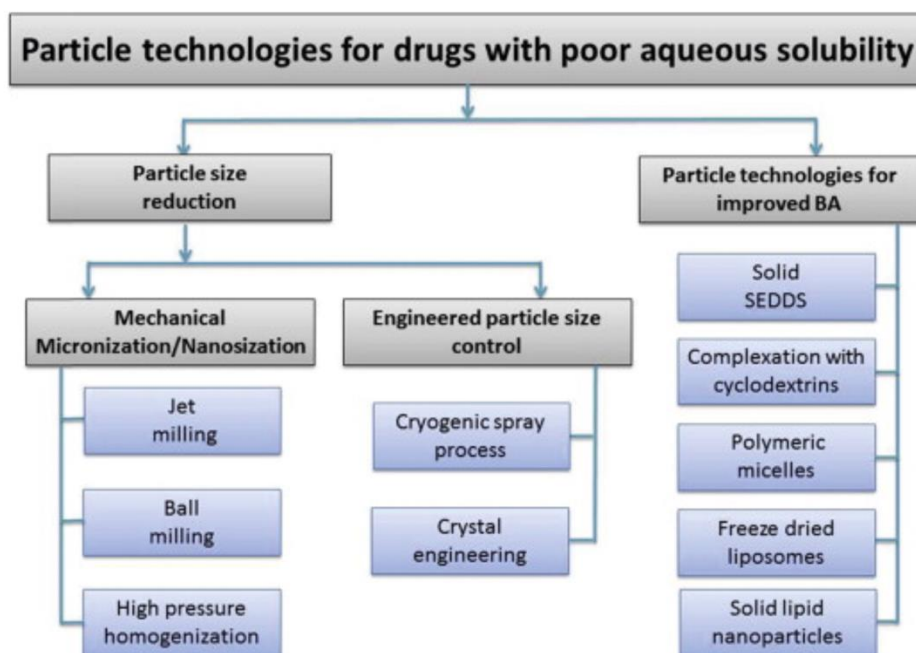


**Figure 10: Pharmaceutical particle technologies for improved solubility, dissolution, and bioavailability of drugs.** <sup>119</sup>

Overall, the enhancement of solubility and permeability for poorly soluble drugs holds tremendous significance in the field of pharmaceutical research and development. The ongoing advancements in academic research have paved the way for innovative strategies to overcome the challenges associated with these drugs, ultimately resulting in improved drug bioavailability, enhanced therapeutic efficacy, and optimizing the potential of pharmaceutical products for better patient outcomes. The continuous exploration of novel approaches, the understanding of underlying mechanisms, and the development of innovative formulations are critical for overcoming solubility and permeability challenges.

#### **5.4.4. New formulations of Ketoprofen**

As a widely used and easy to detect model API, multiple publications can be found about the enhanced oral delivery of ketoprofen, in form of liquid self-nanoemulsifying drug delivery systems, “nanoscale” milled powders or salification.<sup>120–122</sup>

One strategy to enhance the advantages of ketoprofen is to improve its bioavailability, thereby increasing its therapeutic effectiveness. Various formulation approaches have been investigated to achieve the goal. For instance, to improve the solubility and dissolution of KT, Revika et al prepared KT with chitosan polymer and

cross linker tripolyphosphate (TPP) for particles formulation by emulsification ionic gelation.<sup>123</sup> The water solubility of KT-chitosan increased 2.71-fold compared to pure KT. The dissolution of this new compound was elevated in both simulated gastric and intestinal fluid without enzyme which were 1.9-fold and 1.2-fold, respectively. Another investigation was carried out by Sunita et al. to overcome the poor solubility of KT in order to form co-crystal using fumaric acid (FA) as a cofomer.<sup>124</sup> The result from this study showed that the solubility and dissolution rate of this formulation significantly improved. The solubility of the co-crystal compound was increased apprx. 3-4 times compared to the pure KT. The KT released from pure drug solution is only 23.5% while from different batches of KT-FA cocrystals is 62.21-83.68%.

Additionally, solid lipid nanoparticles (SLNs) have demonstrated promising results in enhancing the bioavailability of KT. As a lipid and surfactant, stearic acid and Tween 80 were used in the study by Swati et al. to prepare KT SLNs using the microwave method. Besides, the nanoparticles provide a platform for targeted drug delivery, enabling the selective delivery of KT to specific tissues or cells. Also aiming to increase the solubility and bioavailability of KT, Kiranmai et al. developed silver nanoparticles loaded with KT (Ag-KT).<sup>125</sup> Ag-KT was prepared by the solvent evaporation method using  $\beta$ -cyclodextrin polymer as a capping agent. The optimized formulation exhibited high drug entrapment efficiency (~93%) and showed the amount of released drug as 94.3% compared to the marketed formulation which was 84.6%. In another research, KT-loaded chitosan-chondroitin sulfate (CHS-CS) nanoparticles were formulated via coacervation method by electrostatic interaction.<sup>126</sup> Emulgel was prepared by mixing the nanoparticles into HPMC gel which serves as viscosity agent and then argan oil was added. This work successfully achieved the transdermal delivery of KT enhancement. Comparisons were made between commercial gel and nanoparticle-loaded emulgel with and without argan oil in terms of steady-state flux ( $J_{ss}$ ), permeability coefficient ( $K_p$ ), and enhancement ratio (ER).  $J_{ss}$  for argan oil emulgel was highest and  $J_{ss}$  of nanoparticles was greater as compared to commercial gel. According to ER, drug permeability was increased by nanoparticles by 1.92 times compared to commercial gel. The formulation's ER increased to 2.49 when argan oil was included.

Novel formulations have shown great potential in enhancing the advantages of ketoprofen by improving bioavailability, enabling targeted drug delivery, and reducing adverse effects. The utilization of nanostructured lipid carriers, solid lipid nanoparticles, polymeric nanoparticles, liposomes, and prodrugs has demonstrated promising results in

maximizing the therapeutic benefits of ketoprofen while minimizing its associated limitations. Continued research and development in this field hold great promise for the optimization of ketoprofen therapy. These advancements have the potential to significantly improve patient outcomes and provide safer and more effective treatment options.<sup>127</sup> SLNs demonstrated an efficiency of 74.8% in entrapment. A 40-fold increase in solubility was noted.

#### ***5.4.5. Solid dispersion introduction***

The solubility is an important factor for drug release which is an essential and limiting step for oral drug bioavailability. The poor solubility and low dissolution rate of poorly water-soluble drugs in the gastro intestinal fluid often lead to an insufficient efficacy. For that reason, the solubility enhancement is possible to increase the drugs dissolution rate, the drugs absorption, and the drug bioavailability. It is estimated that most compounds undergoing development at the present time are subjected to poor bioavailability of these compounds.<sup>128</sup> The low solubility of the drugs which leads to low dissolution rate is the biggest obstacle in the performance of poorly water-soluble (PWS) drugs. The solubilization behavior of the drug is the key determinant for the oral bioavailability determination. To solve this problem, various strategies for solubilization enhancement have been developed such as nanoparticle<sup>129</sup>, inclusion complex<sup>130</sup>, lipid formulation<sup>131</sup>, salt formation<sup>132</sup> and solid dispersion<sup>133</sup>.

##### **5.4.5.1. Solid dispersion characterization:**

Among these strategies, solid dispersion is a well-known method for improvement in the solubility, dissolution rate and bioavailability of poorly water-soluble drugs. Solid dispersion is defined as dispersion of one or more active ingredients (hydrophobic) in an inert carrier matrix (hydrophilic) at in the solid state.<sup>134</sup> The overview of solid dispersion compositions is illustrated in Figure 11. Although solid dispersion are mostly binary systems of an API in a carrier, but ternary or multicomponent systems have also been recorded.<sup>135</sup>

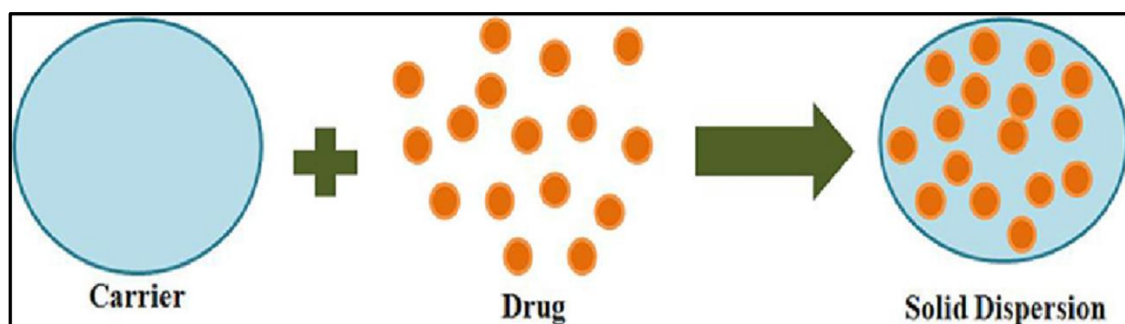


**Figure 11: Components of solid dispersion system** <sup>136</sup>

Since their first mention in 1961, numerous studies have investigated the potential use of solid dispersions<sup>137</sup>. Amorphous solid dispersions (SD) are made from a BCS class II or IV API dispersed into a carrier matrix (usually a hydrophilic polymer). During the manufacturing process, the crystalline API undergoes a phase transition into an amorphous form through solvent evaporation or hot melt extrusion or spray drying to name some more common formulation methods.<sup>138,139</sup> The higher free energy of the amorphous drug and the nanosized particles greatly enhances the poor water solubility of the substance in gastric or intestinal fluids. The carriers can either be amorphous ones like PVP or HPMC, semi-crystalline ones like PEGs or rarely crystalline ones like different sugars.<sup>135,140</sup> It was noted for the hot melt extrusion method that upon cooling, both the crystallization parameters of the API can be influenced by the polymers and the API can influence the properties of the polymer as well.<sup>141,142</sup> Moreover, the bioavailability can be further improved with the addition of surfactants, to the dispersion as well.<sup>143</sup> Even for simple systems, like irbesartan-HPMC, the physical mixture of the two substances caused a sevenfold solubility increase, while the SD a fifteen-fold one.<sup>144</sup> A cyclosporine A-polyoxyethylene (40) stearate system showed ~10% dissolution for pure API, ~60% in case of the physical mixture and over 90% for the solid dispersion.<sup>145</sup>

#### Role of solid dispersion in improving oral absorption:

Solid dispersion shows many mechanisms to become one of the promising techniques for the low solubility drugs. The polymer is dissolved and the drug is released from the SD when exposing in the aqueous media, the drug particle size is reduced as the form of fine particles or colloids.<sup>146</sup> This results in surface area improvement and so with consequence increasing in high dissolution rate of poorly soluble drug. Particles in SD are found to have high porosity which helps to speed up the drug release. The drug

wettability increasing is shown in solid dispersion with or without surface active of the carrier, which can enhance the solubility of the drug. The degree of wettability is higher when surface active carrier or surfactant is added in. The poorly water-soluble crystalline drugs present in amorphous form obtained higher solubility because no energy is required to break up the crystal lattice during the dissolution. Hence, the drug release enhancement can be achieved. In summary, the underlying mechanisms for improvement of the bioavailability of poorly water soluble (PWS) drug by SD technique are<sup>147</sup>:

- Reduce particle size
- Particles with high porosity
- Wettability and dispersibility improvement
- Drug in amorphous state

Understanding the thermodynamics of the solubilization process requires the application of Gibbs free energy of transfer in phase solubility studies. According to Hussain et al., the Gibbs free energy change ( $\Delta G$ ) indicates whether the reaction conditions are favorable or unfavorable for drug solubilization in the carrier.<sup>148</sup> A negative Gibbs free energy ( $\Delta G$ ) indicates spontaneous of the drug solubilization, implying that the solute is more likely to dissolve in the solvent.

Numerous kinetic models have been suggested to describe the overall drug release from dosage forms. Three groups can be distinguished from the approaches applied to investigate the kinetics of drug release:

- Statistical methods (exploratory data analysis method, repeated measures design, multivariate approach [MANOVA: multivariate analysis of variance]<sup>149,150</sup>)
- Model dependent methods

Model dependent methods are based on different mathematical functions, which describe the dissolution profile. After choosing an appropriate function, the dissolution profiles are evaluated depending on the derived model parameters.<sup>149,151</sup>

The in vitro release data were fitted into various release kinetic models, such as first order, zero order, Higuchi, and Korsmeyer and Peppas models, to analyze the mechanism of drug release from the selected formula; the model with the highest correlation coefficient ( $R^2$ ) was considered to be the best model.<sup>152</sup> In vitro drug release data were fitted to some popular models as follows in Table 7.<sup>153</sup>

Model	Equation
Zero order [5]	$Q_t = Q_0 + K_0 t$
First order [5]	$\ln Q_t = \ln Q_0 + K_1 t$
Higuchi [16]	$Q_t = K_H t^{1/2}$
Hixson–Crowell [17]	$Q_0^{1/3} - Q_t^{1/3} = K_S t$
Korsmeyer–Peppas [21]	$Q_t/Q_\infty = K_k t^n$
Weibull Model [22]	$m = 1 - \exp\left[-\frac{(t-T_j)^b}{a}\right]$

where

$Q_t$ : Amount of drug released in time  $t$ ,  
 $Q_0$ : Initial amount of drug in tablet,  
 $Q_t/Q_\infty$ : Fraction of drug released at time  $t$ ,  
 $m$ : The accumulated fraction of the drug in solution at time  $t$   
 $a$ : Scale parameter,  
 $T_j$ : The location parameter,  
 $b$ : The shape parameter,  
 $K_0, K_1, K_H, K_S, K_k$ : Rate order constants.

**Table 7: Mathematical models for comparison of dissolution profiles** <sup>153</sup>

- Model independent methods

Model independent methods using difference factor (f1) and similarity factor (f2).<sup>154,155</sup>

A simple model independent approach compares dissolution profiles using a difference factor (f1) and a similarity factor (f2). The difference factor (f1) calculates the percent difference between the two curves at each time point and measures the relative error between the two curves. It is expressed by the following formula:

$$f1 = \frac{\sum_{j=1}^n |R_j - T_j|}{\sum_{j=1}^n R_j} \times 100 \quad (1)$$

where f1 is the difference factor (relative errors between the two curves), n is the sampling number,  $R_j$  and  $T_j$  are the percent of the dissolved API from the two compared preparations at time point  $j$ .

The similarity factor (f2) is a logarithmic reciprocal square root transformation of the sum of squared error and is a measurement of the similarity in the percent dissolution between the two curves.

$$f2 = 50 \times \log \left\{ \left[ 1 + (1/n) \sum_{j=1}^n w_j |R_j - T_j|^2 \right]^{-0.5} \times 100 \right\} \quad (2)$$

where  $f_2$  is the similarity factor (the logarithmic reciprocal square root transformation of the sum of squared error is a similarity factor which provides percentage dissolution between the two curves) and  $w_j$  is an optional weight factor which was 1 in our experiment.

It is suggested to compare pairwise dissolution profiles using the two factors,  $f_1$  and  $f_2$ . It is possible to calculate the degree of similarity between pairs of dissolution profiles based on  $f_1$  and  $f_2$ . According to guidelines of Food and Drug Administration (FDA), range of  $f_1$ ,  $f_2$  should be  $0 < f_1 < 15$  and  $50 < f_2 < 100$ . When three to four or more dissolution time points are available, this model independent method is best suited for comparing dissolution profiles.

#### **5.4.5.2. Solid dispersion classification**

There are several ways to categorize solid dispersions. Depending on the physical state of carrier, solid dispersions can be divided into 3 main categories:

- Amorphous SD
- Semi-crystalline SD
- Crystalline SD

Solid dispersions may also be classified into 4 generation based on the recent advancement as the following.<sup>156</sup>

1. First generation solid dispersion
2. Second generation solid dispersion
3. Third generation solid dispersion
4. Fourth generation solid dispersion

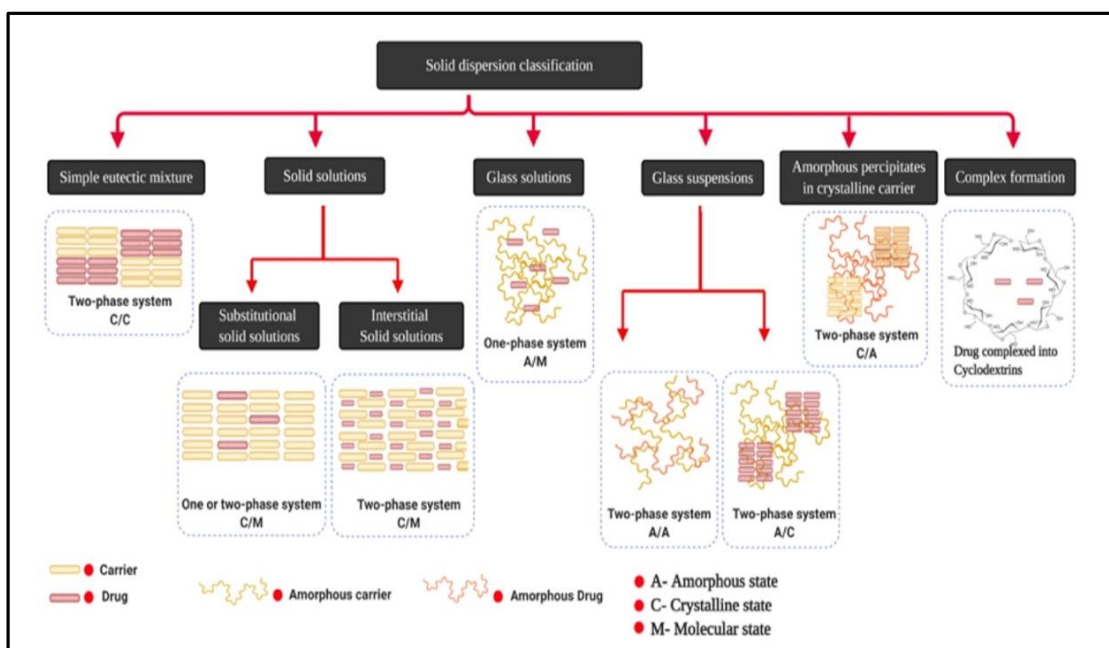


**Figure 12: Classification of solid dispersions** <sup>156</sup>

The SDs are also classified into 6 types according to the molecular arrangement of the resulting mixture (physical states of carriers and incorporated drugs) (shown in Figure 12) including <sup>156</sup>

- Simple eutectic mixtures:
- Solid solution:
- Glass suspension/glass solution:
- Amorphous precipitations:
- Complex or new compound formation

#### 5.4.5.3. Carrier

Carrier is an inactive substance that acts as a vehicle for an active substance, or we can say that by incorporating the carrier to any PWS medicament, solubility may be enhanced. The features of the carrier have a reflective impact on the dissolution properties of the medicament which is dispersed. Table 3 demonstrates different classes of carriers which are used in solid dispersion. A carrier should meet the following prerequisites for the improvement of the dissolution rate of a API

- Be freely water-soluble
- Nontoxic and pharmacologically inert
- Heat stability for the melt method with low melting point

- Solubility in a diversity of solvents
- Economical to process
- Chemical compatibility with the medicament
- Should not form strongly bonded complexes with the medicament

Notably, the carrier is an important factor in any kind of solid dispersion. We can say that the solubility of the poor water-soluble drugs is improved by incorporating the carrier. The features of the carrier have a reflective effect on the dissolution properties of the drug dispersed. A carrier should meet some requirements to be considered to the drug dispersed. A carrier should meet some requirements to be considered to formulate SD with a drug. Carriers used in SD method are listed in Table 8.<sup>156,157</sup>

Type of Carrier	Carrier Examples
Acids	Citric acid, Tartaric acid, Succinic acid, Phosphoric acid
Sugars	Dextrose, Mannitol, Sorbitol, Sucrose, Maltose, Galactose, Xylitol, Lactose, Soluble Starch, Chitosan, Galactomannan, British Gum, Amylodextrins
Polymer material	PVP, PEG4000, PEG6000, Methylcellulose, CMC, HPC, Xanthan Gum, Guar Gum, Sodium Alginate, MC, HPMC, Dextrin, $\beta$ -CD, HP $\beta$ -CD, Eudragit® L100 sodium salts
Surfactant	Polyethylene Stearate, Poloxamer, Deoxycholic acid, Tween and Spans, docusate sodium, Myrj-52, Pluronic F68, SLS, Vitamine E, Gelucire 44/14
Miscellaneous	Pentaerythritol, Urea, Urethane, Hydroxyalkyl xanthenes

**Table 8: Different class of carriers used in solid dispersion method**<sup>146,157</sup>

#### **5.4.5.4. Solid dispersion preparation**

There are various techniques used to prepare solid dispersion which are shown in Figure 13. These methods are presented as the following. To select correct method, the characteristics of the API, the carriers or the excipient should be evaluated carefully because each method have its own advantages and disadvantages.

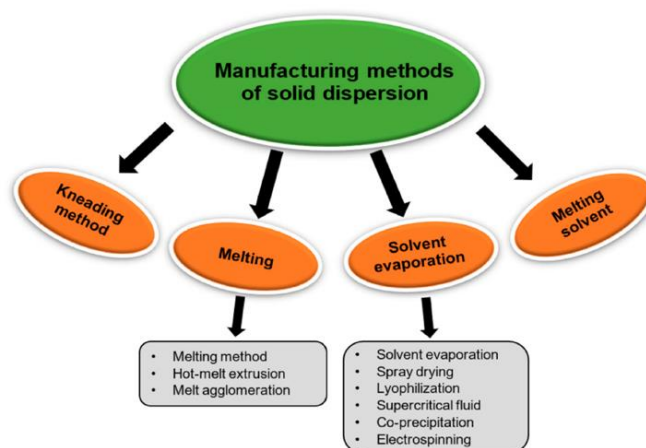


**Figure 13: Techniques for solid dispersion preparation** <sup>158</sup>

There are various techniques used to prepare solid dispersion. These methods are presented below.

- Melting Method (Fusion method)
- Solvent evaporation method (Solvent method)
- Melting solvent method: (Hybrid method)
- Hot melt extrusion method
- Melt agglomeration
- Freeze-Drying method
- Electrospinning method
- Supercritical fluid (SCF) technology
- Kneading method

#### **5.4.5.5. Application and dosage form development of solid dispersion**

There are some commercially available SD-based products. These products are listed in Table 9 along with their manufacturers, brand names, and carriers for preparation.

<b>Drug</b>	<b>Brand name</b>	<b>Carrier used</b>	<b>Manufacturer</b>
Griseofulvin	Gris-PEG <sup>®</sup>	Polyethyleneglycol	Novartis Pharmaceuticals, Switzerland
Nabilone	Cesamet <sup>®</sup>	Polyvinylpyrrolidone	Eli Lilly & Company, USA
Itraconazole	Sporanox <sup>®</sup>	HPMC, PEG 20,000	Janssen Pharmaceutica, Belgium
Nifedipine	Afeditab <sup>®</sup>	HPMC	Elan corporation, USA
Fenofibrate	Fenoglide <sup>®</sup>	Polyethyleneglycol	LifeCycle Pharma, USA
Everolimus	Certican <sup>®</sup>	HPMC	Novartis Pharmaceuticals, Switzerland
Lopinavir /Ritonavir	Kaletra <sup>®</sup>	Polyvinylpyrrolidone /vinylacetate matrix	Abbott laboratories, USA

**Table 9: Market products with solid dispersion<sup>159</sup>**

Besides, various researches were reported that applied the SD technique to improving the disadvantages of many poorly soluble APIs. Jia Cao et.al enhanced the water solubility of Magnolol (MAG).<sup>160</sup> The SD was prepared using hydroxypropyl methylcellulose succinic acid as a carrier via antisolvent coprecipitation. The MAG SD investigation was shown the improvement of the dissolution rate and the bioavailability compared to MAG alone. In another research, curcumin was formulated with hydroxypropyl methylcellulose (HPMC) with ratio 20:80 to produce solid dispersion.<sup>161</sup> The water solubility of curcumin was increased to 238 µg/mL and the encapsulation efficiency was over 93% for all SDs. Meloxicam is also a target to improve its poor solubility and slow onset of action because delayed gastric motility.<sup>162</sup> To enable rapid oral absorption of Meloxicam in patients with severe pain, Hiroki et al. developed an amorphous SD of the drug HPMC and polymethacrylates and polyacrylates. The AUC<sub>0-4</sub> was observed on rats which were orally administered by the amorphous SD and the drugs alone. The result was shown that there were 9-fold increase of AUC<sub>0-4</sub> (area under the drug concentration-time curve )for the SDs compared with crystalline Meloxicam. Deepa Pathak et al. aimed to increase the dissolution properties of Meloxicam by formulating Meloxicam SD with hydroxyethyl cellulose, mannitol and PEG 4000 for geriatric population.<sup>163</sup> Solid dispersions showed greater in vitro dissolution than their corresponding physical mixtures and the pure drug. The highest drug release was seen

with PEGS 4000 in a 1: 9 drug to carrier ratio (100.2%), followed by mannitol (98.2%) and HEC (89.5%) in the same ratio. The in vitro dissolution studies of SD of NSAID piroxicam drug in PEG 4000 and in urea gave faster dissolution than the corresponding simple mixtures.<sup>164</sup> R.N.Pan et. al. prepared these SD systems by fusion and solvent methods, respectively. These dispersion systems provided statistically significant to a higher extent and rate of bioavailability than the corresponding physical mixture, according to a single-dose study with rabbits. Using spray-drying techniques and cycloamylose as the solubilizing agent at a weight ratio of 1:1, Hyung Hee Baek et al developed a novel ibuprofen-loaded solid dispersion with enhanced bioavailability.<sup>165</sup> Drug solubility was increased by about 14 times with this ibuprofen-loaded SD. Additionally, the dispersion demonstrated a 2-fold higher AUC value in comparison to an ibuprofen powder, indicating that it enhanced the oral bioavailability of ibuprofen in rats. Indomethacin (IND), a poorly water-soluble drug, and polyoxyethylene 32 distearate (POED), a novel surfactant polymer, were combined in a solid dispersion preparation that was studied using the melting method.<sup>166</sup> Studies on in vitro dissolution revealed that the formation of solid dispersion significantly increased IND release (5.5–12 times faster).

Poorly water-soluble drugs present a significant challenge to the pharmaceutical industry because their rate of dissolution affects both their bioavailability and therapeutic effectiveness. Solid dispersion techniques have the potential to significantly increase the bioavailability and dissolution rate of drug with poor water solubility, such as NSAIDs. The case studies above demonstrated how solid dispersion can effectively increase the rate at which medications dissolve, particularly NSAIDs. Overall, the solid dispersion technique offers a useful method for increasing the bioavailability of medications that are poorly water-soluble, allowing for more effective and efficient pharmacotherapy.

## 6. THESIS OBJECTIVES

General objective of my thesis was to investigate various PEG derivatives and their characteristics and followed by the preparation of ketoprofen-containing solid dispersion using selected PEG derivatives. As most studies involved only a limited number of derivatives and I wished to better understand the cytotoxicity of these compounds, eleven substances of various molecular weights on a much wider scale: PEG 200, PEG 300, PEG 400, PEG 600, PEG 1000, PEG 1500, PEG 4000, PEG 8000, PEG 10000, PEG 12000, PEG 20000 were examined.

Also, I would like to check how the change of PEGs' molecular weight affects the properties of PEGs and their SDs. My thesis objectives design can be seen in Figure 14.

**In the first part of my thesis** the aim was to examine the toxicity of various PEG derivatives based on cellular effects (cytotoxicity and autophagy) and *in vivo* toxicity which is a necessary step before investigating the solid dispersion containing PEG derivatives and poorly soluble API.

PEGs are commonly used excipients to increase the solubility of active pharmaceutical ingredients, I looked for an API that is not well soluble. The solubility of ketoprofen was improved by solid dispersion preparation using PEG derivatives that I had previously studied for the first section of my thesis.

**In the second part of the thesis**, the aim is to formulate binary ketoprofen - PEG hot melt homogenization solid dispersions with low molecular weight polymers which were PEG 1000, 1500 and 2000. The physicochemical characteristics and the dissolution profiles of these solid dispersions were examined. The relationship between low molecular weight PEG derivatives and ketoprofen-SD characterization were also investigated regarding the effects of molecular weight of PEGs.

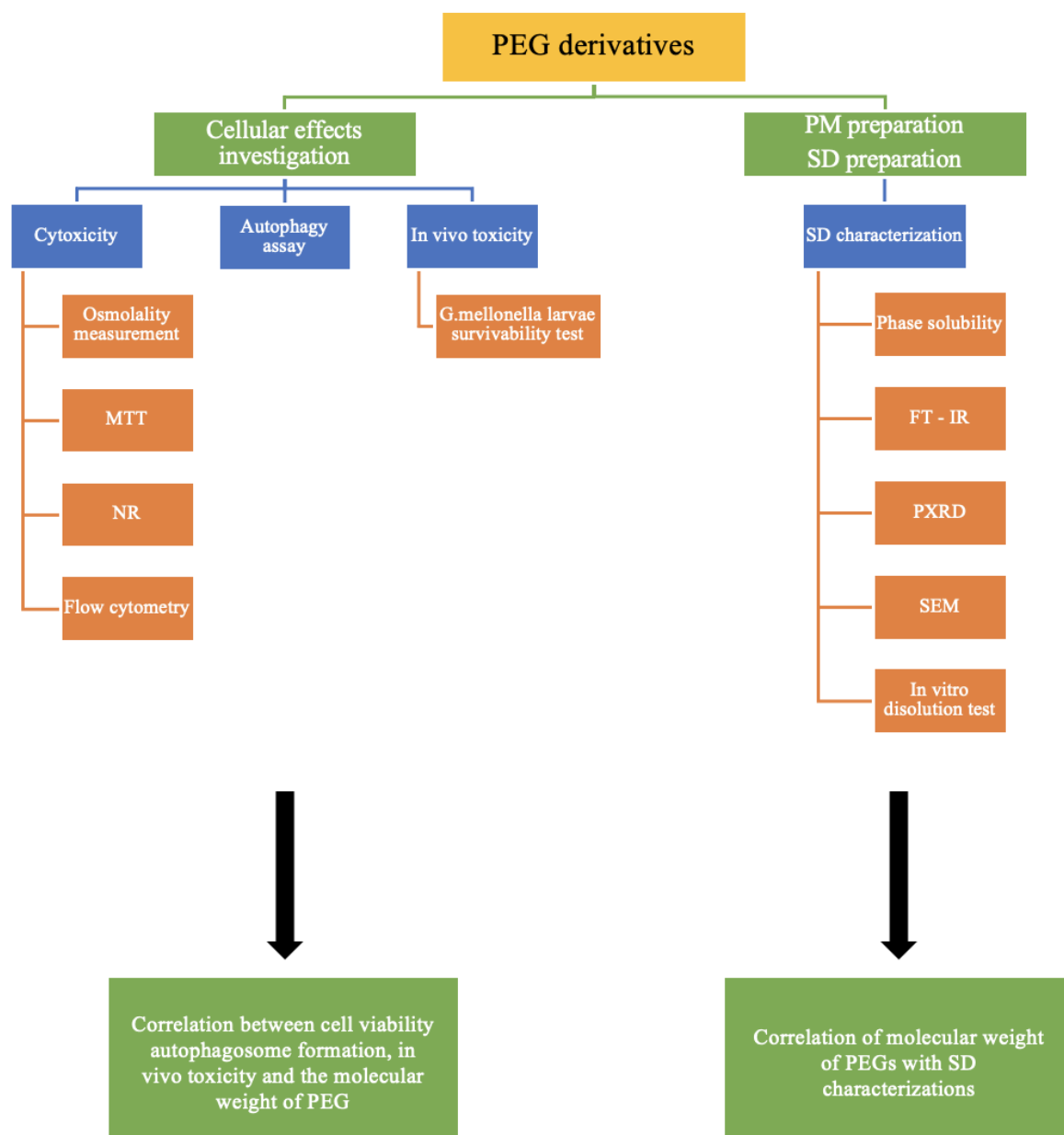


**Figure 14: Experimental design of the thesis.**

## 7. EXPERIMENTAL PART

### 7.1. Materials and sample preparation

A total of 12 polyethylene glycols derivatives were chosen to be investigated based on their average molecular weight. Range of molecular weight provided by the manufacturer is also indicated. All of PEGs are listed below:

- PEG 200 (190-210 MW), PEG 300 (290-305 MW) and PEG 600 (550-650 MW) were obtained from TCI (Zwijndrecht, Belgium).
- PEG 1000 (950-1050 MW), PEG 8000 (7000-9000 MW), PEG 10000 (9000-11250 MW), PEG 12000 (11000-13000 MW) and PEG 20000 (16000-24000 MW) were purchased from Alfa Aesar (Karlsruhe, Germany) and
- PEG 400 (380-420 MW), PEG 1500 (1400-1600 MW), PEG 4000 (3500-4500 MW) and sorbitol were obtained from Molar Chemicals (Halásztelek, Hungary).

The 3-(4,5-dimethylthiazol-2-yl)-2,5-diphenyltetrazolium bromide (MTT), sodium chloride, Dulbecco's Modified Eagle's Medium with high glucose and L-glutamin (DMEM), phosphate-buffered saline (PBS), trypsin from porcine, EDTA, heat-inactivated foetal bovine serum (FBS) and propidium iodide solution were purchased from Sigma-Aldrich (Budapest, Hungary). Non-essential amino acids solution and penicillin-streptomycin mix were obtained from Lonza (Basel, Switzerland). GlutaMax™ supplement and Annexin V Alexa Fluor™ 647 conjugate were purchased from Thermo Fisher (Budapest, Hungary). Neutral Red (3-amino-7-dimethylamino-2-methylphenazine hydrochloride) was obtained from Alfa Aesar (Karlsruhe, Germany). CYTO-ID Autophagy Detection Kit was purchased from Enzo Life Sciences (Farmingdale, NY, USA).

The investigation on the solid dispersion formulating between ketoprofen and polyethylene glycol will focus on 3 polyethylene glycol derivatives which are PEG 1000, PEG 1500, PEG 2000. Molecular weight ranges of PEG 1000 and PEG 1500 were listed above. MW range of PEG 2000 is 1900-2200 MW, (Merck Lifesciences Budapest, Hungary). Ketoprofen to formulate solid dispersion with 3 chosen PEGs was purchased from TCI (Zwijndrecht, Belgium).

All the materials were stored under dry and cool and dark conditions until the measurements and the sample preparation.

The PEGs with different molecular weights were all measured. PEGs were dissolved in PBS at 30 <sup>w/v</sup>% concentration and these solutions were used for all experiments. All of the PEG test solutions were freshly prepared immediately before any given experiment. Different sorbitol solutions were also dissolved with PBS and freshly prepared. All materials were of Pharmacopoeial quality.

## **7.2. Methods**

### **7.2.1. Cell culture**

The Caco-2 cell line was received from the European Collection of Cell Cultures (ECACC), Salisbury, United Kingdom (catalogue No. 8601020). Cells were grown in plastic Nunc™ EasyFlask™ cell culture flasks (Thermo Fisher, Darmstadt, Germany) in Dulbecco's Modified Eagle's Medium, supplemented with 3.7 g/L NaHCO<sub>3</sub>, 10% (v/v) FBS, 1% (v/v) non-essential amino acids solution, 0.584 g/L L-glutamine, 4.5 g/L D-glucose, 100 IU/mL penicillin, and 100 µg/mL streptomycin at 37 °C in an atmosphere of 5% CO<sub>2</sub>. Passaging was routinely done for cell maintenance and glutamine was supplemented by GlutaMax™. For the experiments, cells were between passage numbers 25 and 40.

### **7.2.2. Cytotoxicity tests**

The cytotoxic effects of all PEGs and sorbitol solutions were evaluated by using the MTT and Neutral Red (NR) methods. Caco-2 cells with media were seeded on 96-wells plates at a density of 10.000 cells per well. After 7 days, the medium was removed, and the cells were treated with 100 µl of the test solutions for 30 minutes at 37°C. Concentrations of the test solutions were 30 <sup>w/v</sup>% for all the PEGs solutions and 7-10-12.5-35 <sup>w/v</sup>% for the sorbitol solutions. During the preliminary studies, lower concentrations of PEGs solutions were tested also, but cytotoxicity did not exceed 20%. In case of MTT assay, the test solution was taken out and a 0.5 mg/mL MTT solution (MTT dissolved in PBS) was added to each well. The plate was again incubated for 3 hours at 37°C. In case of Neutral Red assay, a 16.6 mg/mL NR solution (NR dissolved in cell culture medium) was added to each well after removing all test solutions. The plate was incubated for 2 hours in this case. After incubation time, all dyes were completely removed and 0.1 mL of an isopropanol – 1 M hydrochloride acid (25:1) solution was added to each well to dissolve the cells and solubilize the formazan crystals and the incorporated Neutral Red. The absorbance of the wells was measured at 565 nm for MTT

assay and 540 nm for NR assay. We used empty wells of the plate as a reference and all the measurements were carried out with a Thermo-Fisher Multiskan Go (Thermo-Fisher, USA) microplate reader. Cell viability was expressed as a percent of the cell viability of the untreated control cells, which were incubated with PBS for 30 minutes.

### ***7.2.3. Osmolality measurement***

The OSMOMAT 070 vapor pressure osmometer (Gonotec GmbH, Berlin, Germany) is suitable for directly determining the total osmolality of aqueous solutions. The measurement temperature was 45°C and the sampling time was 5 minutes. The solvent chosen was ultrapure (Type 1) water obtained from a Millipore Direct-Q 5 UV system (Millipore SAS, Molsheim, France). Before each experiment, the baseline was determined by ultrapure water. After the baseline was stable, the calibration was carried out with a 1 <sup>w/v</sup>% sodium chloride solution. After the cell constant was calculated and the system calibrated with it, the PEGs and sorbitol samples with increasing concentration were measured sequentially. All liquids were dropped upon the sensors twice and the second drop was used for measurement. The concentrations of the test solutions were 30 <sup>w/v</sup>% for all the PEGs solutions and 7-10-12.5-35 <sup>w/v</sup>% for the sorbitol solutions. The osmolality of the samples was expressed in mOsmol/kg, as an average of 4 individual measurements.

### ***7.2.4. Flow cytometry analysis***

For the flow cytometry measurements, a Guava® easyCyte™ 5HT (Austin, TX, USA) flow cytometer was used. 3 × 6.5 million Caco-2 cells were harvested from cell culture flasks with trypsin-EDTA solution, and 1-1 million cells were treated with 1-1 ml of PEGS test solutions dissolved in PBS. The concentration of the test solutions was 30 <sup>w/v</sup>% for all the PEGS solutions. After 30 min, the cells were centrifuged, the test solutions were removed, and the cells were gently washed with cold PBS and centrifuged again. Supernatant was removed and with annexin-binding puffer a 1 million cells/mL cell suspension was created. 100 µl of this suspension was treated with 5 µl of Alexa Fluor™ 647 and 1 µl of 100 µg/mL propidium iodide solution. The cell suspension was stained for 15 min on ice then immediately analyzed with the flow cytometer. The propidium iodide was excited with a 488 nm laser and detected at the 525/30 nm channel (green parameter). The Alexa Fluor™ 647 was excited with the same laser line and detected at the 695/50 nm channel (red parameter). On the FSC-SSC scatterplot the non-cellular

events were excluded. On the FSC-A-FSC-W scatterplot the duplets were excluded. The remaining events (8000–10.000) were analyzed on a propidium iodide-Alexa Fluor 647 scatterplot, the quadrant gates were determined on non-labelled samples. The double positive cells are regarded as necrotic/late apoptotic cells. The annexin V positive population was regarded as early apoptotic, the double negative population regarded as viable cells.

### **7.2.5. Autophagy Assay**

For the quantitative analysis of autophagy, we used the CYTO-ID Autophagy Detection Kit (Enzo Life Sciences, Farmingdale, NY, USA) which is based on the staining autophagosomes. Caco-2 cells were seeded into black 96-well plates at the density of 10.000 cells per well. After four days, when cells reached the appropriate confluence, they were incubated for 30 minutes with 100  $\mu$ l of the PEGS and sorbitol test solutions at 37 °C. Concentrations of the test solutions were 30  $w/v\%$  for all the PEGS solutions and 7-10-12.5-35  $w/v\%$  for the sorbitol solutions. After this, cells were washed once with PBS and were treated according to the Kit specification. Cells were incubated with a solution which contains 1  $\mu$ L CYTO-ID® Green Detection Reagent and 1  $\mu$ L Hoechst 33,342 Nuclear Stain in 1 mL buffer for 30 min at 37 °C. After incubation time, cells were washed once with PBS. Green fluorescence intensities of the samples were measured with FLUOstar Optima microplate reader (BMG Labtech, Offenburg, Germany) at 485 nm excitation and 520 nm emission wavelengths. Hoechst 33,342 Nuclear Stain was measured at 365 nm excitation and 445 emission wavelengths. According to the instructions of the kit, green fluorescence values were normalized to the blue fluorescence values.

### **7.2.6. *G. mellonella* larvae survivability tests**

Larvae of the sixth developmental stage of *G. mellonella* were obtained from Bugs World Inc. (Budapest, Hungary). Larvae were stored at 10 °C and in a dark environment prior to use. Larvae size was between 2 and 3 cm and they showed no sign of melanisation. For each treatment, 10 healthy larvae were placed in sterile vented Petri dishes. The test solutions were injected into the *G. mellonella* haemocoel through the last pro-leg using a 29 G needle in the volume of 20  $\mu$ l. Concentration of the test solutions was 30  $w/v\%$  for all the PEGS solutions. The injected larvae were incubated at 30 °C for 48 h in dark environment. For the assessment of larval viability, larvae were gently probed

with a blunt-ended needle and if no response was observed, the larvae were considered to be dead. Viability was observed at 19 h, 24 h, 43 h, and 48 h.

### **7.2.7. Statistical analysis**

All data were analysed using GraphPad Prism (version 8; GraphPad Software, San Diego, California, USA). All data were presented as means  $\pm$  SEM. In case of MTT assay and NR assay, each cell viability value represents the mean of ten independent, parallel wells. PEGs and sorbitol treated cells' absorbance values were compared with their given control group as they were measured on multiple microplates. All data groups were analysed with Shapiro–Wilk test for Gaussian distribution and Bartlett's test for equal variances. If the data set passed both tests, a one-way ANOVA was calculated, if Bartlett's test failed, a Welsch's ANOVA was calculated and if Gaussian distribution was not proved, then Kruskal–Wallis test was carried out. As a post test, Dunnett's test was used to compare the treated cells' results to the controls. In each case we used significance level  $p < 0.05$ . Significance is labelled as ns =  $p \geq 0.05$ ; \* =  $p < 0.05$ ; \*\* =  $p < 0.01$ ; \*\*\* =  $p < 0.001$ ; \*\*\*\* =  $p < 0.0001$ . *In vivo* survival curves of *G. mellonella* larvae were plotted according to the Kaplan-Meier analysis, the survival curves were compared with Mantel-Cox log-rank test and Gehan–Breslow–Wilcoxon test. Osmolality, autophagy and flow cytometry results were not analysed because of low number of parallel experiments (n=4, n=4, n=3). Due to this, we used Spearman correlation to calculate the relationship between molecular weight and other measured data ( $p < 0.05$ , two-tailed).

### **7.2.8. Phase solubility**

The phase-solubility test was performed by adding a fixed excess amount of ketoprofen powder to 1 mL solutions containing the different molecular weight PEGs at increasing concentrations (1 – 20  $w_v$  %). The solvent was hydrochloric acid media, set to pH 1.2 without pepsin (simulated gastric fluid without enzyme). The vials were vortexed for 30 seconds to achieve well-mixed dispersions. They were rotated for 24 hours at room temperature at 50 rpm while being protected from light. Then each vial was centrifuged at 4500 rpm for 20 min. The samples were taken from the clear supernatant, and after filtering, the ketoprofen content of the samples was analysed by a UV spectrophotometer (Shimadzu UV-1900) at 258 nm. The phase solubility profiles were plotted as the solubility of ketoprofen versus the w/w% concentration of the given PEGS by GraphPad Prism (version 9; GrapPad Software, San Diego, California, USA).

The Gibbs free energy of transfer ( $\Delta G_{tr}^0$ ) of ketoprofen from pure water to the aqueous solutions of the PEGs was calculated as the following:

$$\Delta G_{tr}^0 = -2.303 \cdot R \cdot T \cdot \log (S_s/S_0) \quad (3)$$

where  $S_s/S_0$  is the ratio of molar solubility of ketoprofen in water (0.41  $\mu\text{g/mL}$  according to our measurements) to that in the aqueous solutions of the PEGs. The apparent stability constant ( $Ka$ ) was determined as:

$$Ka = \text{Slope}/(\text{Intercept} \cdot (1 - \text{Slope})) \quad (4)$$

where slope and intercept were obtained from the plotted curve.

### ***7.2.9. Preparation of solid dispersions and physical mixtures***

The PEGs and the ketoprofen were measured in a ratio of 9:1. We chose this ratio according to literature results, because in this concentration, the properties of the polymer are the dominant factors of dissolution, not that of the API.<sup>135</sup>

### ***7.2.10. Fourier-transform infrared spectroscopy (FTIR)***

The infrared spectra of the pure PEGs, physical mixtures, and solid dispersions were obtained by using a JASCO FT/IR-4600 type (ABL&E-JASCO, Hungary) apparatus coupled with a Zn/Se ATR PRO ONE Single-Reflection ATR accessory. Each sample was directly placed on the cleaned crystal of the equipment; the scanning was running in the wavelength range of 500–4000  $\text{cm}^{-1}$  at the resolution of 1  $\text{cm}^{-1}$  24 times to obtain smooth spectrum. Corrections of environmental  $\text{CO}_2$  and  $\text{H}_2\text{O}$  used the software's built-in method. Spectra were evaluated with SpectraGryph 1.2.16d software (Software for optical spectroscopy by Dr. Friedrich Menges, Oberstdorf, Germany, <http://spectroscopy.ninja> (accessed on 15 January 2021)).

### ***7.2.11. Powder X-ray Diffraction (PXRD)***

The finely powdered samples were fixed onto a Mitegen MicroMeshes sample holder (MiTeGen Co., Ithaca, NY, USA) with a minimal amount of oil. Powder diffraction data of the samples with Debye Scherer geometry were collected using a Bruker-D8 Venture (Bruker AXS. GmbH, Karlsruhe, Germany) diffractometer equipped with INCOATEC I $\mu$ S 3.0 dual (Cu and Mo) sealed tube micro sources (50 kV, 1.4 mA). A Photon 200 Charge-integrating Pixel Array detector and  $\text{CuK}\alpha$  ( $\lambda = 1.54178 \text{ \AA}$ ) radiation was applied. Several frames were collected with various detector-sample distances in phi scan mode. Data collection and integration was performed using the APEX3 and DiffracEva software (Bruker AXS Inc., Madison, WI, USA, Version 4.2.2.3), respectively.

### 7.2.12. Scanning Electron Microscopy (SEM)

Surface area exploration used a Hitachi Tabletop microscope (TM3030 Plus, Hitachi High-Technologies Corporation, Tokyo, Japan) in high-resolution mode. The samples were attached to a fixture with a double-sided adhesive tape containing graphite. Before SEM examination gold-sputtered coating was not deposited on the surface of the samples, as the instrument is suitable for the direct investigation of the specimens without any surface pre-treatments. The measurement requires a vacuum and low, 5kV accelerating voltage. The magnifications were 1000×.

### 7.2.13. In Vitro Dissolution Test

During the experiment, three parallel measurements were performed with size 0 capsules filled with 100 mg of the samples, meaning 90 mg of the given PEGS and 10 mg of ketoprofen in form of either a solid dispersion or a physical mixture. The dissolution media was 450 mL of hydrochloric acid media (same as the media of the phase solubility study). The volume was set as the half of the maximum recommended USP volume to stay within range of the limit of UV spectrophotometric detection of the ketoprofen. USP 2 rotating paddle method was with the rotation speed of 75 rpm and at 37 °C in an Erweka DT 128 light dissolution tester (Erweka GmbH, Langen, Germany). Samples of 1 mL were withdrawn after 5, 10, 15, 20, 30, 45 and 60 minutes and filtered through a 0.2 µm polyethersulfone membrane filter and measured as in case of the phase solubility study. The graphs were plotted by GraphPad Prism 9, all calculations were executed in Microsoft Excel.

In order to compare the dissolution profiles of the different formulations similarity (f1) and difference factors (f2) were calculated, as a model independent approach.<sup>153</sup> The exact calculations were the following:

$$f1 = \frac{\sum_{j=1}^n |R_j - T_j|}{\sum_{j=1}^n R_j} \times 100 \quad (5)$$

where f1 is the difference factor (relative errors between the two curves), n is the sampling number,  $R_j$  and  $T_j$  are the percent of the dissolved API from the two compared preparations at time point  $j$ .

$$f2 = 50 \times \log \left\{ \left[ 1 + (1/n) \sum_{j=1}^n w_j |R_j - T_j|^2 \right]^{-0.5} \times 100 \right\} \quad (6)$$

where  $f_2$  is the similarity factor (the logarithmic reciprocal square root transformation of the sum of squared error is a similarity factor which provides percentage dissolution between the two curves) and  $w_j$  is an optional weight factor which was 1 in our experiment.

For the fitting of dissolution profiles on different dissolution models, the following calculations were used:

<b>Model name</b>	<b>Equations</b> <sup>168,169</sup>	<b>Graphic</b>
Zero-order	$Q_t = Q_0 + k_0 t$ (7)	The graphic of the drug-dissolved fraction versus time is linear.
First-order	$Q_t = Q_0 \times e^{-k_1 t}$ (8)	The graphic of the decimal logarithm of the released amount of drug versus time is linear.
Korsmeyer–Peppas model	$\frac{Q_t}{Q_\infty} = k_{kp} t^n$ (up to $\frac{Q_t}{Q_\infty} \geq 0.6$ ) (9)	The graphic of the released drug versus the square root of time should form a straight line.

**Table 10: Mathematical calculations of drug release profiles.**

where  $Q$  is amount of drug release at time  $t$ ,  $Q_0$  is the initial amount of drug,  $Q_t$  is the amount of drug remaining at time  $t$ , and where  $Q_t/Q_\infty$  is fraction of drug released at time  $t$ .  $k_0$ ,  $k_1$ , and  $k_{kp}$  are the kinetic constants for zero-order, first-order, and Korsmeyer–Peppas models, respectively and  $n$  is the release exponent, indicative of the drug release mechanism.

## **8. RESULTS I.**

In this section, I conducted experiments to explore the impact of PEGs on both Caco-2 cells and *G. mellonella* larvae. The objective was to establish correlations between these effects and the molecular weight and osmolality of the PEGs. Eleven PEGs with varying molecular weights (PEG 200, PEG 300, PEG 400, PEG 600, PEG 1000, PEG 1500, PEG 4000, PEG 8000, PEG 10,000, PEG 12,000, and PEG 20,000) was employed in these experiments. The examined cellular effects encompassed cytotoxicity, assessed through MTT and Neutral Red assays, as well as flow cytometry utilizing propidium iodide and annexin V, along with autophagy. The osmolality of PEG solutions at various concentrations was measured using the vapor pressure osmometer OSMOMAT 070, and *G. mellonella* larvae were injected with the PEG solutions, with sorbitol serving as controls to maintain equivalent osmolality. Statistical analyses revealed noteworthy correlations between osmolality, cytotoxicity assays, flow cytometry data, and larvae mortality with the structural characteristics of the PEGs. However, no statistical correlation was observed between autophagosome formation and the proportion of early apoptotic cells, as well as the molecular weight of the PEGs.

### **8.1. Osmolality results**

Initially, the osmolality of PEGs was standardized at 30  $w/v$  %. Our preliminary findings indicate minimal cytotoxicity of PEGs, as cell viability consistently exceeded 80% for all derivatives at concentrations below 30  $w/v$ %. To comprehensively assess the impact of all derivatives on both cells and in vivo specimens, a further escalation in concentration was deemed necessary. Additionally, we employed sorbitol solutions to differentiate between biological effects linked to osmolality and those unrelated to it. Figure 15 illustrates a noteworthy decline in osmolality from PEG 200 to PEG 4000, with marginal increases observed until PEG 10000, 12000, and 20000, which exhibited nearly identical values.

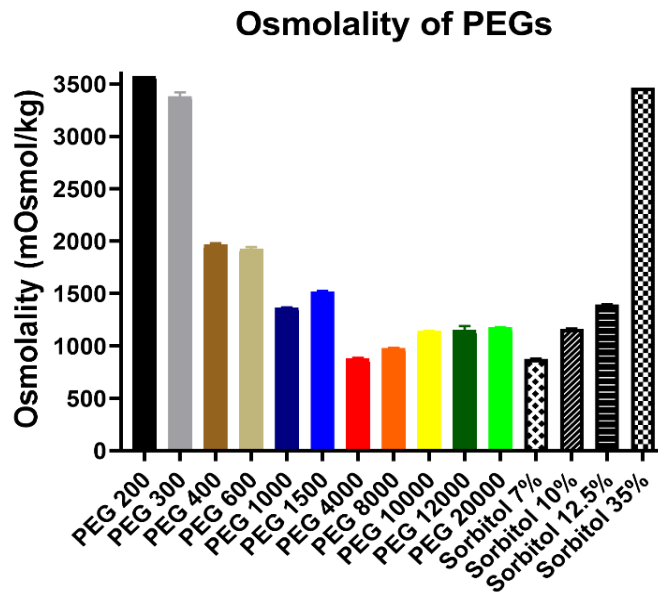


**Figure 15: Osmolality of PEG and sorbitol solutions measured by vapor pressure osmometer OSMOMAT 070.** Concentrations of all PEG solutions were 30 w/v% and volumes were 1 drop of the solutions each time. Data expressed as mean,  $\pm$  SEM  $n=4$ . Osmolality of the samples in mOsmol/kg (mean  $\pm$ SEM): PEG 200: 3574  $\pm$ 0; PEG 300: 3381  $\pm$ 38; PEG 400: 1963  $\pm$ 17; PEG 600: 1926  $\pm$ 17; PEG 1000: 1363  $\pm$ 4; PEG 1500: 1515  $\pm$ 11; PEG 4000: 877  $\pm$ 9; PEG 8000: 977  $\pm$ 3; PEG 10000: 1140  $\pm$ 4; PEG 12000: 1151  $\pm$ 38; PEG 20000: 1174  $\pm$ 5; Sorbitol 7 w/v%: 876  $\pm$ 2; Sorbitol 10 w/v%: 1164  $\pm$ 1; Sorbitol 12.5 w/v%: 1395  $\pm$ 4; Sorbitol 35 w/v%: 3464  $\pm$ 0.

## 8.2. Cytotoxicity assay results

As shown in Figure 16, sorbitol solutions did not exert a notable influence on the cell viability of treated Caco-2 cells, as evidenced by the MTT assay. Conversely, low molecular weight PEGs, such as PEG 200, 300, and 400, exhibited a significant reduction in the number of surviving cells. The remaining derivatives had a comparatively milder effect on cell viability, with none of them yielding values higher than 85%. It is crucial to highlight the substantial variation in results across different molecular weights.

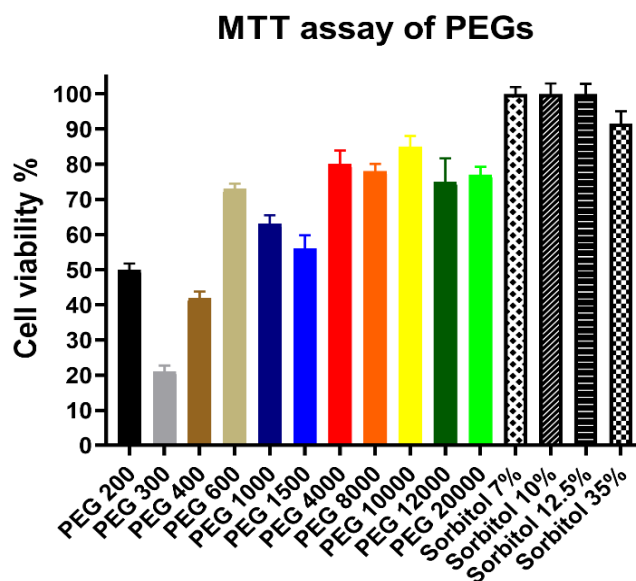


**Figure 16: Cytotoxicity of PEGs and sorbitol solutions measured by MTT assay.** Concentrations of all PEGs solutions were 30 w/v% and volumes were 100  $\mu$ l. Cell viability expressed as the percentage of the absorbance of the untreated control cells. Data expressed as mean,  $\pm$  SEM n=10. Cell viability of the samples (mean  $\pm$ SEM): PEG 200: 50%  $\pm$ 2%; PEG 300: 21%  $\pm$ 2%; PEG 400: 42%  $\pm$ 2%; PEG 600: 73%  $\pm$ 2%; PEG 1000: 63%  $\pm$ 3%; PEG 1500: 56%  $\pm$ 4%; PEG 4000: 80%  $\pm$ 4%; PEG 8000: 78%  $\pm$ 2%; PEG 10000: 85%  $\pm$ 3%; PEG 12000: 75%  $\pm$ 7%; PEG 20000: 77%  $\pm$ 2%; Sorbitol 7 w/v%: 100%  $\pm$ 2%; Sorbitol 10 w/v%: 100%  $\pm$ 3%; Sorbitol 12.5 w/v%: 100%  $\pm$ 3%; Sorbitol 35 w/v%: 92%  $\pm$ 3.6%; Levels of significance after statistical analysis treated cells compared against their respective untreated control group: PEG 200: \*\*\*\*; PEG 300: \*\*\*\*; PEG 400: \*\*\*\*; PEG 600: \*\*\*\*; PEG 1000: \*\*\*\*; PEG 1500: \*\*\*\*; PEG 4000: \*; PEG 8000: \*\*\*\*; PEG 10000: \*\*; PEG 12000: \*; PEG 20000: \*\*\*\*; Sorbitol 7 w/v%: ns; Sorbitol 10 w/v%: ns; Sorbitol 12.5 w/v%: ns; Sorbitol 35 w/v%: ns.

The results from the Neutral Red assay in Figure 17 display similar trends to those observed in the MTT assay. The sorbitol solutions did not exhibit any cytotoxic effects. Low molecular weight PEGs had a more pronounced impact on cell viability, with a narrower difference between high and low molecular weight derivatives. Nevertheless, notable variation was evident in the results for high molecular weight derivatives.

## Neutral Red assay of PEGs

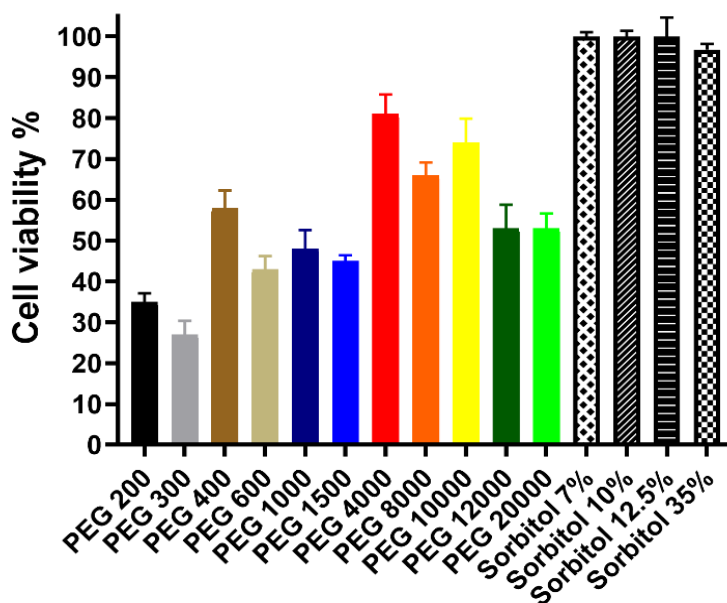


**Figure 17: Cytotoxicity of PEGs and sorbitol solutions measured by NR assay.** Concentrations of all PEGS solutions were 30 w/v% and volumes were 100 µl. Cell viability expressed as the percentage of the absorbance of the untreated control cells. Data expressed as mean, ± SEM n=10.

Cell viability of the samples (mean ±SEM): PEG 200: 35% ±2%; PEG 300: 27% ±3%; PEG 400: 58% ±4%; PEG 600: 43% ±3%; PEG 1000: 48% ±5%; PEG 1500: 45% ±1%; PEG 4000: 81% ±5%; PEG 8000: 66% ±3%; PEG 10000: 74% ±6%; PEG 12000: 53% ±6%; PEG 20000: 53% ±4%; Sorbitol 7 w/v%: 100% ±1%; Sorbitol 10 w/v%: 100% ±1%; Sorbitol 12.5 w/v%: 100% ±5%; Sorbitol 35 w/v%: 97% ±1%; Levels of significance after statistical analysis treated cells compared against their respective untreated control group: PEG 200: \*\*\*\*; PEG 300: \*\*\*\*; PEG 400: \*\*\*\*; PEG 600: \*\*\*\*; PEG 1000: \*\*\*\*; PEG 1500: \*\*\*\*; PEG 4000: \*\*; PEG 8000: ns; PEG 10000: ns; PEG 12000: \*\*; PEG 20000: \*\*\*\*; Sorbitol 7 w/v%: ns; Sorbitol 10 w/v%: ns; Sorbitol 12.5 w/v%: ns; Sorbitol 35 w/v%: ns.

### 8.3. Autophagy assay results

The results depicted in Figure 18 indicate that nearly all treatments led to an increase in the number of autophagosomes. Notably, there was a decreasing trend in fluorescence intensity from PEG 200 to PEG 1500, which then changed and started to increase again. The sorbitol solutions produced similar results to their PEG counterparts, except for 12.5 w/v%, , which yielded higher results than PEG 1000. It is worth mentioning that PEG 200

exhibited significantly higher intensity than any other treatment, while the remaining chemicals produced results in the range of approximately 180% to 100%.

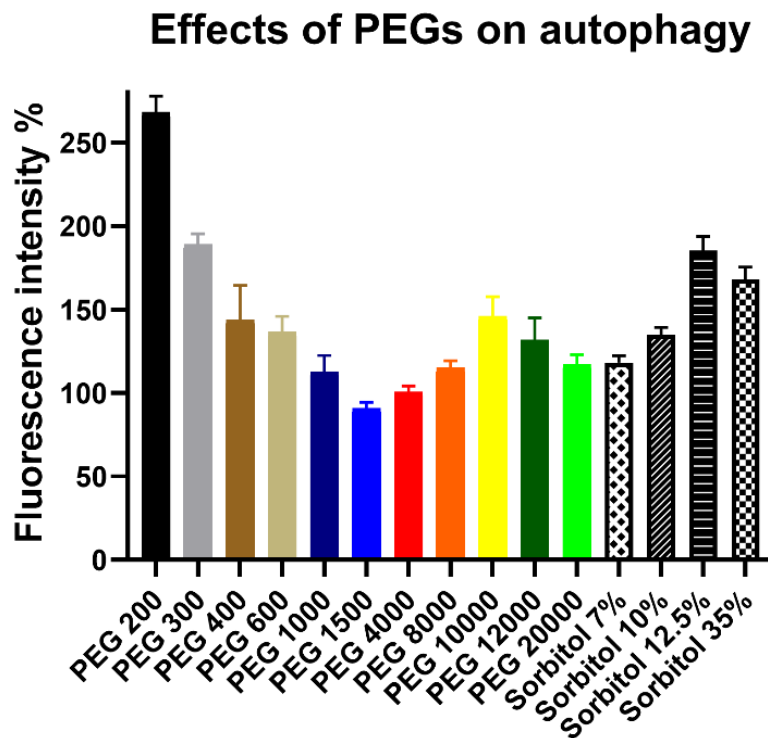


**Figure 18: Effect of PEGs and sorbitol solutions on the number of autophagosomes.** Concentrations of all PEG solutions were 30 w/v% and volumes were 100 µl. Fluorescence intensity is expressed as the percentage of the intensity of the untreated control cells. Data expressed as mean, ± SEM n=4, highest and lowest values were excluded. Fluorescence intensity of the samples (mean ±SEM): PEG 200: 268% ±10%; PEG 300: 189% ±6%; PEG 400: 144% ±21%; PEG 600: 136% ±10%; PEG 1000: 113% ±10%; PEG 1500: 91% ±4%; PEG 4000: 101% ±4%; PEG 8000: 115% ±4%; PEG 10000: 146% ±12%; PEG 12000: 132% ±13%; PEG 20000: 117% ±6%; Sorbitol 7 w/v%: 118% ±4%; Sorbitol 10 w/v%: 135% ±5%; Sorbitol 12.5 w/v%: 185% ±8%; Sorbitol 35 w/v%: 168% ±7%.

#### 8.4. Flow cytometry results

The sorbitol solutions were excluded from further experiments due to their minimal impact on cells. In the flow cytometry analysis, Caco-2 cells were stained with propidium iodide and annexin V labeling to distinguish between necrotic and early apoptotic cells. Figure 19 depicts the distribution of gated cells, revealing that the proportion of unstained, living cells (PI- AV-) increases with molecular weight. Remarkably, for low molecular weight PEGs, necrotic cells (PI+ AV+) predominate among the deceased cells. However, with increasing molecular weight, the ratio of early apoptotic cells (PI- AV+) also rises.

## Flow cytometry analysis of PEG treated Caco-2 cells

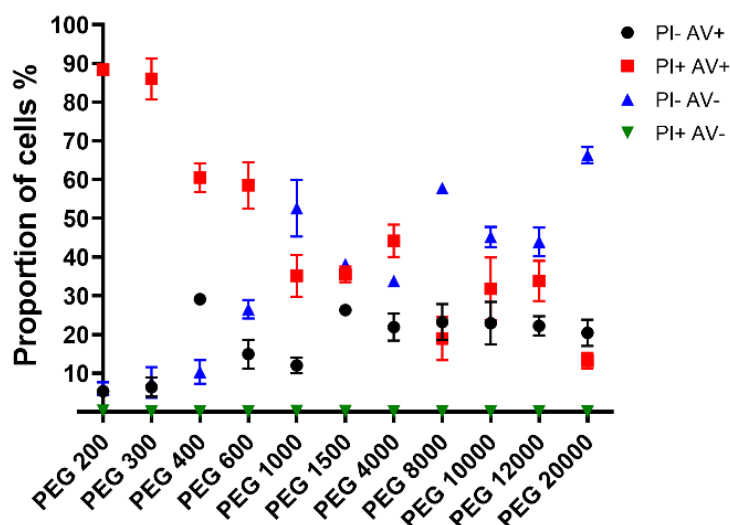


**Figure 19: Flow cytometric measurement of Caco-2 cells.** The cells were treated with 1 ml of 30 <sup>w/v</sup>% solutions of PEGs, stained with propidium iodide (PI) and annexin V (AV). Data is represented as mean of triplicates. Data represented as percentage distribution of cells between necrotic (PI+ AV+), early apoptotic (PI- AV+), living (PI- AV-) and incorrectly stained (PI+ AV-) populations of three independent experiments. Distribution of the samples as mean  $\pm$ SEM (PI- AV+; PI+ AV+; PI- AV-; PI+ AV-):

PEG 200: 5,3%  $\pm$ 1,3%; 88,4%  $\pm$ 0,6%; 6 %  $\pm$ 1,6%; 0,3%  $\pm$ 0,3%;  
 PEG 300: 6,4%  $\pm$ 2,5%; 86%  $\pm$ 5,3; 7,6%  $\pm$ 4%;  $\pm$ 0%  $\pm$ 0%;  
 PEG 400: 29,1%  $\pm$ 0,6%; 60,5%  $\pm$ 3,7%; 10,3%  $\pm$ 3,1%;  $\pm$ 0%  $\pm$ 0%;  
 PEG 600: 14,9%  $\pm$ 3,7%; 58,5%  $\pm$ 6%; 26,5%  $\pm$ 2,4%; 0,1%  $\pm$ 0,1%;  
 PEG 1000: 12%  $\pm$ 2%; 35,1%  $\pm$ 5,4%; 52,6%  $\pm$ 7,3%; 0,2%  $\pm$ 0,1%;  
 PEG 1500: 26,3%  $\pm$ 0,7%; 35,5%  $\pm$ 2; 38,1%  $\pm$ 1,2%; 0,2%  $\pm$ 0,1%;  
 PEG 4000: 21,9%  $\pm$ 3,5%; 44,2%  $\pm$ 4,2%; 33,8%  $\pm$ 0,8%; 0,1%  $\pm$ 0%;  
 PEG 8000: 23,2%  $\pm$ 4,6%; 18,9%  $\pm$ 5,6%; 57,8%  $\pm$ 1,1%; 0,1%  $\pm$ 0,1%;  
 PEG 10000: 22,9%  $\pm$ 5,5%; 31,8%  $\pm$ 8,1%; 45,2%  $\pm$ 2,6%; 0%  $\pm$ 0%;  
 PEG 12000: 22,2%  $\pm$ 2,5%; 33,8%  $\pm$ 5,2%; 43,9%  $\pm$ 3,7%; 0,1%  $\pm$ 0,1%.

## 8.5. In vivo toxicity test

Over the course of the two-day experiment, *G. mellonella* larvae received 20  $\mu$ l injections of PEGS solutions, and their viability was assessed four times. Each group consisted of 10 healthy larvae. The analysis presented in Figure 20 unveiled notable mortality rates for low molecular weight PEG 200 and 300, as well as medium molecular weight PEG 4000. Importantly, no other PEG exhibited a substantial impact on larval survival.

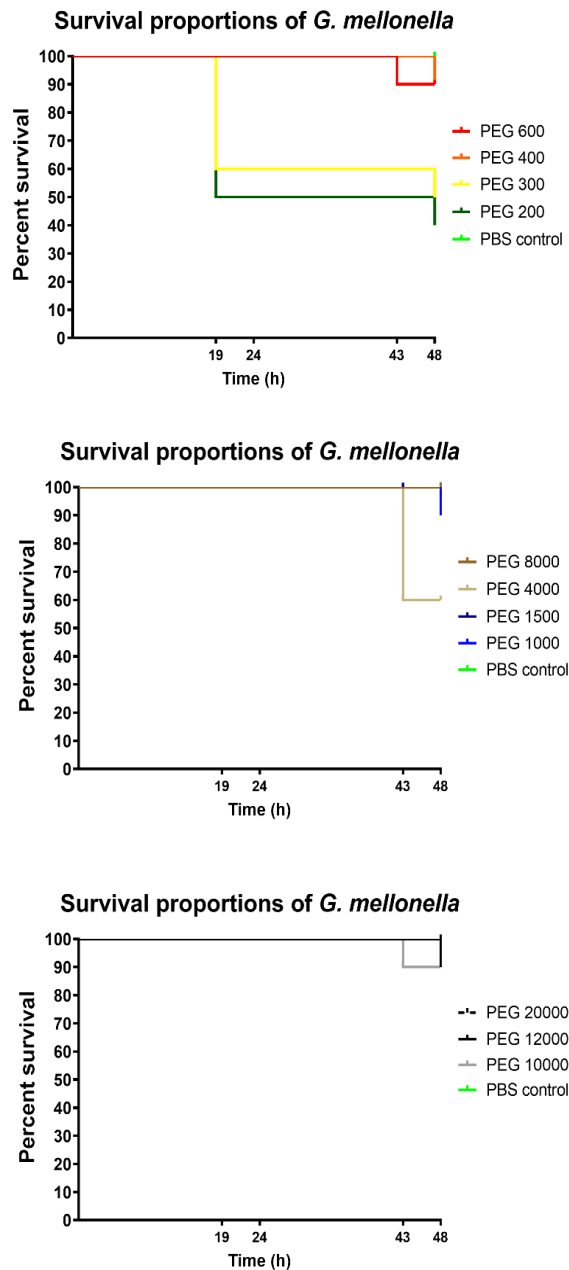


**Figure 20: Survival curve of *G. mellonella* larvae.** Larvae were injected with 20  $\mu$ l of test samples, each group had 10 larvae. Death events of the experiment: 19 h: PEG 200: 5; PEG 300:

4; 43 h: PEG 600: 1; PEG 4000: 4; PEG 10000: 1; 48 h: PEG 200: 1; PEG 300: 1; PEG 400: 1; PEG 1000: 1; PEG 12000: 1; Significance of treated groups compared to PBS control according to Mantel-Cox log-rank test, and Gehan–Breslow–Wilcoxon test: PEG 200: \*\*/\*\*; PEGS 300: \*/\*; PEG 4000: \*/\*; all others were insignificant.

## 8.6. Correlation of results with molecular weight

We employed Spearman correlation analysis to establish the statistical relationship between the measured data and the average molecular weight of PEGs. Interestingly, as the molecular weight of PEGs increased, we observed a significant decrease in osmolality, the proportion of necrotic cells (PI+ AV+ cells according to flow cytometry), and total larvae mortality. Furthermore, the ratio of living cells, as determined by both cytotoxicity assays and flow cytometry, increased with the average molecular weight of PEGs. However, we found no statistical relationship between autophagy and the proportion of apoptotic cells with the chemical structure of PEGs.

	Spearman correlation coefficient	Level significance
Osmolality	-0.8091	**
Cell viability - MTT	0.7909	**
Cell viability - NR	0.6241	*
Autophagy	ns	
Proportion of PI- AV+ cells	ns	
Proportion of PI+ AV+ cells	-0.9273	***
Proportion of PI- AV- cells	0.8455	**
Total larvae mortality	-0.6357	*

**Table 11: Correlation of measured data (only PEGs) with average molecular weight calculated by Spearman method. Significance levels are shown as: ns =  $p \geq 0.05$ ; \* =  $p < 0.05$ ; \*\* =  $p < 0.01$ ; \*\*\* =  $p < 0.001$ ; \*\*\*\* =  $p < 0.0001$ .**

In Table 12, the correlation matrix was calculated to analyze the relationships between the different data sets. It was observed that autophagy showed no statistical relationship overall. However, the proportion of early apoptotic cells exhibited a negative correlation with larvae mortality and a positive correlation with the NR assay. Additionally, the various cell viability measurements, including MTT, NR assays, and the proportion of necrotic and living cells according to flow cytometry, displayed

significant correlations with each other and with osmolality. The last data set, the total larvae mortality was only linked to the flow cytometry results. Notably, the most significant correlation was found between the distribution of necrotic and living cells in the flow cytometry analysis.

	Osmolality	Cell viability - MTT	Cell viability - NR	Autophagy	Proportion of PI-AV+ cells	Proportion of PI+ AV+ cells	Proportion of PI- AV- cells	Total larvae mortality
<b>Osmolality</b>	-	0.909/ ****	- 0.843/ **	ns	ns	0.755/*	-0.709/*	ns
<b>Cell viability - MTT</b>	0.909/**	-	0.770/ **	ns	ns	-0.736/*	0.664/*	ns
<b>Cell viability - NR</b>	0.843/**	0.770/ **	-	ns	0.620/*	ns	ns	ns
<b>Autophagy</b>	ns	ns	ns	-	ns	ns	ns	ns
<b>Proportion of PI-AV+ cells</b>	ns	ns	0.620/ *	ns	-	ns	ns	- 0.626/ *
<b>Proportion of PI+ AV+ cells</b>	0.755/*	0.736/ *	ns	ns	ns	-	0.973/ ***	0.771/ **
<b>Proportion of PI- AV- cells</b>	-0.709/*	0.664/ *	ns	ns	ns	- 0.973/ ***	-	- 0.771/ **
<b>Larvae mortality</b>	ns	ns	ns	ns	-0.626/*	0.771/ *	- 0.771/ *	-

**Table 12: Correlation of matrix of all measured data sets (only PEGs). Spearman correlation coefficient and significance levels are shown as: ns =  $p \geq 0.05$ ; \* =  $p < 0.05$ ; \*\* =  $p < 0.01$ ; \*\*\* =  $p < 0.001$ ; \*\*\*\* =  $p < 0.0001$ .**

## 9. RESULTS II.

In the second part of my thesis, I developed solid dispersions using low molecular weight PEGs (PEG 1000, PEG 1500, PEG 2000) and the active pharmaceutical ingredient (API) ketoprofen through the hot melting method. A phase solubility study was conducted in hydrochloric acid media, and the physicochemical properties of the solid dispersions prepared with hot melt homogenization, along with their respective physical mixtures, were examined using Fourier transform infrared spectroscopy, powder X-ray diffraction, and scanning electron microscopy techniques. The primary goal was to investigate the relationship between selected PEGs and ketoprofen, with a specific focus on the impact of molecular weight. The phase solubility study unveiled no difference among the three polymers, but notable distinctions were observed in the dissolution curves. Particularly, PEG 1000 exhibited a higher percentage of released drugs compared to PEG 1500 and 2000, which demonstrated similar outcomes. These results suggest that, while multiple low molecular weight PEGs can serve as suitable matrix polymers for solid dispersions, the molecular weight has only a limited impact on physicochemical characteristics and interactions.

### 9.1. Phase solubility

Figure 21 illustrates the impact of PEGs on the solubility of ketoprofen. Our research has shown that the solubility of ketoprofen in simulated gastric juice was 41  $\mu\text{g/mL}$ . On the solubility of the API 1  $\text{w/v}\%$  PEGs only had a minimal effect. However, as the concentration increased, a linear correlation was observed up to 10  $\text{w/v}\%$ , with a significant increase at 20  $\text{w/v}\%$ , concentration. No significant differences were observed among different molecular weight PEGs regarding their ability to increase solubility. The apparent stability constants ( $K_a$ ) of ketoprofen for PEG 1000, PEG 1500, and PEG 2000 were calculated to be  $3.317 \cdot 10^{-5}$ ,  $3.346 \cdot 10^{-5}$ , and  $3.569 \cdot 10^{-5}$ , respectively (Table 13).

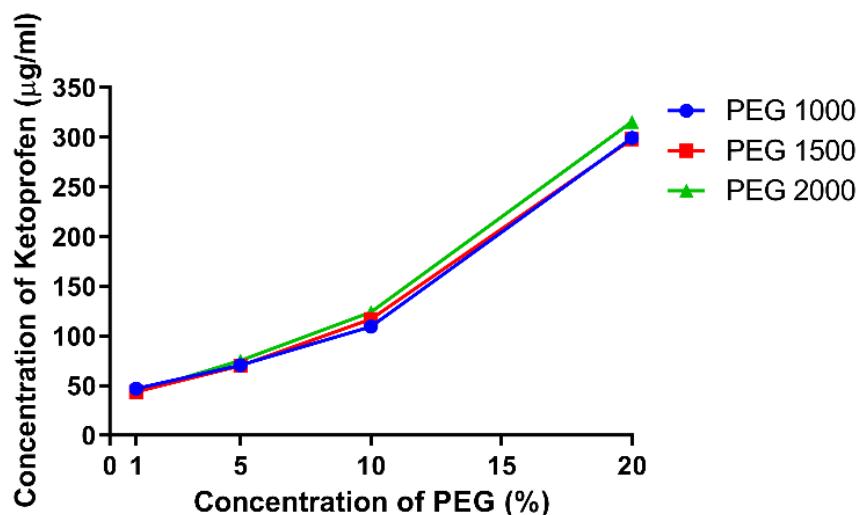


Figure 21: Phase-solubility diagram of ketoprofen in simulated gastric juice.

Concentration (w/w%)	$\Delta G_{tr}^0$ (J/mol)		
	PEGs 1000	PEGs 1500	PEGs 2000
1	-331.6	-144.5	-116.6
5	-1342	-1316	-1491
10	-2420	-2585	-2731
20	-4911	-4901	-5042

Table 13: Gibbs free energy values of ketoprofen and the tested PEGs.

## 9.2. Fourier-transform infrared spectroscopy (FT-IR)

Ketoprofen was prepared for further experimentation in two different forms: solid dispersion by hot melt homogenization (SD) and gently mixed powders (physical mixture, PM) of ketoprofen and PEGs. FTIR spectroscopy was employed to scrutinize potential interactions between ketoprofen and PEGs in these formulations. Remarkably, in the 1650-1700  $\text{cm}^{-1}$  range, ketoprofen exhibited characteristic peaks absent in the PEGs. For PEGs 1000 (Figure 22. A), the spectra of the solid dispersion and physical mixture were nearly identical. In contrast, for PEG 1500 (Figure 22. B) and 2000 (Figure 23. C), the characteristic ketoprofen peaks were discernible in the physical mixture within the same range as the pure API. However, in the solid dispersions, the formation of a new hydrogen bond caused a shift in the ketoprofen bands from 1693  $\text{cm}^{-1}$  to 1732  $\text{cm}^{-1}$ .

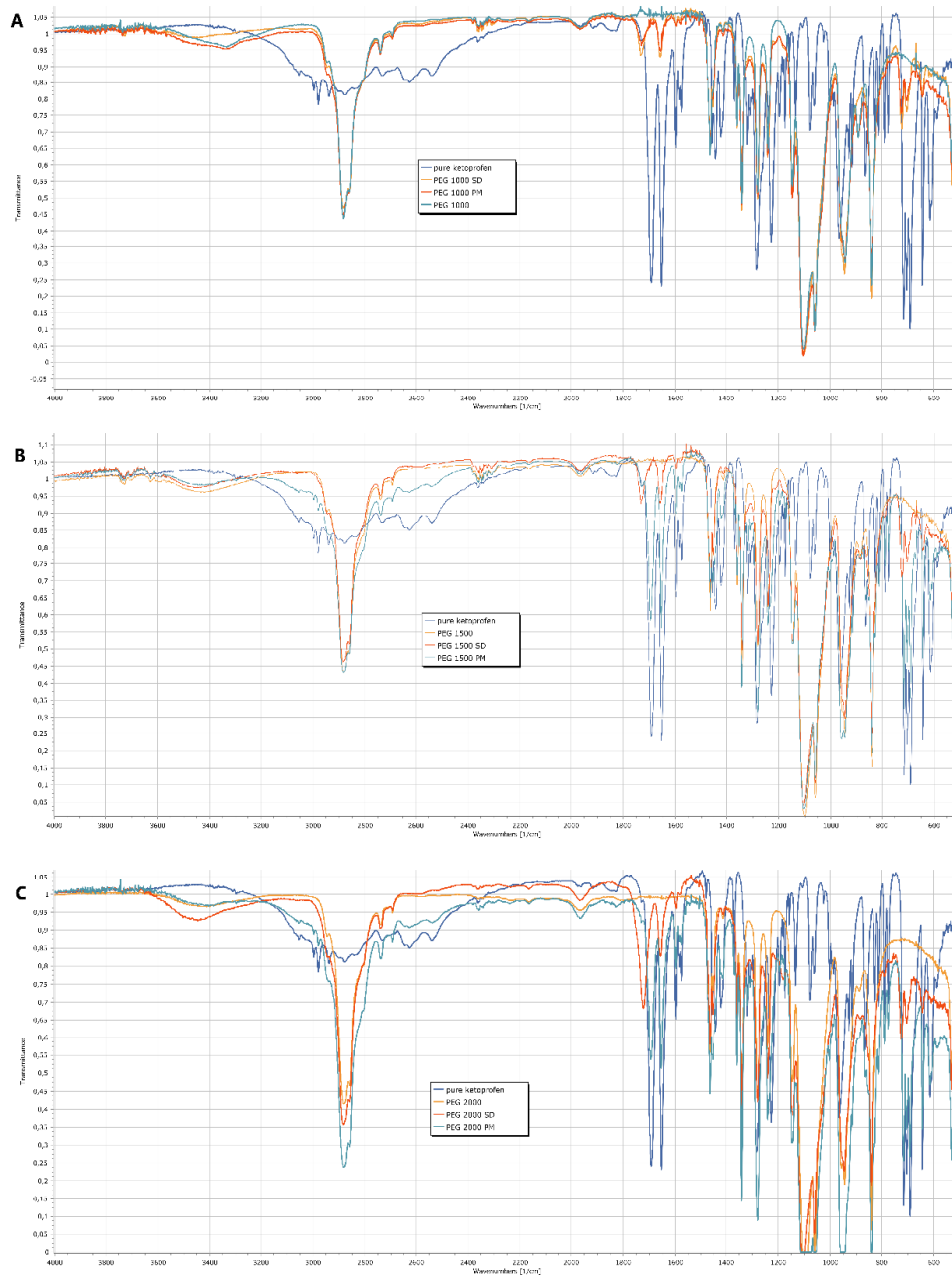


**Figure 22: FTIR spectra of KT, pure PEGs, PM, SD for PEG 1000, 1500, 2000.**

### 9.3. Powder X-ray Diffraction (PXRD)

The PXRD results (Figure 23) confirm that for PEG 1500 and 2000, the physical mixture contains ketoprofen in a crystalline form. In contrast, in the case of solid dispersions, there are no indicative signals of a crystalline structure. This suggests that in the solid dispersions, the active ingredient primarily exists in an amorphous form, indicating that the API was dissolved in PEG. In comparison to the FT-IR results, both PEG 1000 PM and PEG 1500 SD exhibit nearly identical characteristics.

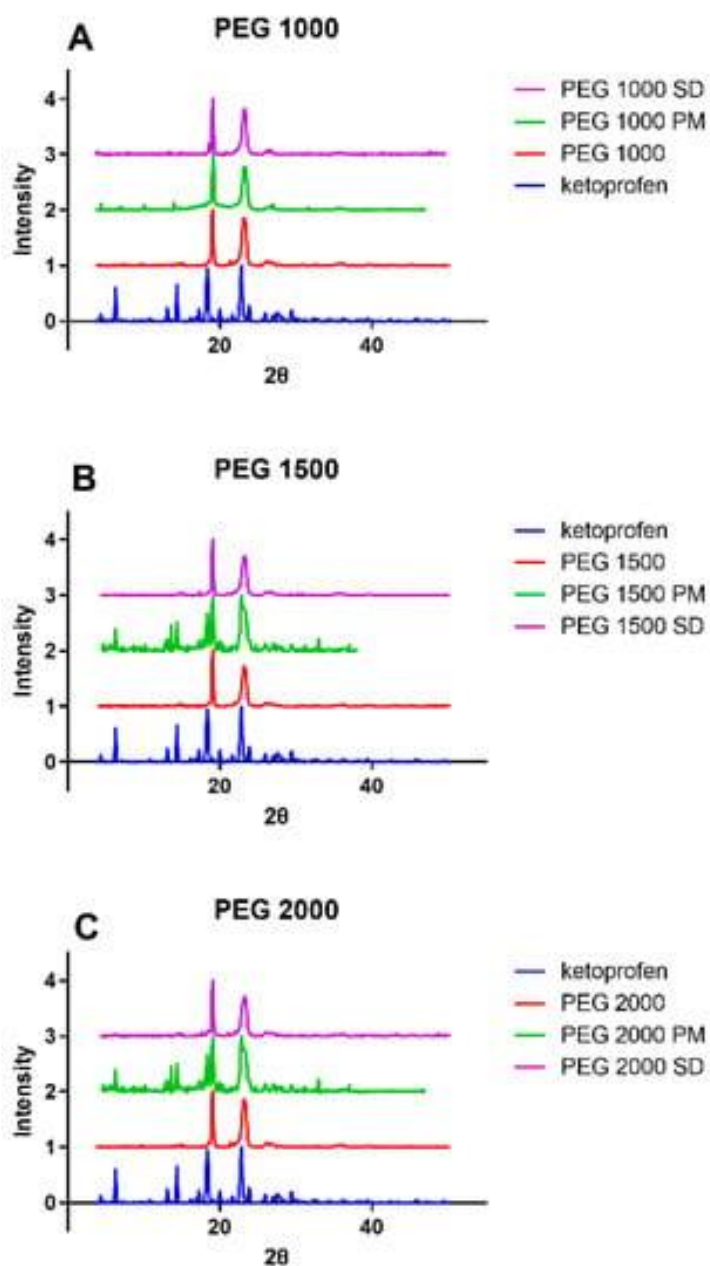
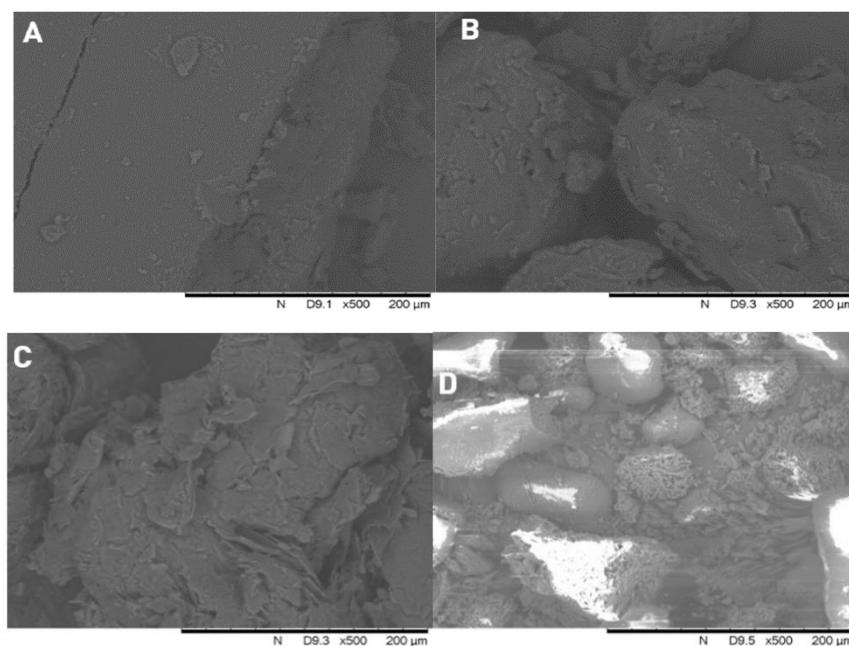


Figure 23: PXRD spectra of KT, pure PEGs, PM, SD for PEG 1000, 1500, 2000.

## 9.4. Scanning Electron Microscopy (SEM)

Figure 24 presents the SEM images of pure ketoprofen, and the three type of PEGs polymers (PEG 1000, PEG 1500, PEG 2000). In the center of 24D the typical crystalline form of ketoprofen is visible with particle size below  $\sim 100 \mu\text{m}$ . In the case of the polymers, there is not any detectable crystalline form, they are amorphous particles. Upon magnification at 500x, the electron microscope images (Figure 25) confirm that the crystals of the active ingredient can be found between the larger particles of the PEGS, whereas, in the case of solid dispersion (SD), a predominantly homogeneous, molten substance is observed. In physical mixtures, the crystals of ketoprofen are detectable, except PEGS 1000, which again shows similarities to its respective solid dispersions. The lack of ketoprofen crystals indicates the successful formation of a solid dispersion. In the case of PEGS 1000, the solid dispersion is achieved due to its low melting point, allowing ketoprofen to dissolved during the gentle homogenization process in the experiment.



**Figure 24: SEM images of PEG 2000, 1500, 1000, and crystalline ketoprofen.**

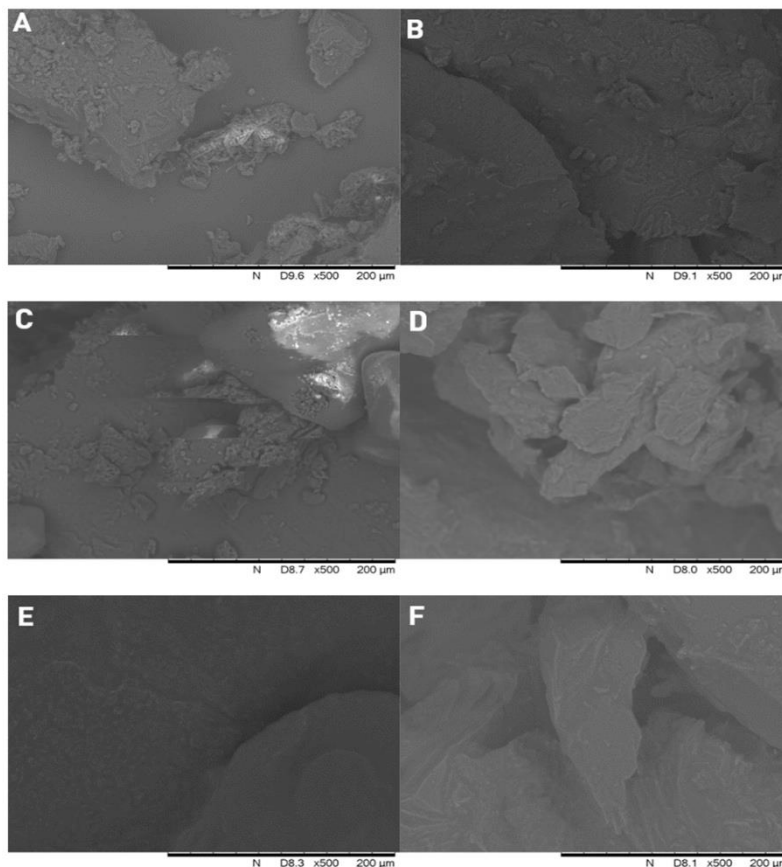


**Figure 25: SEM images of PM and SD of PEG 2000, PEG 1500, PEG 1000.**

## 9.5. In Vitro Dissolution Test

The dissolution test results depicted in Figure 26 reveal that the highest amount of dissolved drug was observed for PEG 1000, with the other two PEGs exhibiting mostly similar profiles. Table 14 presents the calculated difference and similarity factors for the solid dispersions. The compared curves are statistically similar when  $f_1$  values fall between 0 and 15 and  $f_2$  values exceed 50. The graph illustrates the similarity between PEG 1500 SD and 2000 SD. It also must be noted, in all cases, the concentration of the dissolved ketoprofen was multiple times the amount calculated from the phase solubility study results (Figure 26), indicating the formation of a supersaturated solution.

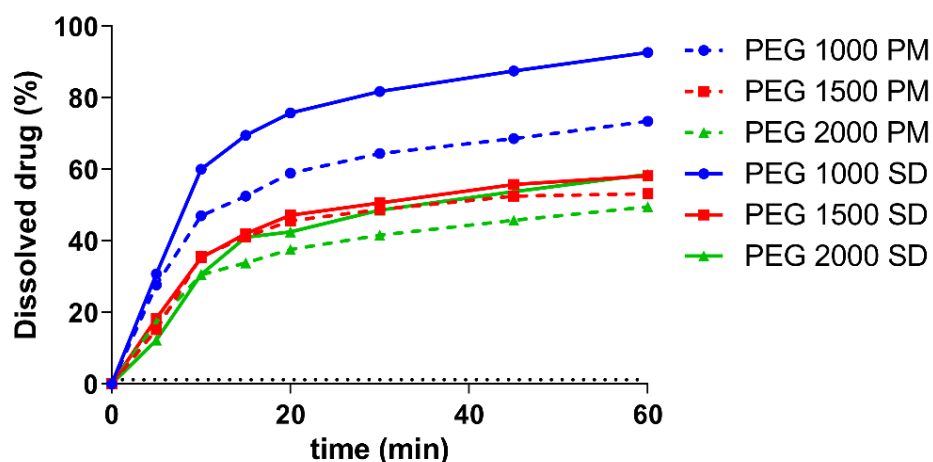


**Figure 26: Dissolution profiles of SDs and PMs in simulated gastric juice.** Data is represented as the average ( $\pm$ SD) detected amount of ketoprofen compared to the average amount of ketoprofen loaded into the capsules. N=3. The dotted line represents the theoretical maximum solubility of ketoprofen in the presence of the PEGs based on the phase solubility study (90 mg of PEG in 450 mL of hydrochloric acid media, average is calculated and plotted from the result of the three polymers).

Comparison of compositions	f1	f2
<b>PEG 1000 PM vs. SD</b>	29.80	39.84
<b>PEG 1500 PM vs. SD</b>	<b>5.00</b>	<b>76.78</b>
<b>PEG 2000 PM vs. SD</b>	<b>10.84</b>	<b>59.19</b>
<b>PEG 1000 SD vs. PEG 1500 SD</b>	38.27	25.74
<b>PEG 1000 SD vs. PEG 2000 SD</b>	42.30	27.59
<b>PEG 1500 SD vs. PEG 2000 SD</b>	<b>6.54</b>	<b>71.39</b>

**Table 14: Difference and similarity factors of the dissolution profiles of the samples.**

Further analysis of the dissolution curves is presented in Table 15. The majority of samples were best described by the Korsmeyer-Peppas equation, commonly used to characterize release from polymeric systems.<sup>148</sup> Though, in specific instances, the zero-

order model was the most suitable, particularly for matrix tablets containing low solubility API.

Type of kinetics profile		Zero-order model	First order model	Korsmeyer-Peppas model
<b>Physical mixture*</b>	PEG 1000	0.8440	0.8854	<b>0.9321</b>
	PEG 1500	<b>0.8371</b>	0.7104	0.7859
	PEG 2000	0.8588	0.8715	<b>0.9109</b>
<b>Solid dispersions</b>	PEG 1000	0.8416	0.9469	<b>0.9592</b>
	PEG 1500	0.8547	0.8242	<b>0.8710</b>
	PEG 2000	<b>0.8823</b>	0.8543	0.8444

**Table 15: Coefficient determination for different models of the dissolution profiles.**

In various articles, multiple PEGs have been studied to understand how changes in their molecular weight affect specific characteristics. The relationship between molecular weight and these characteristics can be either proportional or inversely proportional, but some studies have failed to find any correlation. Table 16 provides a summary of some of these investigations. The upcoming chapters will detail my findings on the relationship between molecular weight and properties related to PEGs (cellular effect and solid dispersion formulation).

<b>Publication</b>	<b>Tested characteristics</b>	<b>PEGs</b>	<b>Relationship of molecular weight and tested characteristics</b>
B.Chakrabarty et al. <sup>169</sup>	Permeation performances of polysulfone polymeric membranes	400, 6000, 20000	Proportionality
S. Chibowski and M.Paszkwicz <sup>170</sup>	Adsorption and electrochemical properties of the titania/electrolyte solution interface	2000, 35000, 100000, 300000	Proportionality
Ruilong Li et al. <sup>171</sup>	Crystallization behaviors, Thermal properties, Tensile performance of polylactic acid stereocomplexes (PLLA)	2000, 4000, 6000, 8000	Proportionality
Ping Qu et al. <sup>172</sup>	Biodegradation and morphology properties of cellulose nanofibrils/poly(lactic) composite materials	600, 1000, 4000	Inverse proportionally
Mansi Singh et al. <sup>173</sup>	Rheological properties of fumed silica-PEGs shear thickening fluid	200, 4600, 6000, 10000	Proportional
Tatiana V. et al. <sup>174</sup>	Polysulfone solution and hollow fiber membranes - Structure - Permeability - Homogenous - Viscosity of solution	400, 1000, 2000, 6000, 20000, 40000	- None -Proportional -Inverse proportionally -None

**Table 16: Some publications about the correlation between MW of PEGs.**

## 10. DISCUSSION I.

Polyethylene glycols, referred to as Macrogols in the European Pharmacopoeia,<sup>6</sup> play a pivotal role as excipients in both oral and parenteral dosage forms. Their primary applications include constipation treatment and colonoscopy preparation.<sup>175,176</sup> These polymers exhibit noteworthy characteristics, including chemical neutrality, hydrophilicity, and high to moderate solubility in aqueous and organic solvents. Such attributes make them widely employed for enhancing the pharmacological and biological properties of diverse pharmaceutical formulations.<sup>177</sup> Additionally, PEGs are recognized for their contribution to the development of stealth coatings on nanoparticle surfaces, leveraging the interaction between opsonins and the PEGSylated surface.<sup>178</sup> While the physical properties and cellular effects of PEGs hold significance, most literature tends to focus on individual PEGs, with limited studies involving multiple derivatives. Our study aimed to delve into the cellular effects of PEGs spanning a broad range of molecular weights, seeking to establish correlations among different measured properties. Prior research has indicated that fundamental biological effects, such as the cytotoxicity of PEGs, are influenced by osmolality and can be predicted based on the molecular weight.<sup>171</sup>

Our study sought to conduct a comprehensive exploration of the biological effects of PEGs. Initially, we measured osmolality and subsequently delved into cytotoxicity, autophagy, and the distribution of necrotic/apoptotic/living cells, along with *in vivo* toxicity assessment. To ascertain the osmolality of our solutions, we employed the OSMOMAT 070 osmometer, given its suitability for assessing osmolality or molecular weight through the vapor pressure method.<sup>32,179,180</sup> In our *in vitro* cytotoxicity experiments, we utilized Caco-2 human colorectal adenocarcinoma cells. These cells were chosen for their role as a general model cell line and their ability to reflect the susceptibility of the gastrointestinal tract, given their morphological resemblance to the intestinal epithelium.<sup>181,182</sup> Cytotoxicity evaluation was conducted through the commonly employed MTT and Neutral Red assays, both of which complement each other. The MTT assay detects cell viability through enzymatic conversion, while the Neutral Red assay measures cellular uptake and the incorporation of neutral red. The combination of these assays is often utilized in various studies to explore the cytotoxicity of different chemicals, benefiting from their distinct mechanisms of action.<sup>183-185</sup> To delve deeper into the cytotoxic characteristics of PEGs, we utilized labeled annexin V and propidium

iodide in conjunction with flow cytometry. This approach allowed us to distinguish between necrotic and early apoptotic cells.<sup>184,186,187</sup> Additionally, we measured autophagosome formation through cellular organelle staining as a marker of autophagy, an inducible mechanism of cytotoxicity.<sup>188–190</sup> We complemented our cytotoxic experiments by employing the *Galleria mellonella* injection method, an emerging *in vivo* model organism that serves to assess the toxicity of different xenobiotics.<sup>191–193</sup> This method has shown a robust correlation with cellular and other *in vivo* techniques in studies focusing on acute toxicity.<sup>194</sup>

In the field of cytotoxicity, there has been limited research on the cytotoxic properties of PEGs across a wide range of molecular weights. Liu et al. conducted a study on a variety of PEG derivatives using the MTT assay, focusing on HeLa (human cervical cancer cells) and the L929 cell line (fibroblasts derived from mice).<sup>195</sup> The PEGS derivatives involved in the study included TEG (triethylene glycol), PEG oligomers (PEG 400, PEGS 1000, PEG 2000, PEG 4000), and PEGS-based monomers such as PEG methyl ether acrylate (mPEGSA) and PEG methyl ether methacrylate (mPEGsMA-500, mPEGsMA-950). Previous research suggested that PEG 400 and PEG 2000 exhibited minimal cytotoxicity at a concentration of 5 mg/mL, while PEG 1000 and PEG 4000 displayed higher toxicity, particularly towards the L929 cell line. This implies that molecular weight and osmolality might not be directly correlated with cytotoxicity. However, our study contradicts this report, as we found that the cytotoxicity of PEG 400, PEG 1000, and PEG 4000 increased based on the MTT assay. Discrepancies between the studies may arise from differences in the MTT assay protocols. In our approach, cells were exposed to a higher concentration of PEGs for a shorter duration, emphasizing acute effects, whereas Lie et al. incubated cells for 24 hours, emphasizing the impact of PEGs on cell proliferation. Furthermore, Hodaei et al. reported that after 24 hours of incubation, PEG 4000, PEG 6000, PEG 10000, and PEG 35000 at 4 w/v% had no cytotoxic effect on Caco-2 cells. In contrast, our study revealed significant toxicity for PEG 400 and PEG 15000 at 4 w/v%, indicating a distinct pattern with acute, high-concentration treatment compared to long-term incubation. Postic et al. explored the impact of PEG 200, 2000, 20000, and poly(vinyl pyrrolidone) 8000 on various cellular parameters in metastatic melanoma A375, mouse fibroblast 3T3, and human corneal epithelial cells over a 72-hour incubation period. Their results indicated that higher concentrations of low molecular weight PEGs significantly altered the number and morphology of A375 cells compared to PVP 8000. The Resazurin assay revealed that PEG 200 was more cytotoxic to A375

and 3T3 cells than other PEGs, while PVP 8000 exhibited a unique dose-dependent killing action against the cells. The effects on human corneal epithelial cells varied among all three PEGs. Caspase 3/7 activation displayed a time-dependent pattern, showing no correlation with molecular weight. In summary, the diverse cellular effects of PEGs are strongly influenced by incubation time and the specific cell types under investigation.

Collectively, the Spearman correlation analysis, as detailed in Table 8, unveiled significant positive correlations between the average molecular weight of the investigated PEGs and cell viability, as indicated by both MTT ( $p=0.0055$ ) and NR assays ( $p=0.0444$ ), along with the percentage of living cells according to flow cytometry ( $p=0.0018$ ). In contrast, a negative correlation was noted between molecular weight and osmolality ( $p=0.0039$ ), as well as the proportion of necrotic cells ( $p=0.0001$ ). These findings suggest that lower molecular weight PEGs exhibit heightened cytotoxic activity, with this effect diminishing as the average PEG chain length increases. Additionally, the correlation matrix revealed associations between osmolality and MTT ( $p<0.0001$ ), NR ( $p=0.0018$ ), the proportion of living cells ( $p=0.0182$ ), and necrotic cells ( $p=0.0098$ ). These results reinforce the concept that the cytotoxicity of PEGs may be attributed to the severe osmotic shock induced during cell exposure to 30  $w/v$  % PEG solutions over a 30-minute incubation period. However, sorbitol solutions did not manifest cytotoxic effects in both the MTT and NR assays, despite comparable osmolality to PEGs. This suggests that osmolality alone might not be solely responsible for the observed decrease in cell viability. There may be an unexplored factor or cellular effect related to molecular weight contributing to the cytotoxicity of PEGs.

Wang et al. discovered that the cellular uptake mechanism of PEGs depended on their molecular weight. They found that low molecular weight PEGs (750-2000) were exclusively taken up through passive diffusion, while longer derivatives also utilized endocytosis as a significant mechanism.<sup>182</sup> Additionally, the study highlighted that cellular uptake was influenced by factors such as incubation time and temperature. Notably, mesenchymal stem cells exhibited varying tolerance levels to sodium chloride, sorbitol, and PEG 3000, despite being applied at the same osmolality.<sup>196</sup> Additionally, the type of osmolyte had a significant impact on various factors related to chondrogenesis, regardless of osmolality. This suggests that only low molecular weight PEGs could penetrate the cells within the brief incubation period, possibly explaining our results. Furthermore, the specific sensitivity of Caco-2 cells to PEGs and their tolerance to sorbitol could also contribute to these findings.

Unfortunately, there is a dearth of prior research on the influence of non-modified PEGs in *G. mellonella* larvae and their role in autophagosome formation. This absence of pre-existing studies poses a challenge in comparing our findings with previous literature. Nevertheless, the well-established correlation between osmotic stress and the induction of autophagy has been extensively explored, revealing a substantial impact.<sup>197,198</sup> Autophagosome formation did not show any correlation with molecular weight, suggesting that autophagy is generally a late-phase response to osmotic stress.<sup>198</sup> The significant increase in autophagosome formation observed in this investigation can be attributed to the facile penetration of low molecular weight PEGs into the cells. Past research has demonstrated that a mere 30 minutes of hyperosmotic incubation can initiate the formation of proteasomes.<sup>199</sup> It is essential to conduct additional research to identify the specific property of PEGs that exerts the most substantial influence on the process. Notably, unexpected cellular effects of PEGs have been documented, including the capacity of PEGS 35 to influence the uptake of exosomes and diminish the levels of IL-1 $\beta$ .<sup>200</sup> Unmodified PEGs had not been previously injected into *G. mellonella* for toxicity evaluation. Our findings showed that only molecular weight ( $p=0.0403$ ) demonstrated a notable correlation with overall larvae mortality. Macromolecules are infrequently examined in this novel model organism; nevertheless, at elevated concentrations, they display toxicity that is dependent on concentration.<sup>201</sup> Moreover, labeled annexin V served as an indicator for early-stage apoptosis, and our results indicated no correlation between the proportion of stained cells and osmolality. Literature suggests that the conjugation of PEG 12000 to interferon- $\alpha 2b$  did not lead to a noteworthy increase in apoptotic activity, in contrast to observations with PEG 5000-coated silver nanoparticles compared to citrate-coated counterparts.<sup>202,203</sup> Additional flow cytometry experiments are required to clarify the division of cells between necrotic and early apoptotic populations after PEGS treatment. We hypothesize it is significantly influenced by the PEG concentration and the duration of incubation.

In summary, the analysis indicates a significant correlation between osmolality, cell viability (measured by various methods), and the molecular weight of PEGs. However, more intricate phenomena such as early-stage apoptosis, autophagosome formation, and in vivo toxicity (larvae survival) do not display a direct association with molecular weight.

When anticipating the biological effects of a previously untested PEG, only straightforward cellular interactions, such as (cyto)toxicity through necrosis, can be

approximated based on prior experiments with PEGs of varying molecular weights. Further investigation is essential to unveil which properties of PEGs influence more complex mechanisms like autophagosome formation or apoptosis. Through thorough testing, the contributing factors can be identified, and statistical correlations can be established to elucidate the connection between biological effects and chemical or physical attributes.

Until additional research is conducted, it is prudent to approach the estimation of cellular actions of PEGs cautiously, particularly when comparing new derivatives to established ones based solely on molecular characteristics.

## 11. DISCUSSION II.

Ketoprofen, a widely utilized NSAID with diverse therapeutic applications, exhibits remarkably low water solubility. Enhancing its solubility is imperative for improved bioavailability, and various methods can be employed to achieve this. Solid dispersions have become increasingly popular due to their favorable characteristics.<sup>204</sup> In our study, we aimed to investigate the binary dispersions of ketoprofen with three polymers of distinct molecular weights: PEG 1000, 1500, and 2000. Our objective was to delineate the variations among the solid dispersions produced by these three molecules and their dissolution properties.

Our phase solubility study (Figure 21) reveals a significant increase in PEGs solubility. Specifically, we observed an augmentation in ketoprofen solubility from 41  $\mu\text{g/mL}$  to 300  $\mu\text{g/mL}$ . Importantly, there was no statistically significant difference among the three polymers. This observation aligns with the findings of Khattab et al., who demonstrated minimal differences in the solubility-enhancing properties of PEGs 4000, 10000, and 20000 for gliclazide.<sup>205</sup> Our results, within the 1-10  $w/v\%$  range, also correspond well with the previous research by Mura et al., indicating a proportional increase in the solubility of ketoprofen when using PEGs within this range.<sup>206</sup> Table 13 illustrates the negative free energy transfer across all concentrations and polymers, indicating the spontaneity of the drug solubilization process. This process is even more advantageous at higher concentrations of the polymers, as evident from the decreasing free energy for the solutions with higher concentrations. Furthermore, based on the  $K_a$  values, it is observed an increase in the binding affinity between ketoprofen and the PEGs as the molecular weight of the PEGs increases.

When examining the six samples, outcomes from both the FT-IR (Figure 22) and the PXRD (Figure 23) analyses suggest the formation, albeit partial, of a solid dispersion even at room temperature, particularly in the case of the physical mixture involving PEGs 1000. Despite the initial mixing being conducted with liquid and subsequent cooled storage before investigation, the infrequently used PEG 1000 for preparing hot melt solid dispersions is attributed to its low melting range. The shifts observed in the characteristic IR bands are ascribed to hydrogen bond formation between ketoprofen and the polymer, a phenomenon previously reported in different ketoprofen solid dispersions.<sup>118,,188,189</sup> Overall, the noted alterations in the spectra indicate the formation of a solid dispersion, distinguishing it from a mere physical mixture.<sup>209,210</sup> The scanning electron microscopy

images (Figure 25 B, D, F) affirm the homogeneous distribution of the API, but the presence of ketoprofen crystals in the solid dispersion texture suggests incomplete conversion into the amorphous phase.

The primary merit of a solid dispersion lies in its ability to generate supersaturated solutions of the given API. In an ideal system, the API exists 100% in an amorphous state. Consequently, the dissolution of the matrix polymer results in a supersaturated colloidal solution, where the kinetic solubility exceeds the "normal" thermodynamic solubility determined by the physicochemical properties of the crystalline form.<sup>211</sup> Comparing Figure 21 to Figure 26, highlights the difference in solubility values. In the phase solubility studies, a 24-hour interval between initial dissolution and ketoprofen measurement initiated amorphous API particle crystallization, which could be separated by centrifugation, leading to a significant decrease in the dissolved ketoprofen amount.<sup>212</sup> During the dissolution experiment, we observed a sufficiently short time window to detect the formation of a supersaturated solution. In Figure 26, the dotted line illustrates the theoretical maximum solubility of ketoprofen in the presence of the investigated PEGs at concentrations equal to the amount of PEGs in each capsule. This supersaturation phenomenon can be attributed to the prevention of crystallization by the polymer matrix.<sup>213-215</sup> Consequently, enhanced bioavailability can be assumed.<sup>144,216,217</sup>

Table 17 presents a compilation of diverse studies investigating solid dispersions using different PEGs as the polymer matrix. It is evident from the data that establishing a universal correlation between molecular weight and dissolution rate is challenging, as this relationship is significantly influenced by the specific APIs employed. Duong and Van den Mooter propose a potential explanation for this phenomenon in their review.<sup>135</sup> According to them, fenofibrate, which does not form hydrogen bonds with PEGs, and flurbiprofen, which does, show that the dissolution of the solid dispersion is unaffected by molecular weight as PEGs remains neutral.<sup>218,219</sup> However, this explanation does not exclusively account for the observed outcomes. For example, in the case of other potential hydrogen-bond-forming molecules like naproxen, the dissolution profiles of solid dispersions were unaffected by molecular weight. Unfortunately, our findings fall under the "None" classification as outlined in Table 17, with PEG 1000 exhibiting a higher percentage of released drug compared to PEG 1500 and PEG 2000, despite the nearly identical characteristics of the latter two. Despite the confirmed formation of hydrogen bonds in the interaction between ketoprofen and PEG 1000, 1500, and 2000, our study did not reveal a clear correlation between molecular weight and dissolution properties.

<b>Publication</b>	<b>API</b>	<b>PEGs</b>	<b>Relationship of molecular weight and percentage of released drug</b>
Ford et al. <sup>220</sup>	indomethacin, phenylbutazone	1500, 4000, 6000, 20000	Inverse proportionality
Miralles et al. <sup>221</sup>	tolbutamide	4000, 6000	Inverse proportionality
Serajuddin et al. <sup>222</sup>	$\alpha$ -Pentyl-3-(2-quinolinylmethoxy)benzene methanol	1000, 1450, 8000	Inverse proportionality
Chiou and Riegelman <sup>223</sup>	griseofulvin	4000, 20000	Proportional
Betageri and Makarla <sup>224</sup>	glyburide	4000, 6000	Proportional
Anguiano-Igea et al. <sup>225</sup>	clofibrate	10000, 20000, 35000	Proportional
Dordunoo and Rubinstein <sup>226</sup>	triamterene, temazepam	1500, 2000, 4000, 6000	Proportional
Mura et al. <sup>227</sup>	naproxen	4000, 6000, 20000	None
Khattab et al. <sup>228</sup>	gliclazide	4000, 10000, 20000	None
Trapani et al. <sup>229</sup>	zolpidem	4000, 6000	None

**Table 17: Some review of SDs dissolution studies, prepared with multiple PEGs.**

Our findings indicate (Figure 26, Table 14, 15) that both the physical mixtures and solid dispersions of PEG 1500 and 2000 yielded similar. It has been noted that the dissolution rate of the polymer may decrease when it is part of a solid dispersion rather than being freely present as in a physical mixture.<sup>230</sup> However, the low melting ranges of PEG 1500 and 2000 may have led to the in situ formation of a solid dispersion from the physical mixtures while inside the capsule. Even if this phase transition occurred only partially, the physical mixture exhibited the potential to elevate the percentage of released

drug to the level observed in the original solid dispersion. The difference between PEGS 1000 SD and PM could be explained by the lowest  $K_a$  values, indicating a lower binding affinity of ketoprofen toward the carrier. We believe that the unique combination of ketoprofen-PEGs interactions altering the dissolution rate of the polymer and the in-situ phase transition of physical mixtures accounts for our results.

Our observation of the kinetics profile (Table 14) for the samples is consistent with existing literature, when SDs commonly exhibit a good fit for both Korsmeyer-Peppas and zero-order models.<sup>212,231,232</sup>

Overall, our investigation supports the conclusion that the molecular weight of PEGs do not have a straightforward impact on the dissolution profile of ketoprofen. Surprisingly, the physical mixtures of PEG 1500 and 2000 were nearly identical to their respective solid dispersions, suggesting a potential method for easily and simply enhancing the solubility of ketoprofen. Further research confirming the in situ solid dispersion formation could lead to the development of simple powder-loaded capsules that enhance the bioavailability of the API compared to conventional dosage forms.

## 12. SUMMARY

To summarize, our study investigated numerous cellular effects, in vivo toxicity, as well as osmolality of eleven different polyethylene glycols on Caco-2 cells. Data analysis with different statistical methods revealed a notable correlation among cytotoxicity, osmolality, and the molecular weight of PEGs. In general, lower molecular weight PEGs demonstrated a substantial decrease in cell viability, elevated osmolality, and elevated the mortality of larvae, while PEGs with higher molecular weights generally exhibited minimal impact on cells and lowered osmolality. Further scientific inquiries are necessary to gain a deeper understanding of the impact of PEGs on autophagosome formation and early apoptosis. However, it can be affirmed that specific biological effects of PEGs cannot be accurately evaluated solely from their molecular weight.

Overall, it can be concluded, that no rule of thumb can be applied for the molecular weight of PEGs as polymer matrices of solid dispersions, if the question is their ability to modify dissolution curve of a drug molecule. Each PEG-API interaction must be investigated on its own and trial-error methods must be used to test out what is the optimal molecular weight, drug:polymer ratio for each situation. Also, the comparison of physical mixtures and solid dispersions must be carried out especially in case of carriers where the melting point/range is in the physiological range of the gastro-intestinal tract.

We describe the formulation of ketoprofen and PEG physical mixtures as well as solid dispersions in a ratio of 1:9. It was observed that at room temperature, the physical mixture PEGS 1000 began to melt, leading to the creation of a partial solid dispersion. On the contrary, the formulations of PEG 1500 and 2000 exhibited distinct PXRD and FT-IR spectra, and their physical characteristics varied as observed in scanning electron microscopic images. The dissolution study carried out in hydrochloric acid media indicated no difference between the formulations with PEG 1500 and 2000, while demonstrating a notably higher quantity of dissolved API in the PEG 1000 solid dispersion. However, in each case, a supersaturated solution was identified, as the quantity of dissolved ketoprofen exceeded the theoretical maximum suggested by the phase solubility study.

In summary, our findings demonstrate that, in the case of low molecular weight PEGs, polymer's length does no influence dissolution profile of ketoprofen solid dispersions directly. Unfortunately, our results can only be moderately compared to other research articles, as the investigation of binary solid dispersions is currently outside the

scope of researchers, and most publications do not focus on the impact of molecular weight but on other aspects of solid dispersion formulation. Further investigation is required to study the dissolution of different formulations to explain the interesting results of the dissolution study. Only the PEG 1000-ketoprofen solid dispersion surpassed its physical mixture counterpart, with PEG 1500 and 2000 exhibiting considerable similarity to each other. Additionally, the physical mixture of PEG 1000 showed a relatively high amount of dissolved API. These findings indicate that, for low molecular weight PEGs, forming a solid dispersion may not be essential to achieve a supersaturated solution in the stomach, thereby significantly enhancing the bioavailability of the given API. Even a simple physical mixture can improve drug delivery due to the combination of the melting point and dissolution speed of PEGs, along with the unique interaction between ketoprofen and the polymers. Further investigation is necessary to delve into the potential utilization of this characteristic of low molecular weight polyethylene glycol derivatives.

### 13. REFERENCES

1. Herzberger, J., Niederer, K., Pohlit, H., Seiwert, J., Worm, M., Wurm, F. R., & Frey, H. (2016). Polymerization of Ethylene Oxide, Propylene Oxide, and Other Alkylene Oxides: Synthesis, Novel Polymer Architectures, and Bioconjugation. *Chemical Reviews*, *116*(4), 2170–2243. <https://doi.org/10.1021/acs.chemrev.5b00441>
2. Gullapalli, R. P., & Mazzitelli, C. L. (2015). Polyethylene glycols in oral and parenteral formulations—A critical review. *International Journal of Pharmaceutics*, *496*(2), 219–239. <https://doi.org/10.1016/j.ijpharm.2015.11.015>
3. Jang, H.-J., Shin, C. Y., & Kim, K.-B. (2015). Safety Evaluation of Polyethylene Glycol (PEGs) Compounds for Cosmetic Use. *Toxicological Research*, *31*(2), 105–136. <https://doi.org/10.5487/TR.2015.31.2.105>
4. Henning, T. (2001). Polyethylene glycols (PEGs) and the pharmaceutical industry. *Polyethylene Glycols (PEGs) and the Pharmaceutical Industry*, *127*(10), 28–32.
5. Parray, Z. A., Hassan, M. I., Ahmad, F., & Islam, A. (2020). Amphiphilic nature of polyethylene glycols and their role in medical research. *Polymer Testing*, *82*, 106316. <https://doi.org/10.1016/j.polymertesting.2019.106316>
6. D'souza, A. A., & Shegokar, R. (2016). Polyethylene glycol (PEGs): A versatile polymer for pharmaceutical applications. *Expert Opinion on Drug Delivery*, *13*(9), 1257–1275. <https://doi.org/10.1080/17425247.2016.1182485>
7. Veronese, F. M., & Pasut, G. (2005). PEGSylation, successful approach to drug delivery. *Drug Discovery Today*, *10*(21), 1451–1458. [https://doi.org/10.1016/S1359-6446\(05\)03575-0](https://doi.org/10.1016/S1359-6446(05)03575-0)
8. Ensing, B., Tiwari, A., Tros, M., Hunger, J., Domingos, S. R., Pérez, C., Smits, G., Bonn, M., Bonn, D., & Woutersen, S. (2019). On the origin of the extremely different

- solubilities of polyethers in water. *Nature Communications*, 10(1), 2893.  
<https://doi.org/10.1038/s41467-019-10783-z>
9. Gullapalli, R. P., & Mazzitelli, C. L. (2015). Polyethylene glycols in oral and parenteral formulations—A critical review. In *International Journal of Pharmaceutics* (Vol. 496, Issue 2). Elsevier B.V. <https://doi.org/10.1016/j.ijpharm.2015.11.015>
  10. Yang, Z., Peng, H., Wang, W., & Liu, T. (2010). Crystallization behavior of poly( $\epsilon$ -caprolactone)/layered double hydroxide nanocomposites. *Journal of Applied Polymer Science*, 116(5), 2658–2667. <https://doi.org/10.1002/app>
  11. Torsten, H. (2002). Polyethylene glycols (PEGs) and the pharmaceutical industry. *Pharma Chem*, June, 57–59.
  12. Baird, J. A., Olayo-Valles, R., Rinaldi, C., & Taylor, L. S. (2010). Effect of Molecular Weight, Temperature, and Additives on the Moisture Sorption Properties of Polyethylene Glycol. *Journal of Pharmaceutical Sciences*, 99(1), 154–168. <https://doi.org/10.1002/jps.21808>
  13. Harris, J. M., & Chess, R. B. (2003). Effect of PEGsylation on pharmaceuticals. *Nature Reviews Drug Discovery*, 2(3), 214–221. <https://doi.org/10.1038/nrd1033>
  14. Hempel, N.-J., Dao, T., Knopp, M. M., Berthelsen, R., & Löbmann, K. (2020). The Influence of Temperature and Viscosity of Polyethylene Glycol on the Rate of Microwave-Induced In Situ Amorphization of Celecoxib. *Molecules*, 26(1), 110. <https://doi.org/10.3390/molecules26010110>
  15. Ray Foster, L. J. (2010). PEGSylation and BioPEGSylation of Polyhydroxyalkanoates: Synthesis, Characterisation and Applications. In M. Elnashar (Ed.), *Biopolymers*. Sciyo. <https://doi.org/10.5772/10265>
  16. Peacock, A. (2000). *Handbook of Polyethylene: Structures: Properties, and Applications* (0 ed.). CRC Press. <https://doi.org/10.1201/9781482295467>

17. Turecek, P. L., Bossard, M. J., Schoetens, F., & Ivens, I. A. (2016). PEGSylation of Biopharmaceuticals: A Review of Chemistry and Nonclinical Safety Information of Approved Drugs. *Journal of Pharmaceutical Sciences*, 105(2), 460–475. <https://doi.org/10.1016/j.xphs.2015.11.015>
18. Yang, Q., & Lai, S. K. (2015). Anti- PEGS immunity: Emergence, characteristics, and unaddressed questions. *WIREs Nanomedicine and Nanobiotechnology*, 7(5), 655–677. <https://doi.org/10.1002/wnan.1339>
19. Hoang Thi, T. T., Pilkington, E. H., Nguyen, D. H., Lee, J. S., Park, K. D., & Truong, N. P. (2020). The Importance of Poly(ethylene glycol) Alternatives for Overcoming PEGS Immunogenicity in Drug Delivery and Bioconjugation. *Polymers*, 12(2), 298. <https://doi.org/10.3390/polym12020298>
20. Hassan, C., East, J., Radaelli, F., Spada, C., Benamouzig, R., Bisschops, R., Bretthauer, M., Dekker, E., Dinis-Ribeiro, M., Ferlitsch, M., Fuccio, L., Awadie, H., Gralnek, I., Jover, R., Kaminski, M. F., Pellisé, M., Triantafyllou, K., Vanella, G., Mangas-Sanjuan, C., ... Dumonceau, J.-M. (2019). Bowel preparation for colonoscopy: European Society of Gastrointestinal Endoscopy (ESGE) Guideline – Update 2019. *Endoscopy*, 51(08), 775–794. <https://doi.org/10.1055/a-0959-0505>
21. Lee-Robichaud, H., Thomas, K., Morgan, J., & Nelson, R. L. (2010). Lactulose versus Polyethylene Glycol for Chronic Constipation. *The Cochrane Database of Systematic Reviews*, 7, CD007570. <https://doi.org/10.1002/14651858.CD007570.pub2>
22. Knop, K., Hoogenboom, R., Fischer, D., & Schubert, U. S. (2010). Poly(ethylene glycol) in Drug Delivery: Pros and Cons as Well as Potential Alternatives. *Angewandte Chemie International Edition*, 49(36), 6288–6308. <https://doi.org/10.1002/anie.200902672>

23. Luneva, O., Olekhovich, R., & Uspenskaya, M. (2022). Bilayer Hydrogels for Wound Dressing and Tissue Engineering. *Polymers*, *14*(15), 3135. <https://doi.org/10.3390/polym14153135>
24. Maji, S., & Lee, H. (2022). Engineering Hydrogels for the Development of Three-Dimensional In Vitro Models. *International Journal of Molecular Sciences*, *23*(5), 2662. <https://doi.org/10.3390/ijms23052662>
25. Nicodemus, G. D., & Bryant, S. J. (2008). Cell Encapsulation in Biodegradable Hydrogels for Tissue Engineering Applications. *Tissue Engineering Part B: Reviews*, *14*(2), 149–165. <https://doi.org/10.1089/ten.teb.2007.0332>
26. Lutolf, M. P., & Hubbell, J. A. (2005). Synthetic biomaterials as instructive extracellular microenvironments for morphogenesis in tissue engineering. *Nature Biotechnology*, *23*(1), 47–55. <https://doi.org/10.1038/nbt1055>
27. Drury, J. L., & Mooney, D. J. (2003). Hydrogels for tissue engineering: Scaffold design variables and applications. *Biomaterials*, *24*(24), 4337–4351. [https://doi.org/10.1016/S0142-9612\(03\)00340-5](https://doi.org/10.1016/S0142-9612(03)00340-5)
28. Lee, K. Y., & Mooney, D. J. (2001). Hydrogels for Tissue Engineering. *Chemical Reviews*, *101*(7), 1869–1880. <https://doi.org/10.1021/cr000108x>
29. Hadinoto, K., Tran, T.-T., & Cheow, W. S. (2022). Beyond tablets' physical characteristics: Incorporating environmental sustainability metrics into the selection of lubricants for pharmaceutical tableting. *Journal of Cleaner Production*, *362*, 132336. <https://doi.org/10.1016/j.jclepro.2022.132336>
30. Oliveira, C. P., Ribeiro, M. E. N. P., Ricardo, N. M. P. S., Souza, T. V. D. P., Moura, C. L., Chaibundit, C., Yeates, S. G., Nixon, K., & Attwood, D. (2011). The effect of water-soluble polymers, PEGS and PVP, on the solubilisation of griseofulvin in

- aqueous micellar solutions of Pluronic F127. *International Journal of Pharmaceutics*, 421(2), 252–257. <https://doi.org/10.1016/j.ijpharm.2011.10.010>
31. Al-Shdefat, R. (2020). Solubility determination and solution thermodynamics of olmesartan medoxomil in (PEGS-400 + water) cosolvent mixtures. *Drug Development and Industrial Pharmacy*, 46(12), 2098–2104. <https://doi.org/10.1080/03639045.2020.1847136>
32. Owensiii, D., & Peppas, N. (2006). Opsonization, biodistribution, and pharmacokinetics of polymeric nanoparticles. *International Journal of Pharmaceutics*, 307(1), 93–102. <https://doi.org/10.1016/j.ijpharm.2005.10.010>
33. Abdellatif, A. A. H., El-Telbany, D. F. A., Zayed, G., & Al-Sawahli, M. M. (2019). Hydrogel Containing PEGS-Coated Fluconazole Nanoparticles with Enhanced Solubility and Antifungal Activity. *Journal of Pharmaceutical Innovation*, 14(2), 112–122. <https://doi.org/10.1007/s12247-018-9335-z>
34. Kędzierska, M., Potemski, P., Drabczyk, A., Kudłacik-Kramarczyk, S., Głąb, M., Grabowska, B., Mierzwiński, D., & Tyliczszak, B. (2021). The Synthesis Methodology of PEGSylated Fe<sub>3</sub>O<sub>4</sub>@Ag Nanoparticles Supported by Their Physicochemical Evaluation. *Molecules*, 26(6), 1744. <https://doi.org/10.3390/molecules26061744>
35. Salmaso, S., & Caliceti, P. (2013). Stealth Properties to Improve Therapeutic Efficacy of Drug Nanocarriers. *Journal of Drug Delivery*, 2013, 1–19. <https://doi.org/10.1155/2013/374252>
36. Torchilin, V. P. (2005). Recent advances with liposomes as pharmaceutical carriers. *Nature Reviews Drug Discovery*, 4(2), 145–160. <https://doi.org/10.1038/nrd1632>

37. Klinkmann, H., Wolf, H., & Schmitt, E. (1984). Definition of Biocompatibility. In G. Bucciatti (Ed.), *Contributions to Nephrology* (Vol. 37, pp. 70–77). S. Karger AG. <https://doi.org/10.1159/000408553>
38. Bacanlı, M., Anlar, H. G., Başaran, A. A., & Başaran, N. (2017). Assessment of Cytotoxicity Profiles of Different Phytochemicals: Comparison of Neutral Red and MTT Assays in Different Cells in Different Time Periods. *Turkish Journal of Pharmaceutical Sciences*, *14*(2), 95–107. <https://doi.org/10.4274/tjps.07078>
39. Pizzoferrato, A., Ciapetti, G., Stea, S., Cenni, E., Arciola, C. R., Granchi, D., & Savarino, L. (1994). Cell culture methods for testing biocompatibility. *Clinical Materials*, *15*(3), 173–190. [https://doi.org/10.1016/0267-6605\(94\)90081-7](https://doi.org/10.1016/0267-6605(94)90081-7)
40. Komeri, R., Kasoju, N., & Anil Kumar, P. R. (2022). In vitro cytotoxicity and cytocompatibility assays for biomaterial testing under regulatory platform. In *Biomedical Product and Materials Evaluation* (pp. 329–353). Elsevier. <https://doi.org/10.1016/B978-0-12-823966-7.00009-8>
41. Bácskay, I., Nemes, D., Fenyvesi, F., Váradi, J., Vasvári, G., Fehér, P., Vecsernyés, M., & Ujhelyi, Z. (2018). Role of Cytotoxicity Experiments in Pharmaceutical Development. In T. A. Çelik (Ed.), *Cytotoxicity*. InTech. <https://doi.org/10.5772/intechopen.72539>
42. Salih Istifli, E., Tahir Hüsün, M., & Basri Ila, H. (2019). Cell Division, Cytotoxicity, and the Assays Used in the Detection of Cytotoxicity. In E. Salih Istifli & H. Basri Ila (Eds.), *Cytotoxicity—Definition, Identification, and Cytotoxic Compounds*. IntechOpen. <https://doi.org/10.5772/intechopen.88368>
43. Kamiloglu, S., Sari, G., Ozdal, T., & Capanoglu, E. (2020). Guidelines for cell viability assays. *Food Frontiers*, *1*(3), 332–349. <https://doi.org/10.1002/fft2.44>

44. Mosmann, T. (1983). Rapid colorimetric assay for cellular growth and survival: Application to proliferation and cytotoxicity assays. *Journal of Immunological Methods*, 65(1–2), 55–63. [https://doi.org/10.1016/0022-1759\(83\)90303-4](https://doi.org/10.1016/0022-1759(83)90303-4)
45. Kuete, V., Karaosmanoğlu, O., & Sivas, H. (2017). Anticancer Activities of African Medicinal Spices and Vegetables. In *Medicinal Spices and Vegetables from Africa* (pp. 271–297). Elsevier. <https://doi.org/10.1016/B978-0-12-809286-6.00010-8>
46. Segeritz, C.-P., & Vallier, L. (2017). Cell Culture. In *Basic Science Methods for Clinical Researchers* (pp. 151–172). Elsevier. <https://doi.org/10.1016/B978-0-12-803077-6.00009-6>
47. Zhang, L., Zhang, L., Zhang, M., Pang, Y., Li, Z., Zhao, A., & Feng, J. (2015). Self-emulsifying drug delivery system and the applications in herbal drugs. *Drug Delivery*, 22(4), 475–486. <https://doi.org/10.3109/10717544.2013.861659>
48. Li, A. P. (2005). Preclinical in vitro screening assays for drug-like properties. *Drug Discovery Today: Technologies*, 2(2), 179–185. <https://doi.org/10.1016/j.ddtec.2005.05.024>
49. Ali, M. Y., Anand, S. V., Tangella, K., Ramkumar, D., & Saif, T. A. (2015). Isolation of Primary Human Colon Tumor Cells from Surgical Tissues and Culturing Them Directly on Soft Elastic Substrates for Traction Cytometry. *Journal of Visualized Experiments*, 100, 52532. <https://doi.org/10.3791/52532>
50. Ghanemi, A. (2015). Cell cultures in drug development: Applications, challenges and limitations. *Saudi Pharmaceutical Journal*, 23(4), 453–454. <https://doi.org/10.1016/j.jsps.2014.04.002>
51. Arango, M.-T., Quintero-Ronderos, P., Castiblanco, J., & Montoya-Ortíz, G. (2013). Cell culture and cell analysis. In *Autoimmunity: From Bench to Bedside [Internet]*. El Rosario University Press. <https://www.ncbi.nlm.nih.gov/books/NBK459464/>

52. Wiegand, C., & Hipler, U.-C. (2009). Evaluation of Biocompatibility and Cytotoxicity Using Keratinocyte and Fibroblast Cultures. *Skin Pharmacology and Physiology*, 22(2), 74–82. <https://doi.org/10.1159/000178866>
53. Hidalgo, I. J., Raub, T. J., & Borchardt, R. T. (1989). Characterization of the human colon carcinoma cell line (Caco-2) as a model system for intestinal epithelial permeability. *Gastroenterology*, 96(3), 736–749.
54. Fogh, J., Wright, W. C., & Loveless, J. D. (1977). Absence of HeLa Cell Contamination in 169 Cell Lines Derived From Human Tumors<sup>2</sup>. *JNCI: Journal of the National Cancer Institute*, 58(2), 209–214. <https://doi.org/10.1093/jnci/58.2.209>
55. Lea, T. (2015). Caco-2 Cell Line. In K. Verhoeckx, P. Cotter, I. López-Expósito, C. Kleiveland, T. Lea, A. Mackie, T. Requena, D. Swiatecka, & H. Wichers (Eds.), *The Impact of Food Bioactives on Health* (pp. 103–111). Springer International Publishing. [https://doi.org/10.1007/978-3-319-16104-4\\_10](https://doi.org/10.1007/978-3-319-16104-4_10)
56. Cao, W., Feng, B., Cheng, L., Wang, Y., Wang, J., & Wang, X. (2016). The octanol/water distribution coefficients of ardisin and its metabolites, and their permeation characteristics across Caco-2 cell monolayer. *Chemistry Central Journal*, 10(1), 29. <https://doi.org/10.1186/s13065-016-0175-y>
57. Harris, J. M. (Ed.). (1992). *Poly(Ethylene Glycol) Chemistry: Biotechnical and Biomedical Applications*. Springer US. <https://doi.org/10.1007/978-1-4899-0703-5>
58. Caliceti, P. (2003). Pharmacokinetic and biodistribution properties of poly(ethylene glycol)–protein conjugates. *Advanced Drug Delivery Reviews*, 55(10), 1261–1277. [https://doi.org/10.1016/S0169-409X\(03\)00108-X](https://doi.org/10.1016/S0169-409X(03)00108-X)
59. Li, M., Jiang, S., Simon, J., Paßlick, D., Frey, M.-L., Wagner, M., Mailänder, V., Crespy, D., & Landfester, K. (2021). Brush Conformation of Polyethylene Glycol Determines the Stealth Effect of Nanocarriers in the Low Protein Adsorption

- Regime. *Nano Letters*, 21(4), 1591–1598.  
<https://doi.org/10.1021/acs.nanolett.0c03756>
60. Hinderer, S., Layland, S. L., & Schenke-Layland, K. (2016). ECM and ECM-like materials—Biomaterials for applications in regenerative medicine and cancer therapy. *Advanced Drug Delivery Reviews*, 97, 260–269.  
<https://doi.org/10.1016/j.addr.2015.11.019>
61. Wang, H., & Heilshorn, S. C. (2015). Adaptable Hydrogel Networks with Reversible Linkages for Tissue Engineering. *Advanced Materials*, 27(25), 3717–3736.  
<https://doi.org/10.1002/adma.201501558>
62. Soppimath, K. S., Aminabhavi, T. M., Kulkarni, A. R., & Rudzinski, W. E. (2001). Biodegradable polymeric nanoparticles as drug delivery devices. *Journal of Controlled Release*, 70(1–2), 1–20. [https://doi.org/10.1016/S0168-3659\(00\)00339-4](https://doi.org/10.1016/S0168-3659(00)00339-4)
63. Hodaei, D., Baradaran, B., Valizadeh, H., & Zakeri-Milani, P. (2015). Effects of polyethylene glycols on intestinal efflux pump expression and activity in Caco-2 cells. *Brazilian Journal of Pharmaceutical Sciences*, 51(3), 745–753.  
<https://doi.org/10.1590/S1984-82502015000300026>
64. Parnaud, G., Corpet, D. E., & Gamet-Payrastre, L. (2001). Cytostatic effect of polyethylene glycol on human colonic adenocarcinoma cells. *International Journal of Cancer*, 92(1), 63–69. [https://doi.org/10.1002/1097-0215\(200102\)9999:9999<::AID-IJC1158>3.0.CO;2-8](https://doi.org/10.1002/1097-0215(200102)9999:9999<::AID-IJC1158>3.0.CO;2-8)
65. LoBiondo-Wood, G., & Haber, J. (Eds.). (2022). *Nursing research: Methods and critical appraisal for evidence-based practice* (10th edition). Elsevier.
66. Kim, J., Lee, K.-W., Hefferan, T. E., Currier, B. L., Yaszemski, M. J., & Lu, L. (2008). Synthesis and Evaluation of Novel Biodegradable Hydrogels Based on Poly(ethylene

- glycol) and Sebacic Acid as Tissue Engineering Scaffolds. *Biomacromolecules*, 9(1), 149–157. <https://doi.org/10.1021/bm700924n>
67. Herold, D. A., Rodeheaver, G. T., Bellamy, W. T., Fitton, L. A., Bruns, D. E., & Edlich, R. F. (1982). Toxicity of topical polyethylene glycol. *Toxicology and Applied Pharmacology*, 65(2), 329–335. [https://doi.org/10.1016/0041-008X\(82\)90016-3](https://doi.org/10.1016/0041-008X(82)90016-3)
68. Prentice, D. E., & Majeed, S. K. (1978). Oral toxicity of polyethylene glycol (PEGS 200) in monkeys and rats. *Toxicology Letters*, 2(2), 119–122. [https://doi.org/10.1016/0378-4274\(78\)90084-X](https://doi.org/10.1016/0378-4274(78)90084-X)
69. Bruns, D. E., Herold, D. A., Rodeheaver, G. T., & Edlich, R. F. (1982). Polyethylene glycol intoxication in burn patients. *Burns*, 9(1), 49–52. [https://doi.org/10.1016/0305-4179\(82\)90136-X](https://doi.org/10.1016/0305-4179(82)90136-X)
70. Li, B., Dong, X., Fang, S., Gao, J., Yang, G., & Zhao, H. (2011). Systemic toxicity and toxicokinetics of a high dose of polyethylene glycol 400 in dogs following intravenous injection. *Drug and Chemical Toxicology*, 34(2), 208–212. <https://doi.org/10.3109/01480545.2010.500292>
71. Sarzi- Puttini, P., Atzeni, F., Lanata, L., Bagnasco, M., Colombo, M., Fischer, F., & D'Imporzano, M. (2011). Pain and ketoprofen: What is its role in clinical practice? *Reumatismo*, 62(3), 172–188. <https://doi.org/10.4081/reumatismo.2010.172>
72. Kantor, T. G. (1986). Ketoprofen: A review of its pharmacologic and clinical properties. *Pharmacotherapy*, 6(3), 93–103. <https://doi.org/10.1002/j.1875-9114.1986.tb03459.x>
73. López-Muñoz, F., Gama, N., Soria-Arteche, O., Hurtado Y de la Peña, M., Domínguez, A., & Medina Lopez, J. R. (2013). HPLC Method with Solid-Phase Extraction for Determination of (R)- and (S)-Ketoprofen in Plasma without Caffeine Interference:

- Application to Pharmacokinetic Studies in Rats. *Journal of Chromatographic Science*, 52. <https://doi.org/10.1093/chromsci/bmt178>
74. Medina-López, R., Vara-Gama, N., Soria-Arteche, O., Moreno-Rocha, L., & López-Muñoz, F. (2018). Pharmacokinetics and Pharmacodynamics of (S)-Ketoprofen Co-Administered with Caffeine: A Preclinical Study in Arthritic Rats. *Pharmaceutics*, 10(1), 20. <https://doi.org/10.3390/pharmaceutics10010020>
75. Atzeni, F., Masala, I. F., Bagnasco, M., Lanata, L., Mantelli, F., & Sarzi-Puttini, P. (2021). Comparison of Efficacy of Ketoprofen and Ibuprofen in Treating Pain in Patients with Rheumatoid Arthritis: A Systematic Review and Meta-Analysis. *Pain and Therapy*, 10(1), 577–588. <https://doi.org/10.1007/s40122-021-00250-3>
76. Kuczyńska, J., Pawlak, A., & Nieradko-Iwanicka, B. (2022). The comparison of dexketoprofen and other painkilling medications (review from 2018 to 2021). *Biomedicine & Pharmacotherapy*, 149, 112819. <https://doi.org/10.1016/j.biopha.2022.112819>
77. Chawla, G., Ranjan, C., Kumar, J., & A. Siddiqui, A. (2017). Chemical Modifications of Ketoprofen (NSAID) in Search of Better Lead Compounds: A Review of Literature From 2004-2016. *Anti-Inflammatory & Anti-Allergy Agents in Medicinal Chemistry*, 15(3), 154–177. <https://doi.org/10.2174/1871523016666170217094722>
78. Bradley, J.-C., Lang, A., & Williams, A. (2014). *Jean-Claude Bradley Double Plus Good (Highly Curated and Validated) Melting Point Dataset* (p. 312733 Bytes) [dataset]. figshare. <https://doi.org/10.6084/M9.FIGSHARE.1031638>
79. Barbanti, P., Grazzi, L., & Egeo, G. (2019). Pharmacotherapy for acute migraines in children and adolescents. *Expert Opinion on Pharmacotherapy*, 20(4), 455–463. <https://doi.org/10.1080/14656566.2018.1552941>

80. Ziesenitz, V. C., Welzel, T., van Dyk, M., Saur, P., Gorenflo, M., & van den Anker, J. N. (2022). Efficacy and Safety of NSAIDs in Infants: A Comprehensive Review of the Literature of the Past 20 Years. *Paediatric Drugs*, 24(6), 603–655. <https://doi.org/10.1007/s40272-022-00514-1>
81. Almeida, H. F. D., Marrucho, I. M., & Freire, M. G. (2017). Removal of Nonsteroidal Anti-Inflammatory Drugs from Aqueous Environments with Reusable Ionic-Liquid-Based Systems. *ACS Sustainable Chemistry & Engineering*, 5(3), 2428–2436. <https://doi.org/10.1021/acssuschemeng.6b02771>
82. Han, J., Xiao, B., Le, P. K., & Mangwandi, C. (2023). Enhancement of the Solubility of BS Class II Drugs with MOF and MOF/GO Composite Materials: Case Studies of Felodipine, Ketoprofen and Ibuprofen. *Materials*, 16(4), 1554. <https://doi.org/10.3390/ma16041554>
83. Soto, R., Svärd, M., Verma, V., Padrela, L., Ryan, K., & Rasmuson, Å. C. (2020). Solubility and thermodynamic analysis of ketoprofen in organic solvents. *International Journal of Pharmaceutics*, 588, 119686. <https://doi.org/10.1016/j.ijpharm.2020.119686>
84. Czyrski, A. (2019). Determination of the Lipophilicity of Ibuprofen, Naproxen, Ketoprofen, and Flurbiprofen with Thin-Layer Chromatography. *Journal of Chemistry*, 2019, 1–6. <https://doi.org/10.1155/2019/3407091>
85. Sheng, J. J., Kasim, N. A., Chandrasekharan, R., & Amidon, G. L. (2006). Solubilization and dissolution of insoluble weak acid, ketoprofen: Effects of pH combined with surfactant. *European Journal of Pharmaceutical Sciences*, 29(3–4), 306–314. <https://doi.org/10.1016/j.ejps.2006.06.006>
86. Miles, S. (2007). Ketoprofen. In *xPharm: The Comprehensive Pharmacology Reference* (pp. 1–7). Elsevier. <https://doi.org/10.1016/B978-008055232-3.61984-1>

87. Gangishetty, H., Eedara, B. B., & Bandari, S. (2015). Development of ketoprofen loaded proliposomal powders for improved gastric absorption and gastric tolerance: In vitro and in situ evaluation. *Pharmaceutical Development and Technology*, 20(6), 641–651. <https://doi.org/10.3109/10837450.2014.908306>
88. Dahlgren, D., Cano-Cebrián, M.-J., Olander, T., Hedeland, M., Sjöblom, M., & Lennernäs, H. (2020). Regional Intestinal Drug Permeability and Effects of Permeation Enhancers in Rat. *Pharmaceutics*, 12(3), Article 3. <https://doi.org/10.3390/pharmaceutics12030242>
89. Elezović, A., Marić, A., Bišćević, A., Hadžiabdić, J., Škrbo, S., Špirtović-Halilović, S., Rahić, O., Vranić, E., & Elezović, A. (2020). In vitro pH dependent passive transport of ketoprofen and metformin. *ADMET and DMPK*, 9(1), 57–68. <https://doi.org/10.5599/admet.916>
90. Aronson, J. K. (Ed.). (2016). Ketoprofen. In *Meyler's Side Effects of Drugs (Sixteenth Edition)* (pp. 429–430). Elsevier. <https://doi.org/10.1016/B978-0-444-53717-1.00947-1>
91. Jamali, F., & Brocks, D. R. (1990). Clinical Pharmacokinetics of Ketoprofen and Its Enantiomers. *Clinical Pharmacokinetics*, 19(3), 197–217. <https://doi.org/10.2165/00003088-199019030-00004>
92. Vane, J. R. (1971). Inhibition of Prostaglandin Synthesis as a Mechanism of Action for Aspirin-like Drugs. *Nature New Biology*, 231(25), Article 25. <https://doi.org/10.1038/newbio231232a0>
93. Rainsford, K. D. (1999). Profile and mechanisms of gastrointestinal and other side effects of nonsteroidal anti-inflammatory drugs (NSAIDs). *The American Journal of Medicine*, 107(6), 27–35. [https://doi.org/10.1016/S0002-9343\(99\)00365-4](https://doi.org/10.1016/S0002-9343(99)00365-4)

94. Hawkey, C. J. (2001). COX-1 and COX-2 inhibitors. *Best Practice & Research Clinical Gastroenterology*, 15(5), 801–820. <https://doi.org/10.1053/bega.2001.0236>
95. Adelizzi, R. A. (1999). COX-1 and COX-2 in health and disease. *The Journal of the American Osteopathic Association*, 99(11 Suppl), S7-12.
96. Sekiya, I., Morito, T., Hara, K., Yamazaki, J., Ju, Y.-J., Yagishita, K., Mochizuki, T., Tsuji, K., & Muneta, T. (2010). Ketoprofen Absorption by Muscle and Tendon after Topical or Oral Administration in Patients Undergoing Anterior Cruciate Ligament Reconstruction. *AAPS PharmSciTech*, 11(1), 154–158. <https://doi.org/10.1208/s12249-009-9367-2>
97. Mazières, B. (2005). Topical Ketoprofen Patch. *Drugs in R & D*, 6(6), 337–344. <https://doi.org/10.2165/00126839-200506060-00003>
98. Mazières, B., Rouanet, S., Guillon, Y., Scarsi, C., & Reiner, V. (2005). Topical ketoprofen patch in the treatment of tendinitis: A randomized, double blind, placebo controlled study. *The Journal of Rheumatology*, 32(8), 1563–1570.
99. Savjani, K. T., Gajjar, A. K., & Savjani, J. K. (2012). Drug Solubility: Importance and Enhancement Techniques. *ISRN Pharmaceutics*, 2012, 1–10. <https://doi.org/10.5402/2012/195727>
100. Tsume, Y., Mudie, D. M., Langguth, P., Amidon, G. E., & Amidon, G. L. (2014). The Biopharmaceutics Classification System: Subclasses for in vivo predictive dissolution (IPD) methodology and IVIVC. *European Journal of Pharmaceutical Sciences*, 57, 152–163. <https://doi.org/10.1016/j.ejps.2014.01.009>
101. Rautio, J., Kumpulainen, H., Heimbach, T., Oliyai, R., Oh, D., Järvinen, T., & Savolainen, J. (2008). Prodrugs: Design and clinical applications. *Nature Reviews Drug Discovery*, 7, 255–270. <https://doi.org/10.1038/nrd2468>

102. Lipinski, C. A., Lombardo, F., Dominy, B. W., & Feeney, P. J. (2001). Experimental and computational approaches to estimate solubility and permeability in drug discovery and development settings IPII of original article: S0169-409X(96)00423-1. The article was originally published in *Advanced Drug Delivery Reviews* 23 (1997) 3–25. 1. *Advanced Drug Delivery Reviews*, 46(1–3), 3–26. [https://doi.org/10.1016/S0169-409X\(00\)00129-0](https://doi.org/10.1016/S0169-409X(00)00129-0)
103. Leuner, C. (2000). Improving drug solubility for oral delivery using solid dispersions. *European Journal of Pharmaceutics and Biopharmaceutics*, 50(1), 47–60. [https://doi.org/10.1016/S0939-6411\(00\)00076-X](https://doi.org/10.1016/S0939-6411(00)00076-X)
104. Al-Kassas, R., Bansal, M., & Shaw, J. (2017). Nanosizing techniques for improving bioavailability of drugs. *Journal of Controlled Release*, 260, 202–212. <https://doi.org/10.1016/j.jconrel.2017.06.003>
105. Leuner, C., & Dressman, J. (2000). Improving drug solubility for oral delivery using solid dispersions. *European Journal of Pharmaceutics and Biopharmaceutics*, 50(1), 47–60. [https://doi.org/10.1016/S0939-6411\(00\)00076-X](https://doi.org/10.1016/S0939-6411(00)00076-X)
106. Loftsson, T., & Brewster, M. E. (2010). Pharmaceutical applications of cyclodextrins: Basic science and product development. *Journal of Pharmacy and Pharmacology*, 62(11), 1607–1621. <https://doi.org/10.1111/j.2042-7158.2010.01030.x>
107. *The United States pharmacopeia: USP 30 ; The National formulary : NF 25*. (2006). United States Pharmacopeial Convention.
108. *British Pharmacopoeia 2009*. (2008). Stationery Office.
109. Miranda, C., Aceituno, A., Fernández, M., Mendes, G., Rodríguez, Y., Llauro, V., & Cabrera-Pérez, M. Á. (2021). ICH Guideline for Biopharmaceutics Classification System-Based Biowaiver (M9): Toward Harmonization in Latin American

- Countries. *Pharmaceutics*, *13*(3), 363.  
<https://doi.org/10.3390/pharmaceutics13030363>
110. Cook, J. A., Davit, B. M., & Polli, J. E. (2010). Impact of Biopharmaceutics Classification System-Based Biowaivers. *Molecular Pharmaceutics*, *7*(5), 1539–1544. <https://doi.org/10.1021/mp1001747>
111. Bennion, B. J., Be, N. A., McNerney, M. W., Lao, V., Carlson, E. M., Valdez, C. A., Malfatti, M. A., Enright, H. A., Nguyen, T. H., Lightstone, F. C., & Carpenter, T. S. (2017). Predicting a Drug's Membrane Permeability: A Computational Model Validated With *in Vitro* Permeability Assay Data. *The Journal of Physical Chemistry B*, *121*(20), 5228–5237. <https://doi.org/10.1021/acs.jpcc.7b02914>
112. Dahan, A., Zimmermann, E., & Ben-Shabat, S. (2014). Modern Prodrug Design for Targeted Oral Drug Delivery. *Molecules*, *19*(10), 16489–16505. <https://doi.org/10.3390/molecules191016489>
113. Maher, S., Brayden, D., Casettari, L., & Illum, L. (2019). Application of Permeation Enhancers in Oral Delivery of Macromolecules: An Update. *Pharmaceutics*, *11*(1), 41. <https://doi.org/10.3390/pharmaceutics11010041>
114. Khiev, D., Mohamed, Z. A., Vichare, R., Paulson, R., Bhatia, S., Mohapatra, S., Lobo, G. P., Valapala, M., Kerur, N., Passaglia, C. L., Mohapatra, S. S., & Biswal, M. R. (2021). Emerging Nano-Formulations and Nanomedicines Applications for Ocular Drug Delivery. *Nanomaterials*, *11*(1), 173. <https://doi.org/10.3390/nano11010173>
115. Zhang, X., Xing, H., Zhao, Y., & Ma, Z. (2018). Pharmaceutical Dispersion Techniques for Dissolution and Bioavailability Enhancement of Poorly Water-Soluble Drugs. *Pharmaceutics*, *10*(3), 74. <https://doi.org/10.3390/pharmaceutics10030074>
116. Goli, N., Bolla, P. K., & Talla, V. (2018). Antibody-drug conjugates (ADCs): Potent biopharmaceuticals to target solid and hematological cancers- an overview. *Journal*

- of Drug Delivery Science and Technology*, 48, 106–117.  
<https://doi.org/10.1016/j.jddst.2018.08.022>
117. Bolla, P. K., Rodriguez, V. A., Kalhapure, R. S., Kolli, C. S., Andrews, S., & Renukuntla, J. (2018). A review on pH and temperature responsive gels and other less explored drug delivery systems. *Journal of Drug Delivery Science and Technology*, 46, 416–435. <https://doi.org/10.1016/j.jddst.2018.05.037>
118. Tiwari, G., Tiwari, R., Bannerjee, S., Bhati, L., Pandey, S., Pandey, P., & Sriwastawa, B. (2012). Drug delivery systems: An updated review. *International Journal of Pharmaceutical Investigation*, 2(1), 2. <https://doi.org/10.4103/2230-973X.96920>
119. Khadka, P., Ro, J., Kim, H., Kim, I., Kim, J. T., Kim, H., Cho, J. M., Yun, G., & Lee, J. (2014). Pharmaceutical particle technologies: An approach to improve drug solubility, dissolution and bioavailability. *Asian Journal of Pharmaceutical Sciences*, 9(6), 304–316. <https://doi.org/10.1016/j.ajps.2014.05.005>
120. Novelli, R., Aramini, A., Boccella, S., Bagnasco, M., Cattani, F., Ferrari, M. P., Goisis, G., Minnella, E. M., Allegretti, M., & Pace, V. (2022). Ketoprofen lysine salt has a better gastrointestinal and renal tolerability than ketoprofen acid: A comparative tolerability study in the Beagle dog. *Biomedicine & Pharmacotherapy*, 153, 113336. <https://doi.org/10.1016/j.biopha.2022.113336>
121. Ikuse, M., Tagami, T., Ogawa, K., & Ozeki, T. (2022). Contamination-Free Milling of Ketoprofen Nanoparticles Using Mannitol Medium and Hoover Automatic Muller: Optimization of Effective Design of Experiment. *Biological and Pharmaceutical Bulletin*, 45(11), 1706–1715. <https://doi.org/10.1248/bpb.b22-00561>
122. Patel, V. D., Rathod, V., Haware, R. V., & Stagner, W. C. (2023). Optimized L-SNEDDS and spray-dried S-SNEDDS using a linked QbD-DM3 rational design for

- model compound ketoprofen. *International Journal of Pharmaceutics*, 631, 122494.  
<https://doi.org/10.1016/j.ijpharm.2022.122494>
123. Rachmaniar, R., Tristiyanti, D., Hamdani, S., & Afifah. (2018). *Solubility and dissolution improvement of ketoprofen by emulsification ionic gelation*. 030024.  
<https://doi.org/10.1063/1.5021217>
124. Devi, S., Kumar, A., Kapoor, A., Verma, V., Yadav, S., & Bhatia, M. (2022). Ketoprofen–FA Co-crystal: In Vitro and In Vivo Investigation for the Solubility Enhancement of Drug by Design of Expert. *AAPS PharmSciTech*, 23(4), 101.  
<https://doi.org/10.1208/s12249-022-02253-5>
125. Mandava, K., Lalit, K., & Katla, V. M. (2021). Formulation and Evaluation of Ketoprofen Using  $\beta$ -Cyclodextrin Capped Silver Nanoparticles. *International Journal of Pharmaceutical Sciences and Nanotechnology*, 14(3), 5501–5507.  
<https://doi.org/10.37285/ijpsn.2021.14.3.7>
126. Gul, R., Ahmed, N., Ullah, N., Khan, M. I., Elaissari, A., & Rehman, Asim. ur. (2018). Biodegradable Ingredient-Based Emulgel Loaded with Ketoprofen Nanoparticles. *AAPS PharmSciTech*, 19(4), 1869–1881.  
<https://doi.org/10.1208/s12249-018-0997-0>
127. Jagdale, S. C., Bafna, M. S., & Chabukswar, A. R. (2022). Transdermal Anti-inflammatory Delivery for Solid Lipid Nanoparticles of Ketoprofen by Microwave-assisted Microemulsion. *Recent Advances in Inflammation & Allergy Drug Discovery*, 15(2), 87–98. <https://doi.org/10.2174/2772270816666220126105802>
128. Huang, Y., & Dai, W.-G. (2014). Fundamental aspects of solid dispersion technology for poorly soluble drugs. *Acta Pharmaceutica Sinica B*, 4(1), 18–25.  
<https://doi.org/10.1016/j.apsb.2013.11.001>
129. Da Silva Júnior, W. F., De Oliveira Pinheiro, J. G., Moreira, C. D. L. F. A., De Souza, F. J. J., & De Lima, Á. A. N. (2017). Alternative Technologies to Improve Solubility

- and Stability of Poorly Water-Soluble Drugs. In *Multifunctional Systems for Combined Delivery, Biosensing and Diagnostics* (pp. 281–305). Elsevier.  
<https://doi.org/10.1016/B978-0-323-52725-5.00015-0>
130. Yao, Y., Xie, Y., Hong, C., Li, G., Shen, H., & Ji, G. (2014). Development of a myricetin/hydroxypropyl- $\beta$ -cyclodextrin inclusion complex: Preparation, characterization, and evaluation. *Carbohydrate Polymers*, *110*, 329–337.  
<https://doi.org/10.1016/j.carbpol.2014.04.006>
131. Skiba-Lahiani, M., Hallouard, F., Mehenni, L., Fessi, H., & Skiba, M. (2015). Development and characterization of oral liposomes of vegetal ceramide based amphotericin B having enhanced dry solubility and solubility. *Materials Science and Engineering: C*, *48*, 145–149. <https://doi.org/10.1016/j.msec.2014.11.069>
132. Burton, L., Ying, W., Gandhi, R., West, R., Huang, C., Zhou, S., Shah, K., Chen, J., & Shen, X. (2012). Development of a precipitation-resistant solution formulation to increase in vivo exposure of a poorly water-soluble compound. *International Journal of Pharmaceutics*, *433*(1–2), 94–101. <https://doi.org/10.1016/j.ijpharm.2012.04.075>
133. Wlodarski, K., Sawicki, W., Kozyra, A., & Tajber, L. (2015). Physical stability of solid dispersions with respect to thermodynamic solubility of tadalafil in PVP-VA. *European Journal of Pharmaceutics and Biopharmaceutics*, *96*, 237–246.  
<https://doi.org/10.1016/j.ejpb.2015.07.026>
134. Kumar, B. (2017). Solid Dispersion-A Review. *Pharmatutor*, *5*, 24–29.
135. Van Duong, T., & Van den Mooter, G. (2016). The role of the carrier in the formulation of pharmaceutical solid dispersions. Part I: Crystalline and semi-crystalline carriers. *Expert Opinion on Drug Delivery*, *13*(11), 1583–1594.  
<https://doi.org/10.1080/17425247.2016.1198768>

136. Wani, S. U. D., Kakkar, V., Gautam, S. P., Hv, G., Ali, M., Masoodi, M. H., & Moin, A. (2021). Enhancing therapeutic potential of poor aqueous soluble herbal drugs through solid dispersion-An overview. *Phytomedicine Plus*, *1*(4), 100069. <https://doi.org/10.1016/j.phyplu.2021.100069>
137. 慶二関口, & 陞小尾. (1961). Studies on Absorption of Eutectic Mixture. I. A Comparison of the Behavior of Eutectic Mixture of Sulfathiazole and that of Ordinary Sulfathiazole in Man. *Chemical & Pharmaceutical Bulletin*, *9*(11), 866–872. <https://doi.org/10.1248/cpb.9.866>
138. Chiou, W. L., & Riegelman, S. (1971). Pharmaceutical Applications of Solid Dispersion Systems. *Journal of Pharmaceutical Sciences*, *60*(9), 1281–1302. <https://doi.org/10.1002/jps.2600600902>
139. Tambe, S., Jain, D., Meruva, S. K., Rongala, G., Juluri, A., Nihalani, G., Mamidi, H. K., Nukala, P. K., & Bolla, P. K. (2022). Recent Advances in Amorphous Solid Dispersions: Preformulation, Formulation Strategies, Technological Advancements and Characterization. *Pharmaceutics*, *14*(10), 2203. <https://doi.org/10.3390/pharmaceutics14102203>
140. Bertoni, S., Albertini, B., & Passerini, N. (2023). Investigating the physicochemical properties of solid dispersions based on semicrystalline carriers: A case study with ketoprofen. *International Journal of Pharmaceutics*, *632*, 122576. <https://doi.org/10.1016/j.ijpharm.2022.122576>
141. Zhu, Q., Harris, M. T., & Taylor, L. S. (2012). Modification of Crystallization Behavior in Drug/Polyethylene Glycol Solid Dispersions. *Molecular Pharmaceutics*, *9*(3), 546–553. <https://doi.org/10.1021/mp200546p>
142. Duong, T. V., Van Humbeeck, J., & Van Den Mooter, G. (2015). Crystallization Kinetics of Indomethacin/Polyethylene Glycol Dispersions Containing High Drug

- Loadings. *Molecular Pharmaceutics*, 12(7), 2493–2504.  
<https://doi.org/10.1021/acs.molpharmaceut.5b00299>
143. Kaushik, R., Budhwar, V., & Kaushik, D. (2020). An Overview on Recent Patents and Technologies on Solid Dispersion. *Recent Patents on Drug Delivery & Formulation*, 14(1), 63–74. <https://doi.org/10.2174/1872211314666200117094406>
144. Boghra, R. J., Kothawade, P. C., Belgamwar, V. S., Nerkar, P. P., Tekade, A. R., & Surana, S. J. (2011). Solubility, Dissolution Rate and Bioavailability Enhancement of Irbesartan by Solid Dispersion Technique. *Chemical and Pharmaceutical Bulletin*, 59(4), 438–441. <https://doi.org/10.1248/cpb.59.438>
145. Liu, C., Wu, J., Shi, B., Zhang, Y., Gao, T., & Pei, Y. (2006). Enhancing the Bioavailability of Cyclosporine A Using Solid Dispersion Containing Polyoxyethylene (40) Stearate. *Drug Development and Industrial Pharmacy*, 32(1), 115–123. <https://doi.org/10.1080/03639040500388573>
146. Iqbal, B., Ali, A., Ali, J., Baboota, S., Gupta, S., Dang, S., Muhammad, S., & K. Sahni, J. (2011). Recent Advances and Patents in Solid Dispersion Technology. *Recent Patents on Drug Delivery & Formulation*, 5(3), 244–264. <https://doi.org/10.2174/187221111797200551>
147. Sareen, S., Joseph, L., & Mathew, G. (2012). Improvement in solubility of poor water-soluble drugs by solid dispersion. *International Journal of Pharmaceutical Investigation*, 2(1), 12. <https://doi.org/10.4103/2230-973X.96921>
148. Dash, S., Murthy, P. N., Nath, L., & Chowdhury, P. (2010). Kinetic modeling on drug release from controlled drug delivery systems. *Acta Poloniae Pharmaceutica*, 67(3), 217–223.

149. Soni, T., & Chotai, N. (2010). Assessment of Dissolution Profile of Marketed Aceclofenac Formulations. *Journal of Young Pharmacists*, 2(1), 21–26. <https://doi.org/10.4103/0975-1483.62208>
150. Polli, J. E., Rekhi, G. S., Augsburger, L. L., & Shah, V. P. (1997). Methods to Compare Dissolution Profiles and a Rationale for Wide Dissolution Specifications for Metoprolol Tartrate tablets†. *Journal of Pharmaceutical Sciences*, 86(6), 690–700. <https://doi.org/10.1021/js960473x>
151. Shah, V. P., Lesko, L. J., Fan, J., Fleischer, N., Handerson, J., Malinowski, H., Makary, M., Ouderkirk, L., Roy, S., Sathe, P., Singh, G. J. P., Tillman, L., Tsong, Y., & Williams, R. L. (1997). fDA Guidance for Industry 1 Dissolution Testing of Immediate Release Solid Oral Dosage Forms. *Dissolution Technologies*, 4(4), 15–22. <https://doi.org/10.14227/DT040497P15>
152. Changdeo, J. S., Vinod, M., Shankar, K. B., & Rajaram, C. A. (2011). Physicochemical characterization and solubility enhancement studies of allopurinol solid dispersions. *Brazilian Journal of Pharmaceutical Sciences*, 47(3), 513–523. <https://doi.org/10.1590/S1984-82502011000300009>
153. Sheth, T. S., & Acharya, F. (2021). Optimizing similarity factor of in vitro drug release profile for development of early stage formulation of drug using linear regression model. *Journal of Mathematics in Industry*, 11(1), 9. <https://doi.org/10.1186/s13362-021-00104-9>
154. Costa, P. (2001). An alternative method to the evaluation of similarity factor in dissolution testing. *International Journal of Pharmaceutics*, 220(1–2), 77–83. [https://doi.org/10.1016/S0378-5173\(01\)00651-2](https://doi.org/10.1016/S0378-5173(01)00651-2)
155. Conceição, J., Estanqueiro, M., H. Amaral, M., Lobão, P., Costa, P., & M. Sousa Lobo, J. (2014). Development and Characterization of Buccal Bilayer Tablets containing

- Microparticles with Ibuprofen. *American Journal of Medical Sciences and Medicine*, 2(5), 109–114. <https://doi.org/10.12691/ajmsm-2-5-5>
156. Salah Attia, M., Ali Hasan, A., Ghazy, F.-E. S., & Gomaa, E. (2021). Solid Dispersion as a Technical Solution to Boost the Dissolution Rate and Bioavailability of Poorly Water-Soluble Drugs. *Indian Journal of Pharmaceutical Education and Research*, 55(2s), s327–s339. <https://doi.org/10.5530/ijper.55.2s.103>
157. Varshney, M. (2022). Solid dispersion: A potent and lucrative technique to enhance the aqueous solubility of drug. *A Journal Of Composition Theory*, 15(3), 126-136, ISSN: 0731-6755
158. Tran, P., Pyo, Y.-C., Kim, D.-H., Lee, S.-E., Kim, J.-K., & Park, J.-S. (2019). Overview of the Manufacturing Methods of Solid Dispersion Technology for Improving the Solubility of Poorly Water-Soluble Drugs and Application to Anticancer Drugs. *Pharmaceutics*, 11(3), 132. <https://doi.org/10.3390/pharmaceutics11030132>
159. Mandal, U. (2011). *Pharmaceutical application of solid dispersion technology in improving solubility of poorly soluble drug: A review* (pp. 156–177).
160. Cao, J., Zhang, S., Hao, Y., Fan, K., Wang, L., Zhao, X., & He, X. (2023). Amorphous solid dispersion preparation via coprecipitation improves the dissolution, oral bioavailability, and intestinal health enhancement properties of magnolol. *Poultry Science*, 102(6), 102676. <https://doi.org/10.1016/j.psj.2023.102676>
161. Yu, J. Y., Kim, J. A., Joung, H. J., Ko, J. A., & Park, H. J. (2020). Preparation and characterization of curcumin solid dispersion using HPMC. *Journal of Food Science*, 85(11), 3866–3873. <https://doi.org/10.1111/1750-3841.15489>
162. Suzuki, H., Yakushiji, K., Matsunaga, S., Yamauchi, Y., Seto, Y., Sato, H., & Onoue, S. (2018). Amorphous Solid Dispersion of Meloxicam Enhanced Oral Absorption in

- Rats With Impaired Gastric Motility. *Journal of Pharmaceutical Sciences*, 107(1), 446–452. <https://doi.org/10.1016/j.xphs.2017.05.023>
163. Pathak, D., Dahiya, S., & Pathak, K. (2008). Solid dispersion of meloxicam: Factorially designed dosage form for geriatric population. *Acta Pharmaceutica*, 58(1), 99–110. <https://doi.org/10.2478/v10007-007-0048-y>
164. Pan, R.-N., Chen, J.-H., & Chen, R. R.-L. (2000). Enhancement of Dissolution and Bioavailability of Piroxicam in Solid Dispersion Systems. *Drug Development and Industrial Pharmacy*, 26(9), 989–994. <https://doi.org/10.1081/DDC-100101327>
165. Baek, H. H., Kim, D.-H., Kwon, S. Y., Rho, S.-J., Kim, D.-W., Choi, H.-G., Kim, Y.-R., & Yong, C. S. (2012). Development of novel ibuprofen-loaded solid dispersion with enhanced bioavailability using cycloamylose. *Archives of Pharmacal Research*, 35(4), 683–689. <https://doi.org/10.1007/s12272-012-0412-4>
166. Sivert, A., Bérard, V., & Andrès, C. (2010). New binary solid dispersion of indomethacin with surfactant polymer: From physical characterization to in vitro dissolution enhancement. *Journal of Pharmaceutical Sciences*, 99(3), 1399–1413. <https://doi.org/10.1002/jps.21935>
167. Dash, S., Murthy, P. N., Nath, L., & Chowdhury, P. (n.d.). Kinetic modeling on drug release from controlled drug delivery systems. *Acta Poloniae Pharmaceutica*, 67(3), 217-23.
168. Samaha, D., Shehayeb, R., & Kyriacos, S. (2009). Modeling and Comparison of Dissolution Profiles of Diltiazem Modified-Release Formulations. *Dissolution Technologies*, 16(2), 41–46. <https://doi.org/10.14227/DT160209P41>
169. Chakrabarty, B., Ghoshal, A. K., & Purkait, M. K. (2008). Effect of molecular weight of PEGS on membrane morphology and transport properties. *Journal of Membrane Science*, 309(1–2), 209–221. <https://doi.org/10.1016/j.memsci.2007.10.027>

170. Chibowski, S., & Paszkiewicz, M. (1999). Influence of the Molecular Weight of Polyethylene Glycol and Polyethylene Oxide on the Adsorption and Electrochemical Properties of the Titania/ Electrolyte Solution Interface <sup/>. *Adsorption Science & Technology*, *17*(10), 845–855. <https://doi.org/10.1177/026361749901701007>
171. Li, R., Wu, Y., Bai, Z., Guo, J., & Chen, X. (2020). Effect of molecular weight of polyethylene glycol on crystallization behaviors, thermal properties and tensile performance of polylactic acid stereocomplexes. *RSC Advances*, *10*(69), 42120–42127. <https://doi.org/10.1039/D0RA08699A>
172. Qu, P., Gao, Y., Zhou, Y., Zhang, L., & Li, S. (2011). Influence of Molecular Weight of PEGS on Biodegradation and Morphology Properties of Cellulose Nanofibrils/Poly(Lactic Acid) Composite Materials. *5th International Conference on Bioinformatics and Biomedical Engineering, iCBBE 2011*, 1–4. <https://doi.org/10.1109/icbbe.2011.5780330>
173. Singh, M., Verma, S. K., Biswas, I., & Mehta, R. (2018). Effect of molecular weight of polyethylene glycol on the rheological properties of fumed silica-polyethylene glycol shear thickening fluid. *Materials Research Express*, *5*(5), 055704. <https://doi.org/10.1088/2053-1591/aac25c>
174. Plisko, T. V., Bilyukevich, A. V., Usosky, V. V., & Volkov, V. V. (2016). Influence of the concentration and molecular weight of polyethylene glycol on the structure and permeability of polysulfone hollow fiber membranes. *Petroleum Chemistry*, *56*(4), 321–329. <https://doi.org/10.1134/S096554411604006X>
175. Tran, L. C., & Di Palma, J. A. (2005). Lack of Lasting Effectiveness of PEGS 3350 Laxative Treatment of Constipation: *Journal of Clinical Gastroenterology*, *39*(7), 600–602. <https://doi.org/10.1097/01.mcg.0000170769.67320.47>

176. Pampati, V., & Fogel, R. (2004). Treatment options for primary constipation. *Current Treatment Options in Gastroenterology*, 7(3), 225–233.  
<https://doi.org/10.1007/s11938-004-0043-z>
177. Roberts, M. J., Bentley, M. D., & Harris, J. M. (2012). Chemistry for peptide and protein PEGSylation. *Advanced Drug Delivery Reviews*, 64, 116–127.  
<https://doi.org/10.1016/j.addr.2012.09.025>
178. Fam, S. Y., Chee, C. F., Yong, C. Y., Ho, K. L., Mariatulqabtiah, A. R., & Tan, W. S. (2020). Stealth Coating of Nanoparticles in Drug-Delivery Systems. *Nanomaterials*, 10(4), 787. <https://doi.org/10.3390/nano10040787>
179. Misichronis, K., Rangou, S., & Avgeropoulos, A. (2008). Synthesis and Molecular and Morphological Characterization of Poly(p-Trimethylsilyl Styrene) and Diblock Copolymers with Poly(1,3-Cyclohexadiene). *International Journal of Polymer Analysis and Characterization*, 13(2), 136–148.  
<https://doi.org/10.1080/10236660801924149>
180. Gibson, D. J., Yang, Q., Kerekes, D. T., & Schultz, G. S. (2014). Medical Honey and Silver Dressings Do Not Interfere with Each Other's Key Functional Attributes. *Wounds: A Compendium of Clinical Research and Practice*, 26(11), 309–316.
181. De Matteis, V., Rojas, M., Cascione, M., Mazzotta, S., Di Sansebastiano, G. P., & Rinaldi, R. (2021). Physico-Chemical Properties of Inorganic NPs Influence the Absorption Rate of Aquatic Mosses Reducing Cytotoxicity on Intestinal Epithelial Barrier Model. *Molecules*, 26(10), 2885.  
<https://doi.org/10.3390/molecules26102885>
182. Wang, T., Guo, Y., He, Y., Ren, T., Yin, L., Fawcett, J. P., Gu, J., & Sun, H. (2020). Impact of molecular weight on the mechanism of cellular uptake of polyethylene

- glycols (PEGs) with particular reference to P-glycoprotein. *Acta Pharmaceutica Sinica B*, *10*(10), 2002–2009. <https://doi.org/10.1016/j.apsb.2020.02.001>
183. Alam, F., Najum Us Saqib, Q., & Waheed, A. (2017). Cytotoxic activity of extracts and crude saponins from *Zanthoxylum armatum* DC. against human breast (MCF-7, MDA-MB-468) and colorectal (Caco-2) cancer cell lines. *BMC Complementary and Alternative Medicine*, *17*(1), 368. <https://doi.org/10.1186/s12906-017-1882-1>
184. Plackal Adimuriyil George, B., Tynga, I. M., & Abrahamse, H. (2015). *In Vitro* Antiproliferative Effect of the Acetone Extract of *Rubus fairholmianus* Gard. Root on Human Colorectal Cancer Cells. *BioMed Research International*, *2015*, 1–8. <https://doi.org/10.1155/2015/165037>
185. Florkiewicz, W., Malina, D., Pluta, K., Rudnicka, K., Gajewski, A., Olejnik, E., Tyliczszak, B., & Sobczak-Kupiec, A. (2019). Assessment of cytotoxicity and immune compatibility of phytochemicals-mediated biosynthesised silver nanoparticles using *Cynara scolymus*. *IET Nanobiotechnology*, *13*(7), 726–735. <https://doi.org/10.1049/iet-nbt.2018.5357>
186. Nozari, S., Faridvand, Y., Etesami, A., Ahmad Khan Beiki, M., Miresmaeili Mazrakhondi, S. A., & Abdolalizadeh, J. (2019). Potential anticancer effects of cell wall protein fractions from *Lactobacillus paracasei* on human intestinal Caco-2 cell line. *Letters in Applied Microbiology*, lam.13198. <https://doi.org/10.1111/lam.13198>
187. Dino, P., D'Anna, C., Sangiorgi, C., Di Sano, C., Di Vincenzo, S., Ferraro, M., & Pace, E. (2019). Cigarette smoke extract modulates E-Cadherin, Claudin-1 and miR-21 and promotes cancer invasiveness in human colorectal adenocarcinoma cells. *Toxicology Letters*, *317*, 102–109. <https://doi.org/10.1016/j.toxlet.2019.09.020>
188. Akter, M., Atique Ullah, A. K. M., Banik, S., Sikder, Md. T., Hosokawa, T., Saito, T., & Kurasaki, M. (2021). Green Synthesized Silver Nanoparticles-Mediated Cytotoxic

- Effect in Colorectal Cancer Cells: NF- $\kappa$ B Signal Induced Apoptosis Through Autophagy. *Biological Trace Element Research*, 199(9), 3272–3286. <https://doi.org/10.1007/s12011-020-02463-7>
189. Zhao, C., Qiu, S., He, J., Peng, Y., Xu, H., Feng, Z., Huang, H., Du, Y., Zhou, Y., & Nie, Y. (2020). Prodigiosin impairs autophagosome-lysosome fusion that sensitizes colorectal cancer cells to 5-fluorouracil-induced cell death. *Cancer Letters*, 481, 15–23. <https://doi.org/10.1016/j.canlet.2020.03.010>
190. Lauzier, A., Normandeau-Guimond, J., Vaillancourt-Lavigne, V., Boivin, V., Charbonneau, M., Rivard, N., Scott, M. S., Dubois, C. M., & Jean, S. (2019). Colorectal cancer cells respond differentially to autophagy inhibition in vivo. *Scientific Reports*, 9(1), 11316. <https://doi.org/10.1038/s41598-019-47659-7>
191. Moya-Andérico, L., Vukomanovic, M., Cendra, M. D. M., Segura-Feliu, M., Gil, V., Del Río, J. A., & Torrents, E. (2021). Utility of *Galleria mellonella* larvae for evaluating nanoparticle toxicology. *Chemosphere*, 266, 129235. <https://doi.org/10.1016/j.chemosphere.2020.129235>
192. Wijesinghe, G. K., Maia, F. C., De Oliveira, T. R., De Feiria, S. N. B., Joia, F., Barbosa, J. P., Boni, G. C., Sardi, J. D. C. O., Rosalen, P. L., & Höfling, J. F. (2020). Effect of *Cinnamomum verum* leaf essential oil on virulence factors of *Candida* species and determination of the in-vivo toxicity with *Galleria mellonella* model. *Memórias Do Instituto Oswaldo Cruz*, 115, e200349. <https://doi.org/10.1590/0074-02760200349>
193. Ignasiak, K., & Maxwell, A. (2017). *Galleria mellonella* (greater wax moth) larvae as a model for antibiotic susceptibility testing and acute toxicity trials. *BMC Research Notes*, 10(1), 428. <https://doi.org/10.1186/s13104-017-2757-8>

194. Allegra, E., Titball, R. W., Carter, J., & Champion, O. L. (2018). Galleria mellonella larvae allow the discrimination of toxic and non-toxic chemicals. *Chemosphere*, *198*, 469–472. <https://doi.org/10.1016/j.chemosphere.2018.01.175>
195. Liu, G., Li, Y., Yang, L., Wei, Y., Wang, X., Wang, Z., & Tao, L. (2017). Cytotoxicity study of polyethylene glycol derivatives. *RSC Advances*, *7*(30), 18252–18259. <https://doi.org/10.1039/C7RA00861A>
196. Ahmadyan, S., Kabiri, M., Hanaee-Ahvaz, H., & Farazmand, A. (2018). Osmolyte Type and the Osmolarity Level Affect Chondrogenesis of Mesenchymal Stem Cells. *Applied Biochemistry and Biotechnology*, *185*(2), 507–523. <https://doi.org/10.1007/s12010-017-2647-5>
197. Liu, Z., Chen, D., Chen, X., Bian, F., Gao, N., Li, J., Pflugfelder, S. C., & Li, D.-Q. (2020). Autophagy Activation Protects Ocular Surface from Inflammation in a Dry Eye Model In Vitro. *International Journal of Molecular Sciences*, *21*(23), Article 23. <https://doi.org/10.3390/ijms21238966>
198. Nunes, P., Hernandez, T., Roth, I., Qiao, X., Strebel, D., Bouley, R., Charollais, A., Ramadori, P., Foti, M., Meda, P., Féraille, E., Brown, D., & Hasler, U. (2013). Hypertonic stress promotes autophagy and microtubule-dependent autophagosomal clusters. *Autophagy*, *9*(4), 550–567. <https://doi.org/10.4161/auto.23662>
199. Yasuda, S., Tsuchiya, H., Kaiho, A., Guo, Q., Ikeuchi, K., Endo, A., Arai, N., Ohtake, F., Murata, S., Inada, T., Baumeister, W., Fernández-Busnadiego, R., Tanaka, K., & Saeki, Y. (2020). Stress- and ubiquitylation-dependent phase separation of the proteasome. *Nature*, *578*(7794), 296–300. <https://doi.org/10.1038/s41586-020-1982-9>

200. Ferrero-Andrés, A., Closa, D., Roselló-Catafau, J., & Folch-Puy, E. (2020). Polyethylene Glycol 35 (PEG35) Modulates Exosomal Uptake and Function. *Polymers*, 12(12), 3044. <https://doi.org/10.3390/polym12123044>
201. de Sousa, A. K. A., Ribeiro, F. O. S., de Oliveira, T. M., de Araújo, A. R., Dias, J. do N., Albuquerque, P., Silva-Pereira, I., de Jesus Oliveira, A. C., Quelemes, P. V., Leite, J. R. S. A., & da Silva, D. A. (2020). Quaternization of angico gum and evaluation of anti-staphylococcal effect and toxicity of their derivatives. *International Journal of Biological Macromolecules*, 150, 1175–1183. <https://doi.org/10.1016/j.ijbiomac.2019.10.126>
202. Vyas, K., Brassard, D. L., DeLorenzo, M. M., Sun, Y., Grace, M. J., Borden, E. C., & Leaman, D. W. (2003). Biologic Activity of Polyethylene Glycol12000–Interferon- $\alpha$ 2b Compared with Interferon- $\alpha$ 2b: Gene Modulatory and Antigrowth Effects in Tumor Cells. *Journal of Immunotherapy*, 26(3), 202. [https://journals.lww.com/immunotherapy-journal/abstract/2003/05000/biologic\\_activity\\_of\\_polyethylene.4.aspx](https://journals.lww.com/immunotherapy-journal/abstract/2003/05000/biologic_activity_of_polyethylene.4.aspx)
203. Bastos, V., Ferreira de Oliveira, J. M. P., Brown, D., Jonhston, H., Malheiro, E., Daniela-da-Silva, A. L., Duarte, I. F., Santos, C., & Oliveira, H. (2016). The influence of Citrate or PEGS coating on silver nanoparticle toxicity to a human keratinocyte cell line. *Toxicology Letters*, 249, 29–41. <https://doi.org/10.1016/j.toxlet.2016.03.005>
204. Patel, K., Shah, S., & Patel, J. (2022). Solid dispersion technology as a formulation strategy for the fabrication of modified release dosage forms: A comprehensive review. *DARU Journal of Pharmaceutical Sciences*, 30(1), 165–189. <https://doi.org/10.1007/s40199-022-00440-0>
205. Khattab, I. S., Nada, A., & Zaghloul, A.-A. (2010). Physicochemical characterization of gliclazide–macrogol solid dispersion and tablets based on optimized dispersion.

- Drug Development and Industrial Pharmacy*, 36(8), 893–902.  
<https://doi.org/10.3109/03639040903578734>
206. Mura, P., Moyano, J. R., González-Rodríguez, M. L., Rabasco-Alvaréz, A. M., Cirri, M., & Maestrelli, F. (2005). Characterization and Dissolution Properties of Ketoprofen in Binary and Ternary Solid Dispersions with Polyethylene Glycol and Surfactants. *Drug Development and Industrial Pharmacy*, 31(4–5), 425–434.  
<https://doi.org/10.1080/03639040500214621>
207. Chan, S.-Y., Toh, S.-M., Khan, N. H., Chung, Y.-Y., & Cheah, X.-Z. (2016). The improved dissolution performance of a post processing treated spray-dried crystalline solid dispersion of poorly soluble drugs. *Drug Development and Industrial Pharmacy*, 42(11), 1800–1812.  
<https://doi.org/10.3109/03639045.2016.1173054>
208. Browne, E., Charifou, R., Worku, Z. A., Babu, R. P., & Healy, A. M. (2019). Amorphous solid dispersions of ketoprofen and poly-vinyl polymers prepared via electrospraying and spray drying: A comparison of particle characteristics and performance. *International Journal of Pharmaceutics*, 566, 173–184.  
<https://doi.org/10.1016/j.ijpharm.2019.05.062>
209. Dong, C.-L., Zheng, S.-D., Liu, Y.-Y., Cui, W.-Q., Hao, M.-Q., God'spower, B.-O., Chen, X.-Y., & Li, Y.-H. (2020). Albendazole solid dispersions prepared using PEGS6000 and Poloxamer188: Formulation, characterization and *in vivo* evaluation. *Pharmaceutical Development and Technology*, 25(9), 1043–1052.  
<https://doi.org/10.1080/10837450.2020.1783553>
210. Al-kasmi, B., Alsirawan, M. H. D. B., Paradkar, A., Nattouf, A.-H., & El-Zein, H. (2021). Aqueous and pH dependent coacervation method for taste masking of

- paracetamol via amorphous solid dispersion formation. *Scientific Reports*, 11(1), 8907. <https://doi.org/10.1038/s41598-021-88312-6>
211. Hermans, A., Milsmann, J., Li, H., Jede, C., Moir, A., Hens, B., Morgado, J., Wu, T., & Cohen, M. (2022). Challenges and Strategies for Solubility Measurements and Dissolution Method Development for Amorphous Solid Dispersion Formulations. *The AAPS Journal*, 25(1), 11. <https://doi.org/10.1208/s12248-022-00760-8>
212. Vueba, M. L., Batista de Carvalho, L. A. E., Veiga, F., Sousa, J. J., & Pina, M. E. (2013). In vitro release of ketoprofen from hydrophilic matrix tablets containing cellulose polymer mixtures. *Drug Development and Industrial Pharmacy*, 39(11), 1651–1662. <https://doi.org/10.3109/03639045.2012.729146>
213. Vippagunta, S. R., Maul, K. A., Tallavajhala, S., & Grant, D. J. W. (2002). Solid-state characterization of nifedipine solid dispersions. *International Journal of Pharmaceutics*, 236(1–2), 111–123. [https://doi.org/10.1016/S0378-5173\(02\)00019-4](https://doi.org/10.1016/S0378-5173(02)00019-4)
214. Yang, R., Zhang, G. G. Z., Kjoller, K., Dillon, E., Purohit, H. S., & Taylor, L. S. (2022). Phase separation in surfactant-containing amorphous solid dispersions: Orthogonal analytical methods to probe the effects of surfactants on morphology and phase composition. *International Journal of Pharmaceutics*, 619, 121708. <https://doi.org/10.1016/j.ijpharm.2022.121708>
215. Purohit, H. S., & Taylor, L. S. (2015). Phase separation kinetics in amorphous solid dispersions upon exposure to water. *Molecular Pharmaceutics*, 12(5), 1623–1635. <https://doi.org/10.1021/acs.molpharmaceut.5b00041>
216. Guo, X., Guo, Y., Zhang, M., Yang, B., Liu, H., Yin, T., Zhang, Y., He, H., Wang, Y., Liu, D., Gou, J., & Tang, X. (2022). A comparative study on in vitro and in vivo characteristics of enzalutamide nanocrystals versus amorphous solid dispersions and

- a better prediction for bioavailability based on “spring-parachute” model. *International Journal of Pharmaceutics*, 628, 122333. <https://doi.org/10.1016/j.ijpharm.2022.122333>
217. Hens, B., Brouwers, J., Corsetti, M., & Augustijns, P. (2016). Supersaturation and Precipitation of Posaconazole Upon Entry in the Upper Small Intestine in Humans. *Journal of Pharmaceutical Sciences*, 105(9), 2677–2684. <https://doi.org/10.1002/jps.24690>
218. Vippagunta, S. R., Wang, Z., Hornung, S., & Krill, S. L. (2007). Factors Affecting the Formation of Eutectic Solid Dispersions and Their Dissolution Behavior. *Journal of Pharmaceutical Sciences*, 96(2), 294–304. <https://doi.org/10.1002/jps.20754>
219. Lacoulonche, F., Chauvet, A., Masse, J., Egea, M. A., & Garcia, M. L. (1998). An investigation of FB interactions with poly(ethylene glycol) 6000, poly(ethylene glycol) 4000, and poly- $\epsilon$ -caprolactone by thermoanalytical and spectroscopic methods and modeling. *Journal of Pharmaceutical Sciences*, 87(5), 543–551. <https://doi.org/10.1021/js970443+>
220. Ford, J. L., Stewart, A. F., & Dubois, J.-L. (1986). The properties of solid dispersions of indomethacin or phenylbutazone in polyethylene glycol. *International Journal of Pharmaceutics*, 28(1), 11–22. [https://doi.org/10.1016/0378-5173\(86\)90142-0](https://doi.org/10.1016/0378-5173(86)90142-0)
221. Miralles, M. J., McGinty, J. W., & Martin, A. (1982). Combined Water-Soluble Carriers for Coprecipitates of Tolbutamide. *Journal of Pharmaceutical Sciences*, 71(3), 302–304. <https://doi.org/10.1002/jps.2600710309>
222. Serajuddin, A. T. M., Mufson, D., Bernstein, D. F., Sheen, P.-C., & Augustine, M. A. (1988). Effect of Vehicle Amphiphilicity on the Dissolution and Bioavailability of a Poorly Water-Soluble Drug from Solid Dispersions. *Journal of Pharmaceutical Sciences*, 77(5), 414–417. <https://doi.org/10.1002/jps.2600770512>

223. Chiou, W. L., & Riegelman, S. (1969). Preparation and Dissolution Characteristics of Several Fast-Release Solid Dispersions of Griseofulvin. *Journal of Pharmaceutical Sciences*, 58(12), 1505–1510. <https://doi.org/10.1002/jps.2600581218>
224. Betageri, G. (1995). Enhancement of dissolution of glyburide by solid dispersion and lyophilization techniques. *International Journal of Pharmaceutics*, 126(1–2), 155–160. [https://doi.org/10.1016/0378-5173\(95\)04114-1](https://doi.org/10.1016/0378-5173(95)04114-1)
225. Anguiano-Igea, S., Otero-Espinar, F. J., Vila-Jato, J. L., & Blanco-Méndez, J. (1995). The properties of solid dispersions of clofibrate in polyethylene glycols. *Pharmaceutica Acta Helveticae*, 70(1), 57–66. [https://doi.org/10.1016/0031-6865\(94\)00051-V](https://doi.org/10.1016/0031-6865(94)00051-V)
226. Dordunoo, S. K., Ford, J. L., & Rubinstein, M. H. (2011). Physical Stability of Solid Dispersions Containing Triamterene or Temazepam in Polyethylene Glycols. *Journal of Pharmacy and Pharmacology*, 49(4), 390–396. <https://doi.org/10.1111/j.2042-7158.1997.tb06812.x>
227. Mura, P., Faucci, M. T., Manderioli, A., Bramanti, G., & Parrini, P. (1999). Thermal Behavior and Dissolution Properties of Naproxen From Binary and Ternary Solid Dispersions. *Drug Development and Industrial Pharmacy*, 25(3), 257–264. <https://doi.org/10.1081/DDC-100102169>
228. Khattab, I. S., Nada, A., & Zaghloul, A.-A. (2010). Physicochemical characterization of gliclazide–macrogol solid dispersion and tablets based on optimized dispersion. *Drug Development and Industrial Pharmacy*, 36(8), 893–902. <https://doi.org/10.3109/03639040903578734>
229. Trapani, G., Franco, M., Latrofa, A., Pantaleo, M. R., Provenzano, M. R., Sanna, E., Maciocco, E., & Liso, G. (1999). Physicochemical characterization and in vivo properties of Zolpidem in solid dispersions with polyethylene glycol 4000 and 6000.

*International Journal of Pharmaceutics*, 184(1), 121–130.

[https://doi.org/10.1016/S0378-5173\(99\)00112-X](https://doi.org/10.1016/S0378-5173(99)00112-X)

230. Sjökvist, E., & Nyström, C. (1988). Physicochemical aspects of drug release. VI. Drug dissolution rate from solid particulate dispersions and the importance of carrier and drug particle properties. *International Journal of Pharmaceutics*, 47(1), 51–66.  
[https://doi.org/10.1016/0378-5173\(88\)90215-3](https://doi.org/10.1016/0378-5173(88)90215-3)

231. Halder, S., Ahmed, F., Shuma, M. L., Azad, M. A. K., & Kabir, E. R. (2020). Impact of drying on dissolution behavior of carvedilol-loaded sustained release solid dispersion: Development and characterization. *Heliyon*, 6(9), e05026.  
<https://doi.org/10.1016/j.heliyon.2020.e05026>

232. Jain, S. K., Shukla, M., & Shrivastava, V. (2010). Development and *in Vitro* Evaluation of Ibuprofen Mouth Dissolving Tablets Using Solid Dispersion Technique. *Chemical and Pharmaceutical Bulletin*, 58(8), 1037–1042.  
<https://doi.org/10.1248/cpb.58.1037>

## **14. KEYWORDS**

CaCo-2; MTT assay; NR assay; autophagy; flow cytometry; osmolality; G.mellonella; solid dispersion, polyethylene glycole, PEGS; ketoprofen; solubility; dissolution

# 15. PUBLICATIONLIST RELATED TO THE DISSERTATION



UNIVERSITY of  
DEBRECEN

UNIVERSITY AND NATIONAL LIBRARY  
UNIVERSITY OF DEBRECEN

H-4002 Egyetem tér 1, Debrecen  
Phone: +3652/410-443, email: publikaciok@lib.unideb.hu

Registry number: DEENK/65/2024.PL  
Subject: PhD Publication List

Candidate: Ha Pham Le Khanh  
Doctoral School: Doctoral School of Pharmacy

## List of publications related to the dissertation

1. **Pham Le Khanh, H.**, Haimhoffer, Á., Nemes, D., Józsa, L., Vasvári, G., Budai, I., Béneyei, A., Ujhelyi, Z., Fehér, P., Bácskay, I.: Effect of Molecular Weight on the Dissolution Profiles of PEG Solid Dispersions Containing Ketoprofen.  
*Polymers*. 15 (7), 1-15, 2023.  
DOI: <http://dx.doi.org/10.3390/polym15071758>  
IF: 5 (2022)
2. **Pham Le Khanh, H.**, Nemes, D., Rusznyák, Á., Ujhelyi, Z., Fehér, P., Fenyvesi, F., Váradi, J., Vecsernyés, M., Bácskay, I.: Comparative Investigation of Cellular Effects of Polyethylene Glycol (PEG) Derivates.  
*Polymers*. 14, 1-15, 2022.  
IF: 5

**Total IF of journals (all publications): 10**

**Total IF of journals (publications related to the dissertation): 10**

The Candidate's publication data submitted to the iDEa Tudóstér have been validated by DEENK on the basis of the Journal Citation Report (Impact Factor) database.

27 February, 2024



## 16. FUNDING

To The Stipendium Hungaricum scholarship, I offer my sincerest thanks for the generous throughout my doctoral studies in the University of Debrecen. Their financial assistance has been instrumental in enabling me to pursue my research ambitions and advance my academic pursuits.

The work was also supported by the GINOP-2.3.4-15-2020-00008 and the GINOP-2.3.3-15-2016-0002 “Developing Pharmaceutical Technology R & D Infrastructure on the University of Debrecen” projects. The research was supported by the Thematic Excellence Programme (TKP2020-IKA-04) of the Ministry for Innovation and Technology in Hungary. The projects are co-financed by the European Union and the European Regional Development Fund.

The research was supported by project no. TKP2021-EGA-18 has been implemented with the support provided from the National Research, Development, and Innovation Fund of Hungary, financed under the TKP2021-EGA funding scheme. This work was also supported by the GINOP-2.3.4-15-2016-00002 “Developing Pharmaceutical Technology R&D Infrastructure on the University of Debrecen”, the “Debrecen Venture Catapult Program” EFOP-3.6.1-16-2016-00022 and the Debrecen Venture Table S Catapult (EFOP-3.6.1-16-2016-0002) projects

## 17. ACKNOWLEDGEMENT

First and foremost, from the bottom of my heart I would like to express my deepest gratitude to my research supervisor, Prof. Dr. Ildikó Bácskay, for her pivotal role in guiding me through the doctoral journey. I am profoundly grateful to her for accepting me as a Ph.D. candidate under her mentorship. Her professional guidance has not only enriched my scholarly endeavors but have also provided invaluable supports to resolve the complexities of life as a Ph.D. student. It is truly a great privilege and honor to work and study under her supervision.

I am also thankful to Prof. Dr. Miklós Vecsernyés, the Former Dean of the Faculty of Pharmacy for giving me the opportunity to do my doctoral research at the Department of Pharmaceutical Technology.

I could not have undertaken this journey without Dr. Dániel Nemes, my senior, who constantly encouraged and helped me from the very beginning of my journey. He has generously shared his knowledge and experience, enriching my understanding and propelling my work forward. Whenever challenges arose, he was there, ready to offer guidance and assistance without hesitation.

I would also like to thank my research partners and co-authors, Dr. Ferenc Fenyvesi, Dr. Judit Váradi, Dr. Pálma Fehér, Dr. Zoltán Ujhelyi, for their contribution to the success of my project. Special thanks to Dr. Ádám Haimhoffer, Dr. Gábor Vasvári, Dr. Ruzsnyák Ágnes, Dr. Liza Józsa for their hard working and support in my research. I would like to thank Prof. Dr. Attila Csaba Benyei from Physical Chemistry Department for the powder X-ray diffraction and Dr. István Budai from Engineering Management Department for the scanning electron microscopy images.

I am grateful to Dr. Dóra Kósa and Dr. Ágota Pető and for their professional and friendly support at my crunch time to accomplish my dissertation.

I would be remiss in not mentioning the faculty members of the Department of Pharmaceutical Technology for their considerate support and encouragement over the past years.

I thank all of my friends who supported me and had to put up with my stresses and moans, for their caring sprit and cheering me up in my difficult moments.

Last but not least, I owe my grateful thanks to my loving family for always by my side and motivating me throughout my life. Especially my father, it was him to inspire me to

follow this academic path and to become the person I am today. The unwavering support and sacrifices from my family have been the foundation upon which I could pursue my studies abroad for an extended period without worry or distraction.

To my parents, I offer my deepest thanks for your unconditional love, endless support (both financially and emotionally) and unwavering belief in my abilities. This achievement is as much yours as it is mine and I am profoundly grateful for the sacrifices you have made to make it possible.